

UNIVERSIDADE FEDERAL DE SANTA MARIA
CENTRO DE CIÊNCIAS NATURAIS E EXATAS
PROGRAMA DE PÓS-GRADUAÇÃO EM CIÊNCIAS BIOLÓGICAS:
BIOQUÍMICA TOXICOLÓGICA

Olawande Chinedu Olagoke

**DIABETES PHENOTYPE MODELLING IN *Nauphoeta cinerea*
USING STREPTOZOTOCIN:
FOCUS ON BRAIN GLUCOSE METABOLISM.**

Santa Maria, RS
2021.

Olawande Chinedu Olagoke

**DIABETES PHENOTYPE MODELLING IN *Nauphoeta cinerea*
USING STREPTOZOTOCIN:
FOCUS ON BRAIN GLUCOSE METABOLISM.**

Tese apresentada ao Curso de Pós-Graduação
Ciências Biológicas: Bioquímica Toxicológica,
da Universidade Federal de Santa Maria (UFSM,
RS), como requisito parcial para obtenção do
título de **Doutor em Ciências Biológicas:
Bioquímica Toxicológica.**

Orientador: Prof^o João Batista Teixeira da Rocha.

Santa Maria, RS

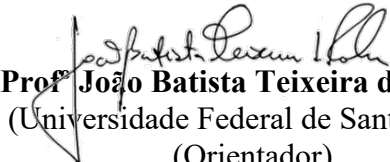
2021

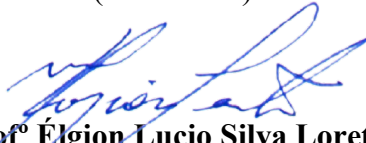
Olawande Chinedu Olagoke


**DIABETES PHENOTYPE MODELLING IN *Nauphoeta cinerea*
USING STREPTOZOTOCIN:
FOCUS ON BRAIN GLUCOSE METABOLISM.**


Tese apresentada ao Curso de Pós-Graduação
Ciências Biológicas: Bioquímica Toxicológica,
da Universidade Federal de Santa Maria (UFSM,
RS), como requisito parcial para obtenção do
título de **Doutor em Ciências Biológicas:
Bioquímica Toxicológica.**

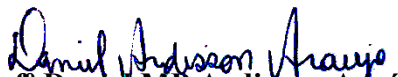
Aprovado em: 16 de maio de 2021.


Profº João Batista Teixeira da Rocha
(Universidade Federal de Santa Maria)
(Orientador)


Profº Elgion Lucio Silva Loreto
(Universidade Federal de Santa Maria)


Profª Vanderlei Folmer
(Universidade Federal do Pampa)


Profº Robson Luiz Puntel
(Universidade Federal do Pampa)


Profº Daniel MP Ardisson-Araújo
(Universidade Federal de Santa Maria)

Santa Maria, RS.
2021.

Olagoke, Olawande
DIABETES PHENOTYPE MODELLING IN Nauphoeta cinerea
USING STREPTOZOTOCIN: FOCUS ON BRAIN GLUCOSE METABOLISM.
/ Olawande Olagoke.- 2021.
152 p.; 30 cm

Orientador: João Batista da Rocha
Tese (doutorado) - Universidade Federal de Santa
Maria, Centro de Ciências Naturais e Exatas, Programa de
Pós-Graduação em Ciências Biológicas: Bioquímica
Toxicológica, RS, 2021

1. GLUT1 2. Insulin signaling 3. RNA-seq 4.
antioxidants 5. Ribosomal protein I. da Rocha, João
Batista II. Título.

Sistema de geração automática de ficha catalográfica da UFSM. Dados fornecidos pelo autor(a). Sob supervisão da Direção da Divisão de Processos Técnicos da Biblioteca Central. Bibliotecária responsável Paula Schoenfeldt Patta CRB 10/1728.

Declaro, OLAWANDE OLAGOKE, para os devidos fins e sob as penas da lei, que a pesquisa constante neste trabalho de conclusão de curso (Tese) foi por mim elaborada e que as informações necessárias objeto de consulta em literatura e outras fontes estão devidamente referenciadas. Declaro, ainda, que este trabalho ou parte dele não foi apresentado anteriormente para obtenção de qualquer outro grau acadêmico, estando ciente de que a inveracidade da presente declaração poderá resultar na anulação da titulação pela Universidade, entre outras consequências legais.

DEDICATION

To El-Roi.

ACKNOWLEDGEMENTS.

I am a recipient of the 2017 CNPq-TWAS Postgraduate Fellowship (FR number: 3240299312). The combined effort of both bodies has added one more shining light to the expanding network of erudite scientists that are creating innovative solutions for Africa by Africans.

The JBT. Rocha Biochemical Toxicology laboratory headed by Prof. Dr. João B.T Rocha gave me a unique platform to experience science across cultural boundaries. I thank the professor and my colleagues for this beautiful experience. I have seen further because my teachers lent shoulders to stand on; some were Professors, others were students like me, there were also cleaners who ensured a safe environment for our research and learning activities. Callused hand by callused hand, it has taken a whole orchestra to produce the symphony that would now be called my doctoral thesis.

The love of family and friends gives me strength in my pursuit of meaning.

“Nobody realises that some people expend tremendous amount of energy merely to be normal”.

Albert Camus

RESUMO

Modelagem do fenótipo de diabetes em *Nauphoeta cinerea* usando estreptozotocina: Foco no metabolismo da glicose no cérebro.

Autor: Olawande Chinedu Olagoke

Orientador: João Batista Teixeira da Rocha

O cérebro é altamente dependente do catabolismo de glicose adequado, mas as mudanças no transporte de glicose no cérebro são bem documentadas em condições hiperglicêmicas. Evidências recentes de "memória hiperglicêmica" sugerem ainda que a exposição crônica à hiperglicemia pode predispor a alterações deletérias, mesmo depois que os níveis glicêmicos normais são restaurados. Portanto, é importante não apenas tentar manter os níveis de glicose circulante dentro da faixa normal, mas também evitar as complicações duradouras causadas pela hiperglicemia crônica. No final do século 20, modelos de insetos (como *Drosophila melanogaster*) começaram a ser considerados ferramentas importantes no estudo de patologias humanas relacionadas à insulina. Baratas já se mostraram eficazes experimentais organismos para a pesquisa neurobiológica, portanto, aqui exploramos o metabolismo da energia do cérebro usando um conhecido agente alquilante - estreptozotocina - em *Nauphoeta cinerea*. Primeiro, elucidamos as alterações bioquímicas e moleculares resultantes da exposição aguda de baratas à estreptozotocina (1 dose de 74 nmol ou 740 nmol por g de massa corporal). A estreptozotocina causou um aumento na glicose, níveis de mRNA do transportador de glicose 1, substâncias reativas ao ácido tiobarbitúrico, atividade da glutatona S-transferase total e níveis de glutatona em homogêneos de cabeça. O glicogênio do corpo adiposo, o conteúdo de triglicerídeos na cabeça e a redução de MTT na cabeça foram diminuídos. Nossos resultados mostraram alterações induzidas por estreptozotocina no metabolismo da glicose em *N. cinerea*, e destacamos a conservação evolutiva de GLUT1 entre *N. cinerea* e outros insetos. Em segundo lugar, examinamos como a hiperglicemia induzida por estreptozotocina no CNS de *N. cinerea* afeta a homeostase redox e a expressão de genes relacionados à resposta inflamatória. Encontramos um aumento nos níveis de mRNA do fator de resposta de crescimento precoce (EGR) e reaper (genes alvo da via da quinase c-Jun N terminal); TOLL1 (gene alvo da via Toll / NF-κB); unpaired 3 (UPD 3) e supressor de sinalização de citocina em 36E Socs36E (ativador e gene alvo da via UPD3 / JAK / STAT); superóxido dismutase e catalase (antioxidantes primários) e GST *sigma*. Não houve diferença significativa na expressão de fator 1 relacionado a PDGF e VEGF (PVF1), peroxirredoxina (PRX), tioredoxina (TRX) e GST *delta*. Essas mudanças na sinalização relacionada à inflamação e na atividade das enzimas antioxidantes são semelhantes às mudanças observadas em roedores e humanos com hiperglicemia. Terceiro, mostramos modificações transcricionais que são semelhantes aos resultados de estudos de associação do genoma em mamíferos e moscas, especialmente a regulação positiva da 40S proteína ribossômica S6 e suas moléculas de sinalização. O tratamento de STZ com dose baixa desregulou mais genes do que o tratamento com dose alta, e houve uma taxa maior de regulação positiva do que regulação negativa. Também identificamos a via de sinalização de insulina putativa de *N. cinerea* e observamos uma diminuição na transcrição de componentes do Via PI3K / AKT, mas os genes alvo da cascata RAS, P38 e JNK MAPK foram regulados para cima. Os elementos estrutura-função também foram semelhantes entre os genes MAPK de *N. cinerea* e outros insetos. Juntos, esses dados demonstram que a barata *N. cinerea* pode ser utilizada no estudo das alterações metabólicas causadas pelo aumento dos níveis de glicose no cérebro.

Palavras-chave: *GLUT1*; Sinalização de insulina; Caminho JNK; Caminho TOLL/NF-κB; Caminho UPD3/JAK/STAT; antioxidantes; proteínas ribossômicas; RNA-seq; Análise de transcriptoma.

ABSTRACT

Diabetes phenotype modelling in *Nauphoeta cinerea* using streptozotocin: Focus on brain glucose metabolism.

Author: Olawande Chinedu Olagoke
Supervisor: João Batista Teixeira da Rocha

The brain is highly dependent on adequate glucose catabolism, but changes in brain glucose transport are well documented in hyperglycemic conditions. Recent evidence of "hyperglycemic memory" further suggests that chronic exposure to hyperglycemia may predispose to deleterious alteration even after normal glycemic levels are restored. Therefore, it is important not only to try to maintain circulating glucose levels within the normal range, but also to avoid the lasting complications caused by chronic hyperglycemia. At the end of the 20th century, insect models (such as *Drosophila melanogaster*) began to be considered as important tools in the study of insulin-related human pathologies. Cockroaches have already been shown to be effective experimental organisms for neurobiology research, therefore, we herein explore brain energy metabolism using a known alkylating agent – streptozotocin – in *Nauphoeta cinerea*. First, we elucidate the biochemical and molecular changes resulting from acute exposure of cockroaches to streptozotocin (1 dose of 74 nmol or 740 nmol per g of bodymass). Streptozotocin caused an increase in glucose, mRNA levels of glucose transporter 1, thiobarbituric acid reactive substances, total glutathione *S-transferase* activity, and glutathione levels in head homogenates. Fat body glycogen, head triglyceride content and the reduction of MTT in head homogenates were diminished. Our results showed streptozotocin-induced alterations in the metabolism of glucose in *N. cinerea*, and we also highlight the evolutionary conservation of GLUT1 between *N. cinerea* and other insects. Secondly, we examined how streptozotocin-induced hyperglycemia in the CNS of *N. Cinerea* affects redox homeostasis and the expression of genes related to inflammatory response. We found an increase in mRNA levels of early growth response factor (EGR) and reaper (target genes of the c-Jun N terminal kinase pathway); TOLL1 (target gene of the Toll/NF-κB pathway); unpaired 3 (UPD 3) and suppressor of cytokine signaling at 36E Socs36E (activator and target gene of the UPD3/JAK/STAT pathway); superoxide dismutase and catalase (primary antioxidants) and GST sigma. There was no significant difference in the expression of PDGF -and VEGF -related factor 1 (PVF1), peroxiredoxin (PRX), thioredoxin (TRX) and GST delta. These changes in inflammation-related signaling and antioxidant enzyme activity are similar to changes observed in rodents and humans with hyperglycemia. Third, we showed transcriptional modifications that are similar to results of genome wide association studies in mammals and flies, especially the up regulation of the 40S ribosomal protein S6 and its signaling molecules. Low dose STZ treatment deregulated more genes than the high dose treatment, and there was a higher rate of up regulation than down regulation. We also identified the putative insulin signaling pathway of *N. cinerea* and observed a decrease in the transcription of components of the PI3K/AKT pathway, but target genes of the RAS, P38 and JNK MAPK cascade were up regulated. Structure-function elements were also similar between the MAPK genes of *N. cinerea* and other insects. Together, these data demonstrate that the cockroach *N. cinerea* can be used in the study of metabolic alterations caused by increased brain glucose levels.

Keywords: *GLUT1*; Insulin signaling; JNK pathway; TOLL/NF-κB pathway; UPD3/JAK/STAT pathway; antioxidants; ribosomal proteins; RNA-seq; Transcriptome analysis.

TABLE OF CONTENT.

Title page	i
Approval page	iii
Catalogue Page	iv
Dedication	v
Acknowledgements	vi
Epigraph	vii
Resumo	viii
Abstract	ix
Table of content	x
1. INTRODUCTION	11
1.1.Insect carbohydrate digestion and metabolism	11
1.2.Brain glucose transport and autoregulation	12
1.3.Brain Insulin signalling	13
1.4.Clinical and experimental diabetes mellitus phenotypes	14
1.5.Glucose analogues and diabetes mellitus modelling	15
1.6.Streptozotocin toxicity	15
1.7.Insect models of diabetes mellitus	16
1.8. <i>Nauphoeta cinerea</i> (Lobster cockroach)	17
2. JUSTIFICATION	18
3. OBJECTIVE	18
4. MATERIALS AND METHODS	20
5. SCIENTIFIC ARTICLES	20
5.1.Article 1: Streptozotocin induces brain glucose metabolic changes and alters glucose transporter expression in the Lobster cockroach; <i>Nauphoeta cinerea</i>	20
5.2.Article 2: Streptozotocin activates inflammation-associated signalling and antioxidant response in the lobster cockroach; <i>Nauphoeta cinerea</i>	34
5.3.Manuscript 1: Ribosomal protein associated transcriptional response to streptozotocin treatment in <i>Nauphoeta cinerea</i>	69
5.4.Manuscript 2: Disruption of PI3K/AKT and MAPK insulin signalling in streptozotocin-treated <i>Nauphoeta cinerea</i>	107
6. DISCUSSION	130
7. CONCLUSION	132
8. PERSPECTIVES	133
9. REFERENCES	133

1. INTRODUCTION

1.1 INSECT CARBOHYDRATE DIGESTION AND METABOLISM

The carbohydrate digesting enzyme that an insect harnesses depends on its diet and starch is the most abundant carbohydrate ingested by plant-eating insects. The inner glycosidic linkages of starch are broken down to dextrans by α -amylase which is secreted by the salivary glands and mid-gut epithelium. α -Glucosidase and oligo-1,6-glucosidase then digests dextrin to glucose [1–3]. The molecular basis of glucose transport from gut to target cells has not been fully elucidated in insects, but it is widely agreed that the glucose absorbed by facilitated diffusion from the mid-gut is converted to trehalose and glycogen for storage mainly in the hemolymph and fat body respectively [4], these molecules are subsequently broken down for tissue use like brain energy metabolism.

Trehalose (α -D-glucopyranosyl- α -D-glucopyranoside) is mainly synthesized in the fat body (also in the gut and muscle cells) from two molecules of glucose. Briefly, hexokinase catalyzes the conversion of glucose to glucose 6-phosphate (G6-P), which is converted to uridine diphosphate glucose (UDPG) in a series of reactions. Trehalose 6-phosphate synthetase then catalyses the conversion of UDPG and G 6-P to trehalose 6-phosphate, from which the phosphate group is removed by the corresponding synthetase to form trehalose. Free trehalose inhibits the synthetase from forming more trehalose when trehalose levels are high in hemolymph, thereby enabling glycogen synthetase to act on UDPG to form glycogen. When hemolymph glucose levels are low, hypertrehalosemic hormone (HTH) and cyclic adenosine monophosphate (cAMP) activates glycogen phosphorylase b to phosphorylase a, which cleaves glucose molecules from the glycogen stores [5–7] (Figure 1).

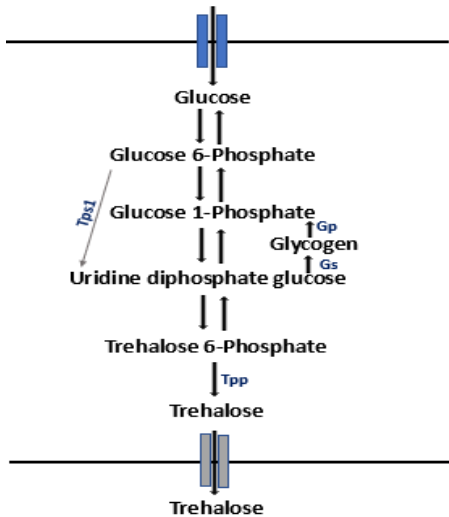


Figure 1: Trehalose and glycogen synthesis in insect fat body.

Tps1: Trehalose phosphate synthase, Gp: Glycogen phosphorylase, Gs: Glycogen synthase, Tpp: Trehalose phosphate phosphatase.

1.2 BRAIN GLUCOSE TRANSPORT AND AUTOREGULATION

The understanding of brain glucose uptake is important because the brain has little or no nutrient store [8], and is anatomically walled off from systemic circulation by functional barriers [9,10]. In flies, glucose sensing by glucose transporter 1 (glut 1) in insulin producing cells (IPCs) of the brain [11] activates glibenclamide – a K_{ATP} channel activator – whose depolarization causes calcium (Ca^{2+}) entry and action potential that induces insulin-like peptide (*ILP*) release from IPCs [12,13] (Figure 2). This is similar to glucose sensing by glut 2 on β cells of mammalian pancreatic islets [14,15], which causes glycolysis and mitochondrial ATP release that activates K_{ATP} channels to depolarize the β cell membrane and initiate calcium (Ca^{2+}) entry and insulin release [16]. While glucose entry into peripheral tissues is largely dependent on *ILP*, the central nervous system (CNS) can absorb glucose simply via facilitated transport through glucose transporter 1 [17–19] – a carrier mediated transport protein marked by Michaelis-Menten kinetics [20,21].

The brain has auto regulatory capacity for glucose use [22] and conditions that affect this ability for self-regulation may disrupt normal brain function [23,24]. The *D. melanogaster* hemolymph-brain barrier (HBB) is crucial for protecting the brain from the fluctuations in solute concentrations that is reminiscent of the insect open circulatory system. [25–27]. At about the 17th embryonic stage, subperineurial glial cells (SPGs), perineurial glial cells (PGs) and a neural lamella form the drosophila HBB [28–30], a homologue of the vertebrate neurovascular unit (NVU). SPGs express SLC2A1 (glucose transporter 1), amongst other transporters of the solute carrier family (SLC) [31].

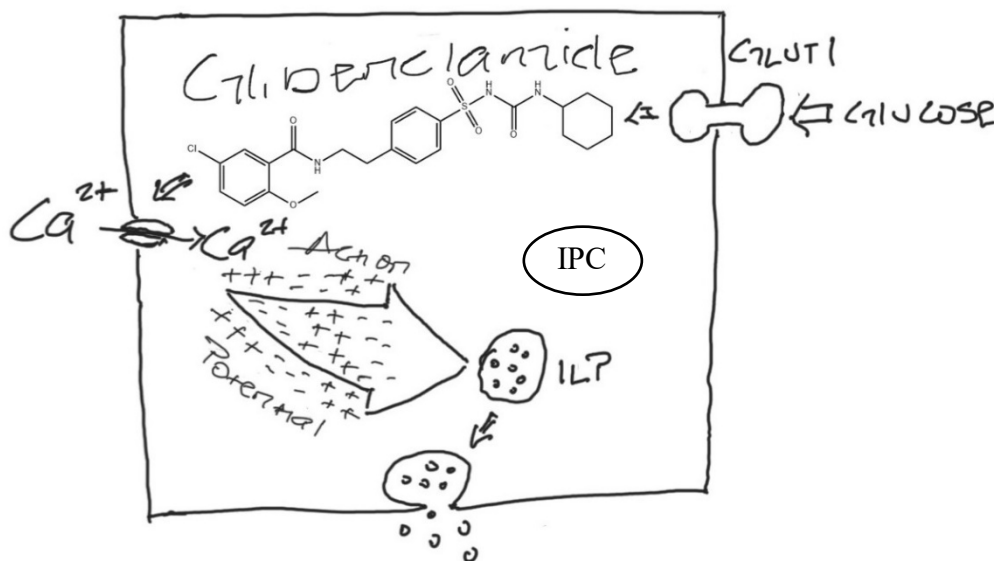


Figure 2: Illustration of insulin-like peptide (ILP) release from insulin producing cells (IPC) in insect brain.

1.3 BRAIN INSULIN SIGNALLING

The detection of insulin and insulin-like peptide in the brain of rodents [32] and insects [33] respectively have raised questions about the synthesis of these hormones in the brain. While it is known that insulin producing cells (IPCs) synthesize and store *ILP* (*ILP*) in the insect brain [34–37], reports vary from those who propose synthesis and storage of insulin in the rodent brain [19,38–42], to those who believe that insulin reaches the mammalian brain from the circulatory system [43–46]. Insulin like peptides are so called because of the similar amino acid sequence that they share with the mammalian insulin [47,48].

The *ILP/PI3K/AKT*, *RAS/MAPK* and *PKC/NF- κ B* pathways are the known mechanisms of action of insulin in the central nervous system of insects [49] (Figure 3), but the *ILP/PI3K/AKT* pathway is more emphasized as some researchers believe it is crucial for determining lifespan [50–52]. It shares evolutionary conservation among invertebrate phyla and with mammals [53,54], and it functions in both the CNS and PNS [55]. Insects differ in the number of *ILPs* that activate this *PI3K/AKT* pathway, for example *Drosophila melanogaster* has 8, *Bombyx mori* has 37, but only 1 has been delineated in *Locusta migratoria*. [36] [56] The pathway is known to be involved in homeostasis [57–59], neuroprotection [60–62] and is said to be neurotrophic [63–65], while there are speculations about the role of the pathway in brain glucose uptake [66–68]. It is therefore not surprising that impaired brain insulin signalling has

been linked with neurodegenerative disorders like Alzheimer's disease [69,70].

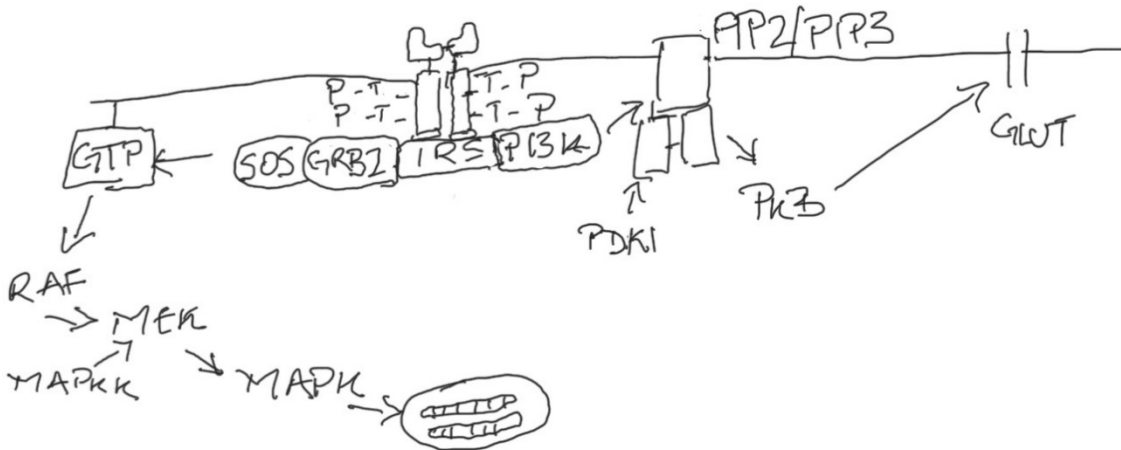


Figure 3: Illustration of PI3K/PKB and MAPK insulin signalling pathways.

1.4 CLINICAL AND EXPERIMENTAL DIABETES MELLITUS PHENOTYPES

Defect in insulin secretion and/or insulin action is known to predispose subjects to a wide range of metabolic disorders termed diabetes mellitus (DM) whose hallmark is hyperglycaemia. The American Diabetes Association has earmarked four general categories of DM, including: Type 1 (insulin insufficiency due to autoimmune β -cell destruction); Type 2 (insulin resistance leading to destruction of β -cells); Gestational DM (diagnosed in the 2nd or 3rd trimester in a previously non-diabetic individual); and Specific types of DM due to other causes (drug/chemical induced DM, exocrine pancreatic diseases etc.) [71]. However, many subjects with diabetes fit into more than one classification or may alternate between euglycemic and hyperglycaemic state, depending on the underlying aetiology. Indeed, an accelerator hypothesis positing that type 1 and type 2 diabetes are both disorders of insulin resistance in different genetic contexts is receiving wide spread consideration [72]. Consequently, effective treatment of hyperglycaemic conditions relies more on understanding the pathogenesis than the need to label the type of diabetes type label. This further makes it possible to model diabetes mellitus in vertebrates and invertebrates in a bid to expand prevailing understanding of the metabolic disorder and gain therapeutic advantage for patient care. This bench to bedside translation is predicated on the integration of clinical context with basic life sciences.

1.5 GLUCOSE ANALOGUES AND DIABETES MELLITUS MODELLING

Biochemical synthetic compounds like Alloxan and Streptozotocin (STZ) that are similar in structure with glucose are often used to mimic diabetes-like phenotypes in insects [73–75] and mammals [76,77]. STZ is an alkylating, natural glucosamine-nitrosourea compound that needs the expression of glucose transporter 2 for its cytotoxic effect on the mammalian pancreatic beta cells, [78]. DNA alkylation [79,80] and nicotinamide adenine dinucleotide (NAD⁺/NADH) depletion [81] are the known mechanisms of STZ toxicity, but there are questions about the role of *O*-GlcNAcase inhibition as a possible mechanism [82]. Consequently, diabetes mellitus phenotypes including insulin dysfunction, hyperglycaemia, polydipsia and polyuria have been replicated in rodent diabetes models using streptozotocin [83]. In insects, the toxicity of Alloxan increases superoxide production [84], as well as other markers of oxidative stress [85] while raising haemolymph glucose levels [86], making insects viable models for studying the pathophysiological mechanisms of metabolic diseases.

1.6 STREPTOZOTOCIN TOXICITY

Streptozotocin (Figure 4) isolated in the 1950s as an antibiotic from the soil bacterium *Streptomyces achromogenes*, and its selective toxicity to the pancreatic beta cells made it useful for modelling insulinitis and diabetes in animals, as well as treating pancreatic beta cell cancers in humans. General exposure to STZ during experimental procedures, manufacturing or the use of pharmaceutical products is via inhalation or contact to eyes and skin. With a half-life of ± 15 minutes, intravenous STZ injection is cleared from plasma in about 3 hours but metabolites remain in plasma for about 24 hours; and though STZ does not cross the blood brain barrier, its metabolites have been found in the cerebrospinal fluid [87]. The alkylating and strand cross-linking effect of STZ on DNA is known to inhibit DNA synthesis and activate poly ADP-ribosylation [79]. There are further reports of pyridine nucleotide and glyconeogenesis inhibition. Topically, STZ irritates human surfaces with which it comes in contact, and IV administration may cause hair loss, nausea, vomiting, and organ injury. STZ may be mutagenic, carcinogenic or teratogenic [87].

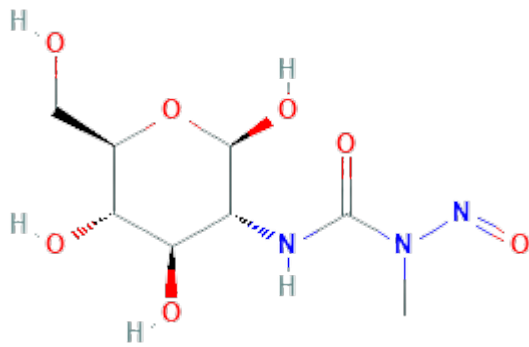


Figure 4: 2D chemical structure of streptozotocin (PubChem Identifier: CID 7067772).

1.7 INSECT MODELS OF DIABETES MELLITUS

The initial scepticism around the differences in carbohydrate metabolism between humans and insects hampered research in this field, but there are emerging evidences in the last two decades that insects can be viable models for diabetes. [88,89]. In addition, the mechanisms that shift carbohydrates between storage and circulation are similar across animal models [90]. The switch between insulin and glucagon in mammals is replicated in a plethora of insects that release insulin-like peptides (*ILPs*) and adipokinetic hormone (*AKH*) when circulating sugar levels are high and low respectively [91–94].

Albeit there are some known differences between the mammalian and insect carbohydrate homeostatic mechanisms: Trehalose – a non-reducing sugar – is the circulatory sugar in insects. Unlike mammals that transport carbohydrates mainly as glucose in blood, glucose levels are low and hardly detectable in insect hemolymph [6,95]. This implies that such complications as non-specific protein glycation that arise from high levels of reducing sugar (glucose) in mammalian models cannot be naturally mirrored in insects. Furthermore, It is yet unclear whether (and how) the circulatory sugars – trehalose – is regulated in insects; while some argue that the switch between trehalose and glycogen synthesis helps to maintain homeostasis, other researchers opine that the non-reducing nature of trehalose and the need for fast energy source for flights makes it unnecessary to regulate circulatory sugars in insects [96–98].

Raised levels of regulatory sugars, reduced size and delayed development have been recorded in *Drosophila* after ablation of insulin producing cells (*IPCs*) in the brain, mimicking the mammalian model of type 1 diabetes [35,36,99]. Also, known mammalian diabetes diagnostic tests like oral glucose tolerance test (*OGTT*) were further used to show increased

postprandial sugar levels in circulation after fast, as well as, increased sugar clearance time from circulation; both of which were rescinded by injecting the flies with bovine insulin [100]. These ‘diabetic’ phenotypes are reproduced when drosophila *ILPs* (*dILP* 1-5) were removed by genomic deletion [101] and further experiments confirmed that *dILP* 2,3 and 5 are involved in regulating sugars in circulation [47] suggesting that IPCs are homologous to mammalian β cells of the islets of pancreas.

An OGTT that shows prolonged glucose clearance time despite normal insulin levels is typical of type II diabetes / insulin resistance. Researchers have shown increased levels of circulating sugars (glucose and trehalose), RNA expression levels of *ILP* 2, 3, 5 and circulating *ILP2* in drosophila larvae exposed to high sugar diet (HSD) [100,102]. Subsequently, exogenous administration of insulin in these HSD fed flies decreased phospho-*AKT* expression (probably due to reduced sensitivity for insulin signalling), as well as, increased triglyceride (TG) and free fatty acid (FFA) content [103,104].

1.8 *Nauphoeta cinerea* (LOBSTER COCKROACH)

The exclusive specie of the *Nauphoeta* genus, *Nauphoeta cinerea* belongs to the family of cockroaches – Blaberidae and originates from North Africa. Its colour ranges from mottled brown to alate (*Invasive Species and Human Health - Google Books*). *Nauphoeta* reproduces either sexually or asexually (facultative parthenogenesis), depending on availability of the male [106] but lifespan and total wellbeing is said to diminish in the parthenogenetic offspring [107]. A little over 30 eggs are incubated in othecas (contained in a brood sac) for about a month, after which the otheca is extruded but hangs on to the female till nymphs emerge from it – making the reproductive process seem ovoviviparous, in contrast to the oviparous nature of other cockroaches [108]. In about 72 days; 7 moults [for males] or 85 days; 8 moults [for females], the nymph reach maturity and have a lifespan of about a year (Figure 5). Observations from our laboratory have shown that *Nauphoeta* cannot fly, can survive for weeks without nutrition, can feed on paper-made materials, and continues to live for between 8 to 12 hours after decapitation. This might be due to some brain parts being located within the body segments as depicted by [109].



Figure 5: Dorsal view of *N. cinerea* showing moult of A. nymph, B. adult and C. Fully formed adult. Adapted from Afolabi, 2019.

2. JUSTIFICATION

The need to develop non mammalian models of biomedical research has been well elucidated, but models must adequately reflect the conditions that they attempt to mimic. Therefore, the evolutionary conservation of glucose transport into the brain, as well as insulin-related signalling from insects to mammals makes it possible to model glucose metabolic diseases in insects. Importantly, several gaps exist in our knowledge of brain specific hyperglycaemic effects and recent evidence of “hyperglycaemic memory” imply that the deleterious effects of increased circulatory sugars may persist even after euglycaemic state is achieved.

It is therefore important to use every available method to broaden our knowledge of glucose-related modifications to brain energy metabolism, in a bid to gain therapeutic advantage and improve human standard of living, in line with goal 3 of the United Nations sustainable development goals – good health and wellbeing.

3. OBJECTIVE

3.1 GENERAL OBJECTIVE

The discovery of insulin in the 1920s by Banting and Best gave hope to the treatment of the erstwhile fatal diabetes mellitus. Ever since, efforts have been made to better understand the metabolic disease and more efficiently manage its presentation. Hence, target 3.4 of the United Nations sustainable development goals is “to reduce premature mortality from non-

communicable diseases by a third by 2030 relative to 2015 levels”. We therefore set out to expand the understanding of brain energy metabolism by using a known alkylating agent – streptozotocin – to possibly derange carbohydrate metabolic processes in *N. cinerea*.

Obviously, insects differ from humans and care must be taken in extrapolating results, but even humans differ in their genetic and cellular response to perturbations. Furthermore, the possible conservation of diabetes-related changes from insects to mammals validates the attempts to model human metabolic diseases in insects. Here, we employed biochemical, molecular and bioinformatics methods to attempt our goal.

3.2 SPECIFIC OBJECTIVES

- To elucidate the biochemical and molecular adjustments that follow alterations in brain glucose level, using streptozotocin treatment in *N. cinerea*. [Study I].
- To demonstrate the relationship that hyperglycaemia may have with redox and inflammation-like responses in *N. cinerea* [Study II].
- To evaluate the transcriptional profile of streptozotocin-treated *N. cinerea* nymphs. [Study III]
- To illustrate the putative *N. cinerea* insulin-signalling pathway and demonstrate evolutionary conservation of structure-function apparatus with other animals [Study IV].

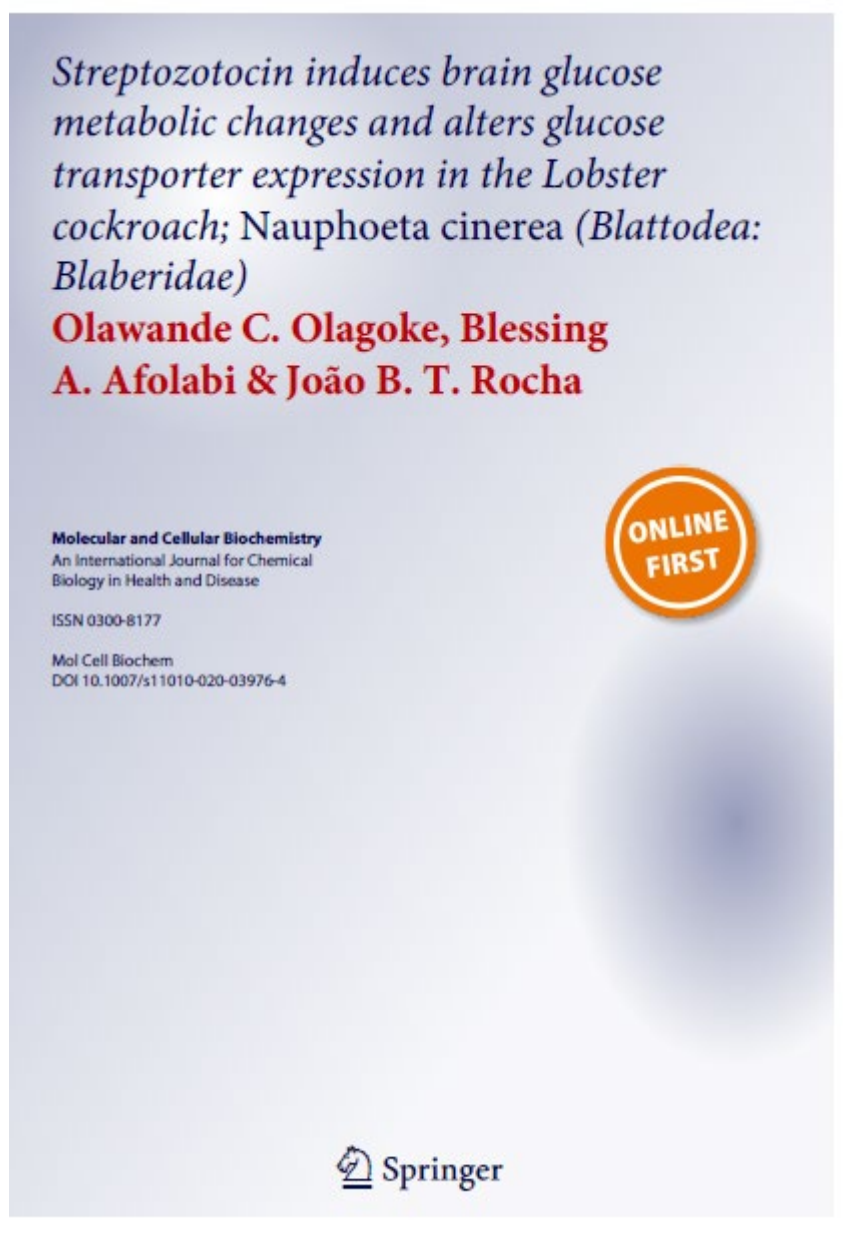
4. MATERIALS AND METHODS

The relevant methodology has been integrated into scientific articles in section 5.

5. SCIENTIFIC ARTICLES

5.1. Article 1: Streptozotocin induces brain glucose metabolic changes and alters glucose transporter expression in the Lobster cockroach; *Nauphoeta cinerea* (Blattodea: Blaberidae).

<https://doi.org/10.1007/s11010-020-03976-4>





Streptozotocin induces brain glucose metabolic changes and alters glucose transporter expression in the Lobster cockroach; *Nauphoeta cinerea* (Blattodea: Blaberidae)

Olawande C. Olagoke¹ · Blessing A. Afolabi² · João B. T. Rocha¹

Received: 27 May 2020 / Accepted: 6 November 2020
© Springer Science+Business Media, LLC, part of Springer Nature 2020

Abstract

The development of new models to study diabetes in invertebrates is important to ensure adherence to the 3R's principle and to expedite knowledge of the complex molecular events underlying glucose toxicity. Streptozotocin (STZ)—an alkylating and highly toxic agent that has tropism to mammalian beta cells—is used as a model of type 1 diabetes in rodents, but little is known about STZ effects in insects. Here, the cockroach; *Nauphoeta cinerea* was used to determine the acute toxicity of 74 and 740 nmol of STZ injection per cockroach. STZ increased the glucose content, mRNA expression of glucose transporter 1 (GLUT1) and markers of oxidative stress in the head. Fat body glycogen, insect survival, acetylcholinesterase activity, triglyceride content and viable cells in head homogenate were reduced, which may indicate a disruption in glucose utilization by the head and fat body of insects after injection of 74 and 740 nmol STZ per nymph. The glutathione *S*-transferase (GST) activity and reduced glutathione levels (GSH) were increased, possibly via activation of nuclear factor erythroid 2 related factor as a compensatory response against the increase in reactive oxygen species. Our data present the potential for metabolic disruption in *N. cinerea* by glucose analogues and opens paths for the study of brain energy metabolism in insects. We further phylogenetically demonstrated conservation between *N. cinerea* glucose transporter 1 and the GLUT of other insects in the Neoptera infra-class.

Keywords GLUT1 · Brain glucose · Fat body glycogen · MTT reduction · Oxidative stress · Insect phylogeny

Introduction

Insects and particularly *Drosophila melanogaster* are established models for toxicity testing [1–3], and they have been instrumental to decipher the molecular mechanisms associated with human pathologies [4, 5]. Recently, *Nauphoeta*

cinerea has been used to examine the toxicity of mercury [6, 7], chlorpyrifos [8], monosodium glutamate [9], vinylcyclohexane [10], and natural occurring toxins [11].

Streptozotocin (STZ) is glucosamine-nitrosourea compound that is structurally similar to glucose and was first isolated from the soil bacterium *Streptomyces achromogenes*. It enters the cells mainly via glucose transporter 2 (GLUT 2) and has a tropism to beta cells in mammals [12]. Two major intracellular mechanisms have been demonstrated to be responsible for its toxicity in eukaryotic cells: DNA alkylation [13] and nicotinamide adenine dinucleotide (NAD⁺/NADH) depletion via Poly (ADP-ribose) polymerase [14], however, little is known about the transport and toxicity of STZ in insects. Indeed, the toxicity of STZ has been rarely studied in insects. In two in vitro studies, the clastogenic activity of STZ in mosquito cells was demonstrated [15, 16]. However, the effects of STZ after in vivo administration in insects has not been reported.

Impaired insulin secretion and signaling, with increased circulatory sugar is the hallmark of type 1 diabetes [17].

Electronic supplementary material The online version of this article (<https://doi.org/10.1007/s11010-020-03976-4>) contains supplementary material, which is available to authorized users.

✉ Olawande C. Olagoke
olagokeco@gmail.com; olawande.olagoke@acad.ufsm.br

✉ João B. T. Rocha
jbrocha@yahoo.com.br

¹ Departamento de Bioquímica e Biologia Molecular, Centro de Ciências Naturais e Exatas (CCNE), Universidade Federal de Santa Maria, Santa Maria, RS 97105-900, Brazil

² Department of Biochemistry, Bowen University, Iwo, Osun State, Nigeria

Despite initial skepticism about the application of insect physiology to the understanding of glucose metabolic disorders, considerable conservation of analogous metabolic pathways, including sugar energy metabolism has been outlined between mammals and insects in the last 2 decades [18], and is further confirmed by alignment of the protein sequences of glucose metabolism genes, as well as the depiction of evolutionary history as a phylogenetic tree [19, 20]. Insect diabetes models have been induced by several methods including exposure to high sugar diet [21], high fat diet [22], the use of biosynthetic glucose analogues like alloxan [23, 24] and the development of Insulin receptor mutants [25], among others.

The discovery of insulin-like peptide in invertebrates [26, 27] and the similarity of their function to the mammalian insulin receptor [28] has helped researchers to probe into the usefulness of *D. melanogaster* as a model for studying Diabetes [29, 30]. Ablation of insulin producing cells in *D. melanogaster* creates phenotypes similar to mammalian beta cell damage, namely; reduced size and delayed development [31], which are further substantiated by other studies reporting a rise in levels of circulating sugars [32] and slower sugar clearance after fasting and feeding flies with glucose solution (oral glucose tolerance test) [33]. These studies culminated in the knowledge that circulating sugar levels in flies are regulated by *ilp 2, 3 and 5* [34], thereby paving new paths for specific application of *Drosophila* in screening genes that genome wide association studies have earmarked as been involved in glucose toxicity [35, 36].

Though *D. melanogaster* has been instrumental to study toxicity mechanisms and the disruption of glucose metabolism [24], the large size of cockroaches over flies provides an easy-to-handle model in terms of administration routes and sources of tissues to be studied. We hereby seek to explore the possible disruption of glucose homeostasis in the lobster cockroach, as has been recorded in the mammalian and *D. melanogaster* models of type 1 diabetes. Upon absorption from the midgut, insects convert glucose to trehalose that circulates in the hemolymph, and glycogen for storage in the fat body [37]. Trehalose is readily hydrolyzed to two molecules of glucose for use by muscles and other tissues [38], and glucose use by eukaryotic cells have been shown to be more efficient than harnessing other energy-yielding molecules [39, 40]. Data about alterations in insect brain glucose metabolism are scarce in literature, particularly, after the administration of the toxin STZ, which is extensively used in rodents to study diabetes and neuropathologies [41, 42].

In view of the necessity of adhering to the 3R's principle regarding the use of vertebrates in biomedical research [43], and to develop additional models in insects bigger than flies, we herein explored brain energy metabolism in *N. cinerea*, using STZ as a model. Furthermore, the potential for facultative parthenogenesis in *N. cinerea* [44] makes it a potential

useful tool for subsequently investigating the genetic basis of degenerative diseases in invertebrates. In *D. melanogaster* models of diet-induced diabetes, an increase in markers of oxidative stress has been reported [21], thus, in addition to determining glucose in the head and glycogen in the fat body, we also investigated markers of oxidative stress in the head of cockroach nymphs. We further examined if *N. cinerea* have similar need for glucose transporter 1 (GLUT1) in the brain like *D. melanogaster* and mammals [45, 46] by identifying for the first time the GLUT1 of *N. cinerea*, estimating the expression of the carrier protein in the head of the cockroaches and phylogenetically demonstrating conservation between *N. cinerea* glucose transporter 1 and the GLUT of other insects in the Neoptera infra-class.

Materials and methods

Chemicals

All chemicals used for these procedures were purchased from Sigma Aldrich (St Louis, MO, USA), except where otherwise stated.

Insect stock

Lobster cockroaches (*N. cinerea*) were obtained from Departamento de Bioquímica e Biologia Molecular, Centro de Ciências Naturais e Exatas (CCNE), Universidade Federal de Santa Maria, Brasil. Nymphs were acclimatized in translucent boxes (21.5 cm × 21.5 cm × 8.2 cm; 2.5 L) for a week, before treatment. Temperature (24 ± 3 °C; mean set temperature and the minimum and maximal recorded temperature during the period of the experiments), humidity (57–75%) and light/dark cycle (12h) were controlled, and insects had access to water and food (composed as shown in Table S1) ad libitum.

Experimental procedure

1440 male and female nymphs weighing between 0.25 and 0.30 g were randomly allotted to a triplicate of four (4) groups of sixty (60) cockroaches each: intact control (not injected), sham injected [20 µl 0.8% NaCl/nymph], streptozotocin treated [20 µl of 74 nmol STZ injection/nymph and 20 µl of 740 nmol STZ injection/nymph]; and monitored for three (3) and seven (7) days, respectively. Streptozotocin was dissolved in normal saline (0.8% NaCl) and injected into the second right dorsal thoracic segment of each nymph. The cockroaches were then subjected to survival analyses, biochemical assays and a gene expression study.

Prior to this experiment, we ran a dose- and time-response pilot study to determine the effective doses and test duration

that are below the LD50 of STZ in *N. cinerea* nymphs, similar to a previous experiment in *Vespa orientalis* and *Manduca sexta* [47, 48]. In the pilot experiments, we injected 0, 74, 740 or 7400 nmol STZ (dissolved in 20 μ l 0.8% NaCl v/v nymph) into the second right dorsal thoracic segment of each nymph and they were observed for 1, 3, 7, 14 and 21 days. In the group treated with the highest dose of STZ, half of the insects died within 1 day. Therefore, the doses of 74 and 740 nmol STZ were selected for the biochemical study. Furthermore, we only found changes in glucose levels after 3 and 7 days, therefore we excluded the groups that were monitored for 1, 14 and 21 days in the biochemical study (data not shown).

Tissue preparation

Cockroaches were anaesthetized on dry ice before head and fat body excision. Heads were homogenized (100 mg Head to 1 ml 0.1 M phosphate buffer, pH 7.4) and centrifuged at 13,000 RPM for 10 min at 4 °C. The supernatant was used for protein measurement (read at 280 nm using NanoDrop 2000 supplied by Thermo Fisher Scientific Inc, USA), glucose quantification and other biochemical assays (using SpectraMax plate reader supplied by Molecular Devices, USA).

Fat body for glycogen assay was collected in test tubes placed in dry ice; dried at 100 °C for 10 min; digested with 500 μ l 30% KOH for 10 min, and precipitated with 1 ml ethanol and 50 μ l Na₂SO₄. The sample was centrifuged at 6000 RPM for 10 min; supernatant was discarded; residue was washed with 1 ml ethanol, centrifuged, dried and dissolved in 1 ml deionized water [49].

Insect body mass and survival profile

Insect mass was measured at the beginning and end of the treatment period using an electronic weighing balance (AUW-D series, supplied by Shimadzu Co., Japan) and results were expressed in milligrams (mg). The beginning of the experiment is reported as day 0 and the end of the experiment is reported as day 3 and day 7, respectively. We did an initial investigation to determine the gross toxicity to cockroaches after injecting 74 and 740 nmol of STZ/cockroach by counting the number of dead nymphs in each group every day and showing the results as percentage survival per sixty (60) cockroaches.

Head glucose content and fat body glycogen estimation

Head glucose was estimated from head homogenate using a commercial glucose monoreagent kit (supplied by Bioclin, Brasil) that utilizes glucose oxidase. The reaction mixture

contained 2 μ l sample and 200 μ l of glucose oxidase (color reagent), according to the manufacturer's protocol.

Glycogen was measured in the fat body by modifying the method of Dubois et al. [50]. 80% phenol and 98.5% H₂SO₄ were added to the solution in the ratio 1:40:100. Special care was taken to gently add the H₂SO₄ to the side of the tube slanted in ice. The setup was left to stand for 10 min at 25–30 °C and then shaken gently. The resultant orange-yellow color was read at 490 nm. Distilled water was used as blank and glycogen for standard curve.

Acetylcholine esterase (AChE) activity

AChE activity was measured by quantifying thiocholine production from AChE hydrolysis [51]. The wells contained 20 μ l 0.1 M phosphate buffer (pH 7.4), 40 μ l sample (0.8 mg/ml protein), 100 μ l distilled water, 20 μ l 10 mM Ellman's reagent (DTNB), and 20 μ l 8 mM acetylthiocholine iodide. Absorbances were read at 412 nm for 30 min (30 s interval) and results expressed as μ mol thiocholine formed/min/mg protein.

Head triglyceride content

Triglycerides are hydrolyzed by lipoprotein lipase to form glycerol which is converted in a series of reactions to quinoneimine that absorbs light at 490 nm [52]. The assay was accomplished with Triglyceride liquiform kit supplied by Labtest, Brasil.

Estimation of thiobarbituric acid reactive substances (TBARS)

Thiobarbituric acid (TBA) reacts with malondialdehyde (MDA) to form a pink solution that absorbs light at 532 nm as illustrated by [53, 54]. 200 μ l of stock reagent [10% trichloroacetic acid (TCA) and 0.75% TBA in the ratio 1:1] was incubated in a water bath with 100 μ l of sample (1 mg tissue: 5 μ l 0.1 M phosphate buffer, pH 7.4) at 95 °C for 60 min. The mixture was cooled and centrifuged at 8000 RPM for 10 min. Results were expressed as units/g tissue.

Analysis of cell viability by the MTT assay

Cell active dehydrogenase reduce the yellow, water soluble 3-(4,5-dimethylthiazol-2-yl)-2,5-diphenyl tetrazolium bromide dye (MTT) to form an insoluble purple formazan [55, 56]. And classically, MTT reduction has been used as colorimetric methodology to determine cell viable dehydrogenases [55]. 100 μ l sample (1 mg/ml protein) was added to 20 μ l 5 mg/ml MTT and incubated for 30 min at 37 °C. 200 μ l dimethyl sulfoxide (DMSO) was added to dissolve the formazan. The samples were incubated for 30 min, and

centrifuged at 3000 RPM for 20 min. The resultant purple formazan was read at 545 nm and 630 nm, the difference in absorbance at these wavelengths was expressed as units of formazan formed per mg protein.

Determination of glutathione-S-transferase (GST) activity

GST assay quantified the conjugation of 1-chloro-2,4-dinitrobenzene (CDNB) with glutathione (GSH) at 340 nm for 20 min (30 s interval) [57]. Wells had 135 μ l 0.1 M phosphate buffer (pH 6.5), 50 μ l sample (0.5 mg/ml protein), 100 μ l 3 mM GSH and 15 μ l 20 mM CDNB incubated for 5 min at 30 °C. Results were expressed as μ mol/min/mg protein.

Estimation of total thiol levels

Total thiol concentration is a measure of the colored products formed by the reaction of DTNB with sulfhydryl groups in the sample [51]. The reaction mixture contained 160 μ l.

0.1 M phosphate buffer (pH 7.4), 20 μ l sample (~ 10 mg/ml protein) and 20 μ l 10 mM DTNB read at 412 nm. Each sample was discounted from a blank containing the head homogenate without DTNB. Results were expressed as units/mg protein.

Identification of *Nauphoeta cinerea* glucose transporter 1 and primer design

Coding sequences of glucose transporter 1 gene, as well as, other normalizer genes for *Zootermopsis nevadensis*, *Blattella germanica*, *D. melanogaster* and *Cryptotermes secundus* were downloaded from the National center for biotechnology information (NCBI) platform (<https://www.ncbi.nlm.nih.gov/>) and used to query our *Nauphoeta* transcriptome [58]. We confirmed similarity of the matched *Nauphoeta* sequence with those of other insects using the NCBI basic local alignment search (Blast) tool—(<https://blast.ncbi.nlm.nih.gov/Blast.cgi>). Requisite *Nauphoeta* sequences were then used to design the primers of interest on the Primer3 input website (<https://primer3.ut.ee/>) and confirmed with OligoAnalyzer (<https://www.idtdna.com/page/tools/oligoanalyzer>).

Sequence alignment, phylogenetic analysis and domain prediction

Coding sequences of the genes of interest were downloaded from flybase (flybase.org), NCBI (<https://www.ncbi.nlm.nih.gov/>) and InsectBase (<https://www.insect-genome.com/>). They included at least one representative for the three Neoptera insect infraclass—Polyneoptera, Paraneoptera

and Holometabola. Multiple sequence alignments were built using MEGA5 [59] and aligned by MUSCLE [60]. Gap penalties were left at default values and poorly aligned positions were eliminated by block mapping and gathering with entropy (NGphylogeny.fr). The sequences were used to build the required phylogenetic tree by neighbor joining method, with bootstrap branch support performed 100 times and branch length (which is synonymous to evolutionary distance) computed by Poisson correction method.

Real-time polymerase chain reaction

Total RNA from head of nymphs was isolated as described in the Trizol™ reagent protocol (ThermoFisher scientific, USA). DNase treatment (Promega Corp, USA) was used to ensure purity of the samples, and quality of the isolated RNA was ascertained by spectrophotometry (using Nanodrop™ 2000 at 260/280 nm) and agarose gel electrophoresis. Reverse transcription of 1 μ g total RNA was performed using GoScript™ protocol (Promega Corp, USA) with a T100™ thermal cycler (BIO-RAD, China). Real-time PCR was carried out using a QuantStudio 3 RT-qPCR system (ThermoFisher scientific, USA). Each well contained 10 μ l cDNA with 10 μ l reaction mix comprising 0.4 μ l 0.2 μ M primers (forward and reverse), 1 X buffer, 0.2 mM dNTP, 2 mM MgCl₂ 0.1 X SYBR green and 0.25 U taq polymerase, made up with deionized water. The cycling procedure consisted of: a hold stage at 94 °C for 5 min; a PCR stage with 1 cycle of 94 °C for 15 s and 40 cycles of 94 °C for 15 s, 60 °C for 10 s and 72 °C for 30 s; and a melt curve stage with 1 cycle of 94 °C for 10 s, 55 °C for 1 min and 94 °C for 15 s. The efficiency of each primer to bind to its target gene was evaluated using pools from all samples for RT-qPCR and analysing the results with the QuantStudio™ design and analysis software. Details of primers used are: GLUT1 sense AAATATGGACACCGGAGAG, antisense TGCCCCGGAAGTGAATATAG; Tubulin sense TTGCCA GTGATGAGTTGCTC, antisense AGCATGTACCAAGGG CAGTT; TBP sense GGTGCGAATGTGGAGTACAG, antisense TAGTGGCTCCAGTGCAAGTC; GaPDH sense CCG TGTCCTGTTCCTAATG, antisense GTCCAAGATGCC CTCAGAG.

Statistical analysis

All data are expressed as mean \pm standard error of mean (SEM). Body mass and biochemical analyses data for days 3 and 7 were analyzed by two-way ANOVA (2 [3 and 7 Days] \times 4 [Control, 0.8% NaCl, 74 nmol STZ and 740 nmol STZ] factorial design). When appropriate, the Tukey's post hoc test ($P < 0.05$) was applied, using Graph Pad Prism 6. The data of cockroach survival were analyzed using the

Log-rank test for trend, and survival curves were significantly different at $P < 0.05$.

C_q values for RT-qPCR were generated with the QuantStudio™ design and analysis software and evaluated using the comparative C_T method. The ensuing data were analyzed with GraphPad Prism 6, using Kruskal–Wallis test, followed by Dunn's multiple comparisons test to determine results that were significantly different from intact control ($P < 0.05$).

Results

Insect body mass and survival profile

Injection of 740 nmol STZ significantly reduced the absolute mass of nymphs after 7 days (Table 1); moreover, both 74 and 740 nmol STZ reduced insect survival after 7 days, compared with the intact control and sham groups (Fig. 1).

STZ-induced increase in head glucose content

The head glucose content was increased in the nymphs treated with 740 nmol STZ on day 3 after injection (Fig. 2). By day 7, head glucose content of both the 74 and 740 nmol STZ treated groups were significantly increased compared with the intact control and sham injected groups (Fig. 2).

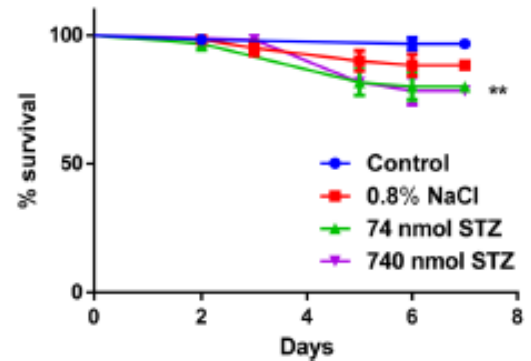


Fig. 1 Kaplan–Meier survival analysis of cockroaches after a single dose of 74 and 740 nmol STZ injection per cockroach. Log-rank test for trend reveals significant reduction in the survival of STZ treated groups compared with intact control and sham injected groups ($P = 0.0023$)

Fat body glycogen levels

Both 74 and 740 nmol STZ treatment significantly reduced fat body glycogen levels by day 3, and by day 7 (Fig. 3). However, the effect was much more evident at 7 days.

Acetylcholinesterase (AChE) activity

There was no significant difference in acetylcholinesterase activity 3 days after STZ treatment, but by day 7, AChE

Table 1 Body mass and body mass gain of cockroaches after a single administration of STZ

	Body mass (mg): Day 0	Body mass (mg): Day 3	Body mass gain (mg): Day 3–Day 0
<i>Body mass on day 3</i>			
Intact control	269 ± 2.5	273 ± 2.3	4 ± 2
0.8% NaCl	272 ± 2.8	273 ± 2.9	1 ± 0.5
74 nmol STZ	271 ± 2.6	271 ± 2.6	0 ± 0
740 nmol STZ	267 ± 2.4	265 ± 2.2	− 2 ± 1
	Body mass (mg): Day 0	Body mass (mg): Day 7	Body mass gain (mg): Day 7–Day 0
<i>Body mass on day 7</i>			
Intact control	269 ± 2.4	273 ± 2.3	4 ± 2
0.8% NaCl	266 ± 2.4	275 ± 2.3	9 ± 4.5
74 nmol STZ	270 ± 2.5	270 ± 2.8	0 ± 0
740 nmol STZ	270 ± 2.6	263 ± 2.3*	− 7 ± 3.5

Body mass was determined either 3 days after the injection (3 days monitoring groups) or after 7 days (7 days monitoring groups). Two-way ANOVA indicated a significant interaction between treatments × time [$F(3,430) = 3.39$; $P = 0.018$], mainly because 740 nmol STZ reduced the body mass of nymphs after 7 days of the STZ injection. All values are mean ± SEM ($N = 60$). Post hoc analysis by Tukey's test indicate a significant difference from intact control and sham groups (* $P < 0.0180$).

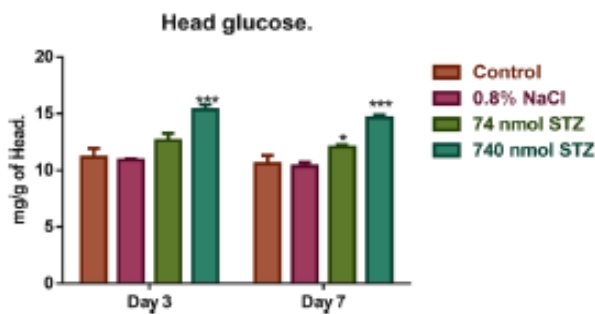


Fig. 2 Head glucose content 3 and 7 days after STZ treatment. Two-way ANOVA indicated a significant interaction between time and treatments [$F(3, 56)=65.0$; $P<0.0001$]. The interaction was significant because head glucose content was increased in STZ treated groups, when compared to intact control and saline-injected groups. Post hoc analysis indicated a significant increase in head glucose content after 740 nmol STZ on days 3 and 7, and a significant increase in group 74 nmol STZ on day 7. All values are mean \pm SEM. Post hoc analysis by Tukey's test indicated differences between groups: * and *** indicate a difference of at least $P<0.05$ between groups; * significant vs intact control; *** significant vs intact control, sham injected and 74 nmol STZ injection

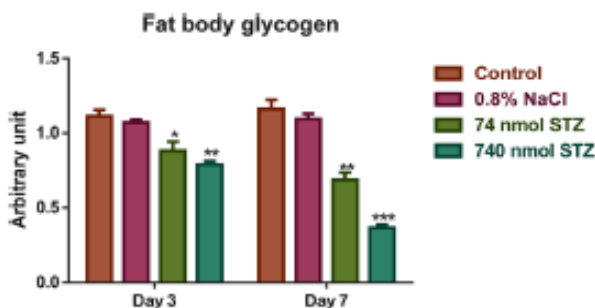


Fig. 3 Fat body glycogen content 3 and 7 days after STZ treatment. The fat body glycogen was reduced after a single injection of STZ both 3 and 7 days after the treatment. This was indicated by the significant interaction between treatments \times time [$F(3, 32)=13.4$; $P<0.0001$]. The greater decrease in glycogen content after 7 days of treatment further contributed to the significant interaction. All values are mean \pm SEM. Post hoc analysis by Tukey's test indicated differences between groups: *, ** and *** indicate a difference of at least $P<0.05$ between groups; * significant vs intact control; ** significant vs intact control and sham injected group; *** significant vs intact control, sham injected and 74 nmol STZ injection. Arbitrary units were derived from the change in absorbance (Δ) at 490 nm

activity in both STZ-treated groups was significantly reduced compared to intact control (Fig. 4).

Head triglyceride content

Triglyceride levels were not modified by a single injection of STZ (74 and 740 nmol) in relation to intact control groups after 3 days of the treatments. However by day 7,

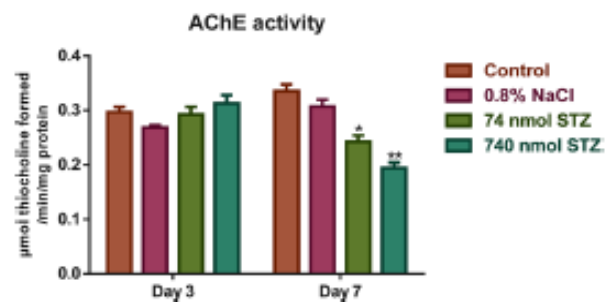


Fig. 4 Acetylcholinesterase activity in the head of cockroaches. In group of cockroaches that were monitored for 7 days, a single injection of STZ (74 and 740 nmol of STZ per cockroach) reduced AChE activity, as indicated by the significant interaction between treatments \times time [$F(3, 56)=21.0$; $P<0.0001$]. All values are mean \pm SEM. Post hoc analysis by Tukey's test indicated differences between groups: * and ** indicate a difference of at least $P<0.05$ between groups; * significant vs intact control; ** significant vs intact control and sham injected group

the triglyceride estimation from head of nymphs (Fig. 5) revealed a significant decrease of triglyceride levels in the 740 nmol STZ treated group compared with intact control.

STZ-induced oxidative stress and reduced cell viability

A single injection of 74 and 740 nmol STZ significantly increased the levels of thiobarbituric acid reactive substances (TBARS) in the head of cockroaches by day 7, but only the highest dose increased TBARS after 3 days (Fig. 6).

Head tissue viability (reduction of MTT) was decreased after 3 days only in the highest dose of STZ. But after 7 days, the reducing capacity of head homogenates was decreased in the two groups injected with STZ, when compared to intact control groups (Fig. 7).

Glutathione S-transferase activity and total thiol levels

GST activity (Fig. 8) was significantly increased in the 74 nmol STZ treated group by day 3. By day 7, both 74 and 740 nmol STZ groups had significant increase in GST activity compared with intact control and sham injected groups. Similarly, total thiol levels (Fig. 9) were significantly increased in the 74 and 740 nmol STZ treated groups on days 3 and 7 compared with intact control and sham injected groups.

Expression of head glucose transporter 1

Injection of STZ (74 and 740 nmol) upregulated the expression of solute carrier family 2, facilitated glucose transporter

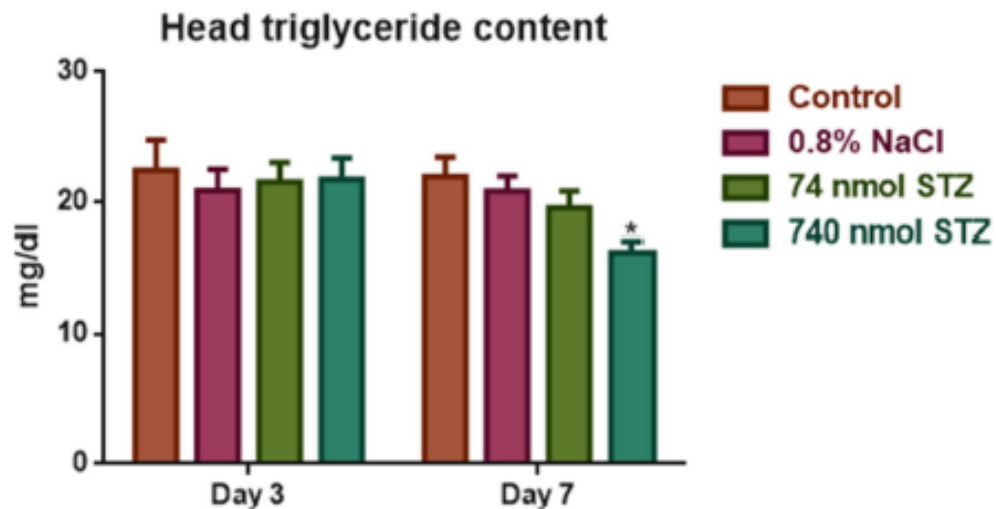


Fig. 5 Triglyceride content in head homogenate 3 and 7 days after a single injection of STZ treatment. Two-way ANOVA indicated a significant interaction between treatments \times time [$F(1, 7)=8.09$; $P=0.0249$]. All values are mean \pm SEM. Post hoc analysis by Tuk-

ey's test indicated differences between groups: * indicates a difference of at least $P < 0.05$ between groups. * significant vs intact control

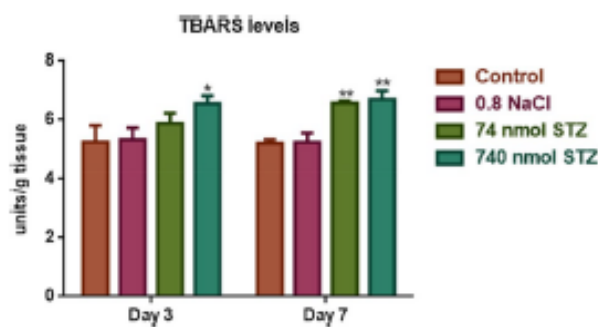


Fig. 6 Estimation of TBARS levels in head homogenate 3 and 7 days after STZ treatment. Two-way ANOVA indicated a significant main effect of streptozotocin treatment [$F(3, 16)=6.99$; $P=0.0032$] because STZ caused an increase in TBARS levels 3 (740 nmol STZ group) and 7 days (both STZ groups) after the injection. All values are mean \pm SEM. Post hoc analysis by Tukey's test indicated differences between groups: * and ** indicate a difference of at least $P < 0.05$ between groups. * significant vs intact control; ** significant vs intact control and sham injected group

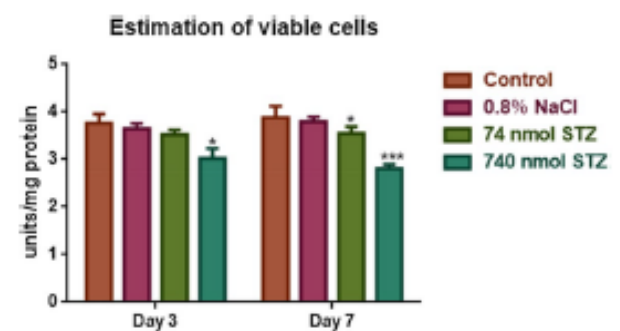


Fig. 7 Estimation of head homogenate reducing ability by MTT reduction. Two-way ANOVA indicated a significant interaction between treatments \times time [$F(3, 56)=13.7$; $P < 0.0001$]. All values are mean \pm SEM. Post hoc analysis by Tukey's test indicated differences between groups: * and *** indicate a difference of at least $P < 0.05$ between groups. * significant vs intact control; *** significant vs intact control, sham injected and 74 nmol STZ injection

member 1 (GLUT1) in the head of *N. cinerea* nymphs, 7 days after STZ administration [$H=19.85$, $P=0.0002$] (Fig. 10).

Phylogenetic relationship between *Nauphoeta cinerea* GLUT1 with the GLUT1 of other insects

In an attempt to examine the evolutionary conservation of our *Nauphoeta cinerea* GLUT1, we compared the GLUT1 sequence of *Nauphoeta cinerea* with those of seven other insects, including at least one representative of the three

subdivisions of the Neoptera infra-class; Polyneoptera, Paraneoptera and Holometabola (Fig. 11). The GLUT1 of *Nauphoeta cinerea* is in the same clade as the GLUT1 of *Zootermopsis nevadensis* and *Cryptotermes secundus*, which is supported by 99% of bootstrap analysis and suggests a common ancestry between *N. cinerea*, *Z. nevadensis* and *C. secundus*.

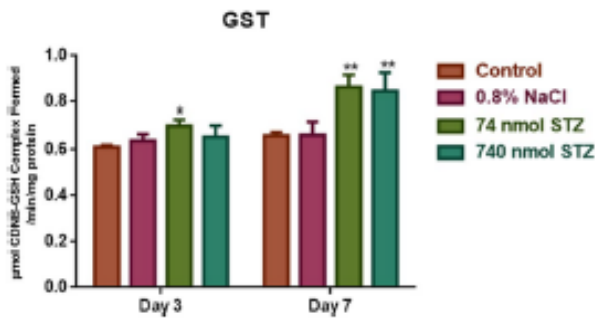


Fig. 8 Glutathione-S-transferase activity in head homogenate 3 and 7 days after STZ treatment. Two-way ANOVA indicated a significant interaction between treatments \times time [$F(3, 56) = 11.0$; $P < 0.0001$]. All values are mean \pm SEM. Post hoc analysis by Tukey's test indicated differences between groups: * and ** indicate a difference of at least $P < 0.05$ between groups. * significant vs intact control; ** significant vs intact control and sham injected group

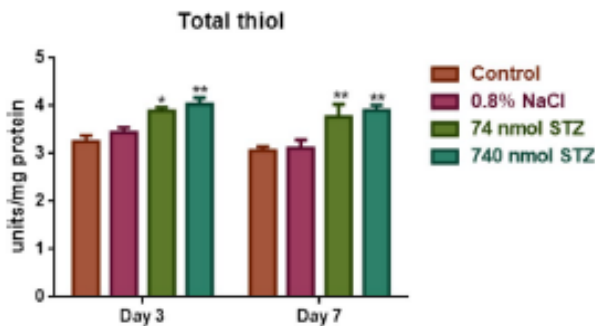


Fig. 9 Total thiol levels 3 and 7 days after STZ treatment. Two-way ANOVA indicated a significant interaction between treatments \times time [$F(1, 28) = 4.36$; $P = 0.0461$]. All values are mean \pm SEM. Post hoc analysis by Tukey's test indicated differences between groups: * and ** indicate a difference of at least $P < 0.05$ between groups. * significant vs intact control; ** significant vs intact control and sham injected group

Discussion

The points of evidence obtained here indicate *N. cinerea* as a viable model for studying glucose dyshomeostasis. Our data demonstrated an increase in head glucose content and oxidative stress of cockroaches injected with STZ, a known alkylating agent. We further delineated substantial reduction in fat body glycogen content, as well as, in acetylcholinesterase activity, triglyceride levels and dehydrogenases in head of STZ-injected nymphs. Therefore, we infer that STZ toxicity interferes with glucose utilization in the head and fat body of cockroaches, while reducing their post-exposure survival.

B cell cytotoxic agents like alloxan and streptozotocin are widely used to induce diabetes-like conditions

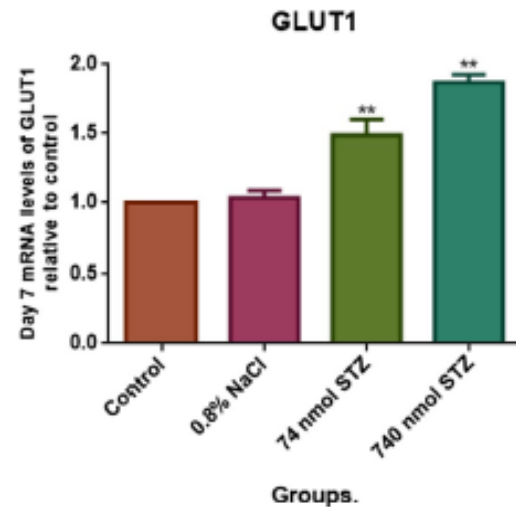


Fig. 10 Glucose transporter 1 (GLUT1) mRNA expression in the head of nymphs after 7 days of a single STZ injection. Kruskal-Wallis test followed by Dunn's multiple comparisons test showed significant upregulation of the glucose transporter 1 [$P = 0.0002$]. All values are mean \pm SEM. ** indicates a difference of at least $P < 0.05$ between groups. ** significant vs intact control and sham injected group

in vertebrates [41, 42], and there are a few reports about alloxan-induced hyperglycemia in *D. melanogaster* and *V. orientalis* [24, 47]. Furthermore, hyperglycemia has been shown to inhibit glycogen synthase activity in mice [61] and in adipocytes in vitro [62], thereby perturbing glycogen synthesis and storage [63]. These lend credence to our finding of reduced fat body glycogen content in STZ treated nymphs. Trehalogenesis in the nymph and trehalose hydrolysis in the central nervous system (CNS) are crucial for neural glucose uptake in insects [64]. We found increased head glucose content in the nymphs treated with STZ, which suggested an increase in trehalose hydrolysis, probably secondary to the reduced capacity for glycogen synthesis and storage in the fat body. These results are in accordance with data from mammals, where almost four-fold increase in brain glucose content of hyperglycemic rats [65, 66] and humans [67] have been reported.

Our data indicated a significant reduction in AChE activity of STZ-treated nymphs after 7 days. Acetylcholine is an important neurotransmitter in the insect CNS [68], STZ-induced hyperglycemic state may therefore be disrupting cholinergic neurotransmission in the lobster cockroach. The inhibition of cholinesterases and subsequent accumulation of acetylcholine is a known mechanism of xenobiotic toxicity to neural and peripheral cells [69, 70]. Hyperglycemia has also been associated with a decrease in AChE activity in rodents [71], and in the fly *D. melanogaster* [21]. This may suggest increased acetylcholine levels in the head of STZ treated cockroaches. STZ treatment also significantly

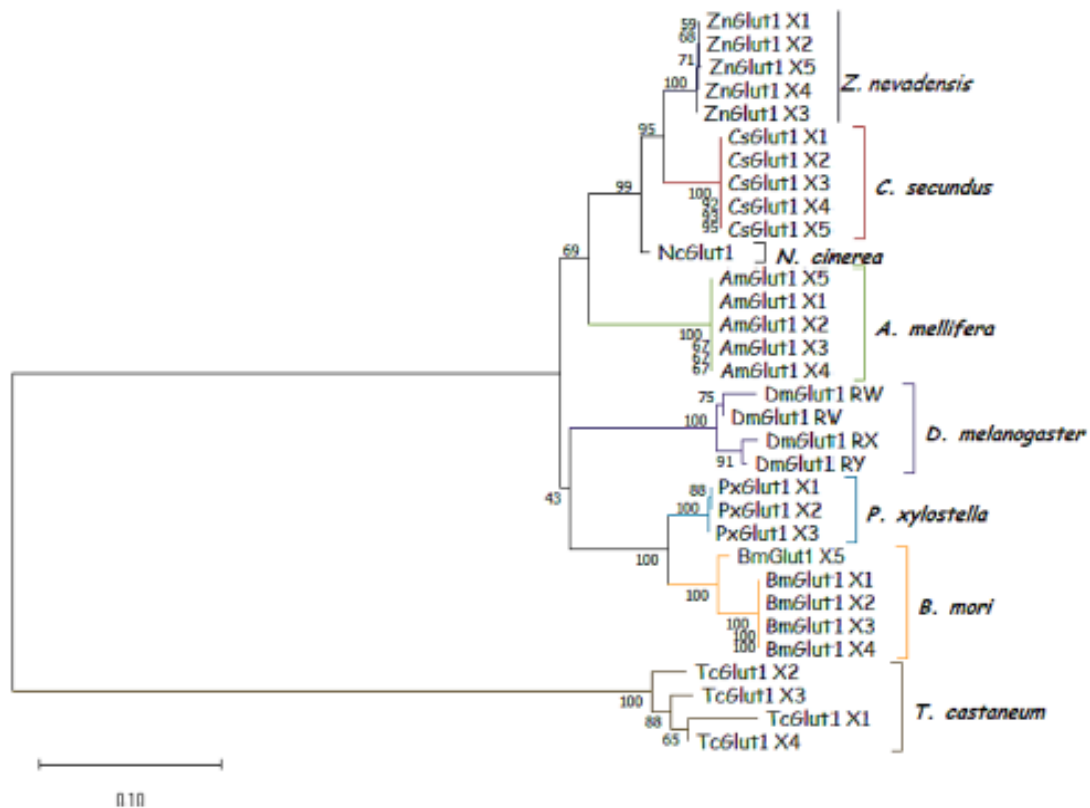


Fig. 11 Phylogenetic relationship between *Nauphoeta cinerea* GLUT1 and the GLUT1 of other insects. Evolutionary history was inferred by neighbor joining method with bootstrap branch support

performed 100 times. Branch length is synonymous to evolutionary distance computed by Poisson correction method

reduced survival of cockroaches as seen in mice models that present upregulation of pro-apoptotic markers and down-regulation of pro-survival proteins [72]. There is a record of increased mortality in *M. sexta* treated with a similar dose of STZ [23]. This was also reflected in our findings of reduced total body mass and head triglyceride content in STZ treated nymphs. Inability to gain weight [73] and reduction in brain triglyceride content have also been recorded in STZ treated rats [74, 75]. Glucose dyshomeostasis is also correlated with reduced body weight and triglyceride content in *D. melanogaster* [76].

We recorded increased levels of TBARS in STZ treated nymphs, which has also been reported in STZ treated rats [77], cell culture models of hyperglycaemia [78], and diabetic humans [79]. Hyperglycemia is known to trigger superoxide production [80] by four mechanisms, one of which is the increased formation of advanced glycation end-product (AGE) [81]. The resultant oxidative stress can activate nuclear factor erythroid 2-related factor (Nrf2) which upregulates the expression of antioxidant genes [78, 82]. In our study, there was a concurrent increase in antioxidant and detoxification profile (GST and GSH) of STZ treated cockroaches, which is similar to the data on increased GST

activity in plasma, kidney and heart of STZ treated rats [83], and the concomitant increase in TBARS levels and total GST recorded in *D. melanogaster* exposed to alloxan [24]. In this study, GST activity showed a hormetic response to STZ dosage, which may indicate a reduced capacity for detoxification after high dose exposure to STZ in the Lobster cockroach. The inverted U shaped dose response of GST to xenobiotics has been earlier reported [84, 85]. MTT reduction revealed significant decrease in reducing capacity of head homogenates of STZ treated nymphs, MTT reduction is mediated by dehydrogenases [55, 86], thus the decrease in reducing activity of head homogenates may be a consequence of NAD-NADH depletion in cockroaches treated with streptozotocin or a direct alkylation of dehydrogenases by STZ.

The open circulatory system in insects require that the nervous system be protected from fluctuating solute concentrations via the hemolymph-brain barrier (HBB) [87, 88]. As early as the 17th embryonic stage, subperineurial glial cells (SPGs), perineurial glial cells (PGs) and a neural lamella are known to constitute the HBB in drosophila [89], similar to the vertebrate neurovascular unit (NVU) [90]. Consequently, partitioning of circulation from the brain is

conserved from vertebrates to invertebrates, and this might explain why SPGs express transporters of the solute carrier family (SLC) [91] like SLC2A1 (glucose transporter GLUT 1)—a carrier mediated transport protein marked by Michaelis–Menten kinetics [92]. Peripheral streptozotocin injection is known to elevate brain glucose content [65, 66] and GLUT 1 mRNA expression [66, 93] in rats, similar to our findings of upregulated GLUT 1 mRNA in heads of STZ treated nymphs of *N. cinerea*. This suggested that the STZ-induced increase in head glucose content could probably be associated with the observed increase in glucose transporter 1 expression in the head (hemolymph-brain barrier) of the lobster cockroach after toxic treatment with STZ.

Conclusion

The lobster cockroach is a viable model for studying diabetes-like phenotypes, as similar glucose dyshomeostases that have been modeled in *D. melanogaster* and mammals are achievable in *N. cinerea*.

Acknowledgements Olawande C. Olagoke is a recipient of the 2017 CNPq-TWAS Postgraduate Fellowship (FR Number: 3240299312).

Funding This work is financially supported by FAPERGS/CNPq 12/2014-PRONEX: nº 16/2551-0/000, CAPES/PROEX (nº 23038.004173/2019-93; nº 0493/2019; nº 88882.182125/2018-01; 88882.182123/2018-01), and INCT-EN: for Cerebral Diseases, Excitotoxicity, and Neuroprotection.

Data availability All data and materials used are available upon reasonable request made to the corresponding author.

Code availability Not applicable.

Compliance with ethical standards

Conflict of interest The authors have no conflict of interest to declare.

Ethical approval Not applicable.

Consent to participate Not applicable.

Consent for publication The authors grant Molecular and Cellular Biochemistry the appropriate consent to publish this work.

References

- Hoang TC, Pryor RL, Rand GM, Frakes RA (2011) Use of butterflies as nontarget insect test species and the acute toxicity and hazard of mosquito control insecticides. *Environ Toxicol Chem* 30:997–1005. <https://doi.org/10.1002/etc.462>
- Lagadic L, Caquet T (1998) Invertebrates in testing of environmental chemicals: are they alternative? *Environ Health Perspect* 106:593–611. <https://doi.org/10.1289/ehp.98106593>
- Mrdaković M, Hijić L, Vlahović M et al (2019) Effects of dietary fluoranthene on nymphs of *Blattica dubia* S. (Blattodea: Blaberidae). *Environ Sci Pollut Res* 26:6216–6222. <https://doi.org/10.1007/s11356-019-04133-1>
- Huang X, Liu G, Guo J, Su Z (2018) The PI3K/AKT pathway in obesity and type 2 diabetes. *Int J Biol Sci* 14:1483–1496. <https://doi.org/10.7150/ijbs.27173>
- Gupta HP, Jha RR, Ahmad H et al (2019) Xenobiotic mediated diabetogenesis: developmental exposure to dichlorvos or atrazine leads to type 1 or type 2 diabetes in *Drosophila*. *Free Radic Biol Med* 141:461–474. <https://doi.org/10.1016/j.freeradbiomed.2019.07.013>
- Afolabi BA, Olagoke OC, Souza DO et al (2020) Modified expression of antioxidant genes in lobster cockroach, *Nauphoeta cinerea* exposed to methylmercury and monosodium glutamate. *Chem Biol Interact* 318:108969. <https://doi.org/10.1016/j.cbi.2020.108969>
- Piccoli BC, Alvim JC, da Silva FD et al (2019) High level of methylmercury exposure causes persisted toxicity in *Nauphoeta cinerea*. *Environ Sci Pollut Res* 27:4799–4813. <https://doi.org/10.1007/s11356-019-06989-9>
- Adedara IA, Rosemberg DB, de Souza D et al (2016) Neurobehavioral and biochemical changes in *Nauphoeta cinerea* following dietary exposure to chlorpyrifos. *Pestic Biochem Physiol* 130:22–30. <http://doi.org/10.1016/j.pe.stp.2015.12.004>
- Afolabi BA, Olagoke OC (2020) High concentration of MSG alters antioxidant defence system in lobster cockroach *Nauphoeta cinerea* (Blattodea: Blaberidae). *BMC Res Notes* 13:217. <https://doi.org/10.1186/s13104-020-05056-8>
- Waczuk EP, Wagner R, Klein B et al (2019) Assessing the toxicant effect of spontaneously volatilized 4-vinylcyclohexane exposure in nymphs of the lobster cockroach *Nauphoeta cinerea*. *Environ Toxicol Pharmacol* 72:103264. <https://doi.org/10.1016/j.etap.2019.103264>
- dos Santos DS, Rosa ME, Zanatta AP et al (2019) Neurotoxic effects of sublethal concentrations of cyanobacterial extract containing anatoxin-a(s) on *Nauphoeta cinerea* cockroaches. *Ecotoxicol Environ Saf* 171:138–145. <https://doi.org/10.1016/j.ecoenv.2018.12.068>
- Elsner M, Guldbakke B, Tiedge M et al (2000) Relative importance of transport and alkylation for pancreatic beta-cell toxicity of streptozotocin. *Diabetologia* 43:1528–1533. <https://doi.org/10.1007/s001250051564>
- Bennett RA, Pegg AE (1981) Alkylation of DNA in rat tissues following administration of streptozotocin. *41:2786–2791*. <https://cancerres.aacrjournals.org/content/41/17/2786>
- Berthiaume JM, Kurdys JG, Muntean DM, Rosa MG (2017) Mitochondrial NAD⁺/NADH redox state and diabetic cardiomyopathy. *Antioxid Redox Signal* 30:375–398. <https://doi.org/10.1089/ars.2017.7415>
- Bolzán AD, Bianchi NO, Bianchi MS (1998) Effects of antioxidants on streptozotocin-induced clastogenesis in mammalian and insect cells. *Mutat Res Toxicol Environ Mutagen* 418:35–42. [https://doi.org/10.1016/S1383-5718\(98\)00107-7](https://doi.org/10.1016/S1383-5718(98)00107-7)
- Bolzán AD, González MC, Bianchi MS (2000) The effect of 1,10-phenanthroline on the chromosome damage and sister-chromatid exchanges induced by streptozotocin in mammalian and insect cells. *Mutat Res Mol Mech Mutagen* 447:221–226. [https://doi.org/10.1016/S0027-5107\(99\)00210-9](https://doi.org/10.1016/S0027-5107(99)00210-9)
- Paschou SA, Papadopoulou-Marketou N, Chrousos GP, Kanaka-Gantenbein C (2018) On type 1 diabetes mellitus pathogenesis. *Endocr Connect* 7:R38–R46. <https://doi.org/10.1530/EC-17-0347>
- Mattila J, Hietakangas V (2017) Regulation of carbohydrate energy metabolism in *Drosophila melanogaster*. *Genetics* 207:1231–1253. <https://doi.org/10.1534/genetics.117.199885>

19. Antonova Y, Arik AJ, Moore W et al (2012) Insulin-like peptides: structure, signaling, and function. *Insect Endocrinol*. <https://doi.org/10.1016/B978-0-12-384749-2.10002-0>
20. Baldwin SA (1994) Mammalian Na⁺-independent sugar transporters and their homologues in other organisms. *Cell Physiol Biochem* 4:242–264. <https://doi.org/10.1159/000154729>
21. Ecker A, do Nascimento Gronzaga TKS, Seeger RL et al (2017) High-sucrose diet induces diabetic-like phenotypes and oxidative stress in *Drosophila melanogaster*: protective role of *Syzygium cumini* and *Bauhinia forficata*. *Borneo J Pharmacother* 89:605–616. <https://doi.org/10.1016/j.biopha.2017.02.076>
22. Birse RT, Choi J, Reardon K et al (2010) High-fat diet-induced obesity and heart dysfunction are regulated by the TOR pathway in *Drosophila*. *Cell Metab* 12:533–544. <https://doi.org/10.1016/j.cmet.2010.09.014>
23. Kramer KJ, Jacobs RM, Speirs RD, Hendricks LH (1978) Effect of vertebrate hypoglycemic and β -cell cytotoxic agents on insects. *Comp Biochem Physiol Part C Comp Pharmacol* 61:95–97. [https://doi.org/10.1016/0306-4492\(78\)90117-X](https://doi.org/10.1016/0306-4492(78)90117-X)
24. Siddique YH, Ansari MS, Rahul JS (2020) Effect of alloxan on the third instar larvae of transgenic *Drosophila melanogaster* (*hsp70-lacZ*) β g9. *Toxin Rev* 39:41–51. <https://doi.org/10.1080/15569543.2018.1472106>
25. Park S, Alfa RW, Topper SM et al (2014) A genetic strategy to measure circulating *Drosophila* insulin reveals genes regulating insulin production and secretion. *PLoS Genet*. <https://doi.org/10.1371/journal.pgen.1004555>
26. O'Connor KJ, Baxter D (1985) The demonstration of insulin-like material in the honey bee, *Apis mellifera*. *Comp Biochem Physiol Part B Biochem* 81:755–760. [https://doi.org/10.1016/0305-0491\(85\)90400-6](https://doi.org/10.1016/0305-0491(85)90400-6)
27. Duvé H, Thorpe A, Lazarus NR (1979) Isolation of material displaying insulin-like immunological and biological activity from the brain of the blowfly *Calliphora vomitoria*. *Biochem J* 184:221–227. <https://doi.org/10.1042/bj1840221>
28. Fernandez-Almonacid R, Rosen OM (1987) Structure and ligand specificity of the *Drosophila melanogaster* insulin receptor. *Mol Cell Biol* 7:2718–2727. <https://doi.org/10.1128/mcb.7.8.2718>
29. Alfa RW, Kim SK (2016) Using *Drosophila* to discover mechanisms underlying type 2 diabetes. *DMM Dis Model Mech* 9:365–376. <https://doi.org/10.1242/dmm.023887>
30. Inoue YH, Katsube H, Hinami Y (2018) *Drosophila* models to investigate insulin action and mechanisms underlying human diabetes mellitus. *Adv Exp Med Biol* 1076:235–256. https://doi.org/10.1007/978-981-13-0529-0_13
31. Rulifson EJ, Kim SK, Nusse R (2002) Ablation of insulin-producing neurons in flies: growth and diabetic phenotypes. *Science* 296:1118–1120. <https://doi.org/10.1126/science.1070058>
32. Broughton SJ, Piper MDW, Ikeya T et al (2005) Longer life span, altered metabolism, and stress resistance in *Drosophila* from ablation of cells making insulin-like ligands. *Proc Natl Acad Sci USA* 102:3105–3110. <https://doi.org/10.1073/pnas.0405775102>
33. Haselton A, Sharmir E, Schrader J et al (2010) Partial ablation of adult *Drosophila* insulin-producing neurons modulates glucose homeostasis and extends life span without insulin resistance. *Cell Cycle* 9:3135–3143. <https://doi.org/10.4161/cc.9.15.12458>
34. Grönke S, Clarke DF, Broughton S et al (2010) Molecular evolution and functional characterization of *Drosophila* insulin-like peptides. *PLoS Genet* 6(2):e1000857. <https://doi.org/10.1371/journal.pgen.1000857>
35. Pendse J, Ramachandran PV, Na J et al (2013) A *Drosophila* functional evaluation of candidates from human genome-wide association studies of type 2 diabetes and related metabolic traits identifies tissue-specific roles for dHHEX. *BMC Genom* 14:136. <https://doi.org/10.1186/1471-2164-14-136>
36. Ugrankar R, Berglund E, Akdemir F et al (2015) *Drosophila* glucose screening identifies Ck1alpha as a regulator of mammalian glucose metabolism. *Nat Commun* 6:7102. <https://doi.org/10.1038/ncomms8102>
37. Kunieda T, Beye M, Takeuchi H et al (2006) Carbohydrate metabolism genes and pathways in insects: insights from the honey bee genome. *Insect Mol Biol* 15:563–576. <https://doi.org/10.1111/j.1365-2583.2006.00677.x>
38. Nwaka S, Holzer H (1997) Molecular biology of trehalase and the trehalases in the yeast *Saccharomyces cerevisiae*. *Prog Nucleic Acid Res Mol Biol* 58:197–237. [https://doi.org/10.1016/S0079-6603\(08\)60037-9](https://doi.org/10.1016/S0079-6603(08)60037-9)
39. Dwyer DS, Liu Y, Bradley RJ (1999) An ethanol-sensitive variant of the PC12 neuronal cell line: sensitivity to alcohol is associated with increased cell adhesion and decreased glucose accumulation. *J Cell Physiol* 178:93–101. [https://doi.org/10.1002/\(SICI\)1097-4652\(199901\)178:1%3e93::AID-JCP12%3e3.0.CO;2-U](https://doi.org/10.1002/(SICI)1097-4652(199901)178:1%3e93::AID-JCP12%3e3.0.CO;2-U)
40. Kan O, Baldwin SA, Whetton AD (1994) Apoptosis is regulated by the rate of glucose transport in an interleukin 3 dependent cell line. *J Exp Med* 180:917–923. <https://doi.org/10.1084/JEM.180.3.917>
41. Barbosa NBV, Rocha JBT, Soares JCM et al (2008) Dietary diphenyl diselenide reduces the STZ-induced toxicity. *Food Chem Toxicol* 46:186–194. <https://doi.org/10.1016/j.fct.2007.07.014>
42. Karganov MY, Alchinova IB, Tinkov AA et al (2020) Streptozotocin (STZ)-induced diabetes affects tissue trace element content in rats in a dose-dependent manner. *Biol Trace Elem Res*. <https://doi.org/10.1007/s12011-020-02090-2>
43. Hackleman N, DeBakey ME, Dodds WJ et al (1988) Use of laboratory animals in biomedical and behavioral research. National Academy Press, Washington, D.C. <https://www.nap.edu/catalog/1098.html>
44. Corley LS, Blankenship JR, Moore AJ (2001) Genetic variation and asexual reproduction in the facultatively parthenogenetic cockroach *Nauphoeta cinerea*: implications for the evolution of sex. *J Evol Biol* 14:68–74. <https://doi.org/10.1046/j.1420-9101.2001.00254.x>
45. Galochkina T, Ng Fuk Chong M, Challali L et al (2019) New insights into Glut1 mechanics during glucose transfer. *Sci Rep* 9:1–14. <https://doi.org/10.1038/s41598-018-37367-z>
46. Volkenhoff A, Hirrlinger J, Kappel JM et al (2018) Live imaging using a FRET glucose sensor reveals glucose delivery to all cell types in the *Drosophila* brain. *J Insect Physiol* 106:55–64. <https://doi.org/10.1016/j.jinsphys.2017.07.010>
47. Ishay J (1975) Glucose levels in *Vespa orientalis*: the effect of starvation. *Comp Biochem Physiol Part A Physiol* 52:91–96. [https://doi.org/10.1016/S0300-9629\(75\)80134-4](https://doi.org/10.1016/S0300-9629(75)80134-4)
48. Kramer KJ, Jacobs RM, Speirs RD, Hendricks LH (1978) Effect of vertebrate hypoglycemic and beta cell cytotoxic agents on insects. *Biochem Physiol* 61:95–97. <https://pubag.nal.usda.gov/download/11675/PDF>
49. Inagaki S, Yamashita O (1986) Metabolic shift from lipogenesis to glycogenesis in the last instar larval fat body of the silkworm, *Bombyx mori*. *Insect Biochem* 16:327–331. [https://doi.org/10.1016/0020-1790\(86\)90043-0](https://doi.org/10.1016/0020-1790(86)90043-0)
50. Dubois M, Gilles KA, Hamilton JK et al (1956) Colorimetric method for determination of sugars and related substances. *Anal Chem* 28:350–356. <https://doi.org/10.1021/ac60111a017>
51. Ellman GL (1959) Tissue sulphydryl groups. *Arch Biochem Biophys* 82:70–77. [https://doi.org/10.1016/0003-9861\(59\)90090-6](https://doi.org/10.1016/0003-9861(59)90090-6)
52. Rifai N, Warnick GR, Dominiczak MH (2000) Handbook of lipoprotein testing. AAC Press. https://books.google.com.br/books?hl=en&lr=&id=9p624M13mIC&oi=fnd&pg=PP25&ots=rhxQu47xHW&sig=tXmtYNUH9V RG abrsUQ3xQYZTmo&redir_esc=y#v=onepage&q&f=false

53. Varshney R, Kale RK (1990) Effects of calmodulin antagonists on radiation-induced lipid peroxidation in microsomes. *Int J Radiat Biol* 58:733–743. <https://doi.org/10.1080/09553009014552121>
54. Salami AT, Odukanmi OA, Olagoke CO et al (2016) Role of nitric oxide and endogenous antioxidants in thyroxine facilitated healing of ischemia-reperfusion induced gastric ulcers. *J Pharm Res* 12:189–206. <https://www.ajol.info/index.php/njpr/article/view/163404>
55. Stockert JC, Horobin RW, Colombo LL, Blázquez-Castro A (2018) Tetrazolium salts and formazan products in cell biology: viability assessment, fluorescence imaging, and labeling perspectives. *Acta Histochem* 120:159–167. <https://doi.org/10.1016/j.acthis.2018.02.005>
56. Berridge MV, Tan AS (1993) Characterization of the cellular reduction of 3-(4,5-dimethylthiazol-2-yl)-2,5-diphenyltetrazolium bromide (MTT): subcellular localization, substrate dependence, and involvement of mitochondrial electron transport in MTT reduction. *Arch Biochem Biophys* 303:474–482. <https://doi.org/10.1006/abbi.1993.1311>
57. Habig WH, Jakoby WB (1981) Assays for differentiation of glutathione S-transferases. *Methods Enzymol* 177:398–405. [https://doi.org/10.1016/S0076-6879\(81\)77053-8](https://doi.org/10.1016/S0076-6879(81)77053-8)
58. Se gatto ALA, Di e s e JF, Loreto ELS, da Rocha JBT (2018) De novo transcriptome assembly of the lobster cockroach *Nauphoeta cinerea* (Blaberidae). *Genet Mol Biol* 41:713–721. <https://doi.org/10.1590/1678-4685-gmb-2017-0264>
59. Tamura K, Peterson D, Peterson N et al (2011) MEGA 5: molecular evolutionary genetics analysis using maximum likelihood, evolutionary distance, and maximum parsimony methods. *Mol Biol Evol* 28(10):2731–2739. <https://doi.org/10.1093/molbev/msr121>
60. Edgar RC (2004) MUSCLE: multiple sequence alignment with high accuracy and high throughput. *Nucleic Acids Res* 32:1792–1797. <https://doi.org/10.1093/nar/gkh340>
61. Parker G, Taylor R, Jones D, McClain D (2004) Hyperglycemia and inhibition of glycogen synthase in streptozotocin-treated mice: role of O-linked N-acetylglucosamine. *J Biol Chem* 279:20636–20642. <https://doi.org/10.1074/jbc.M312139200>
62. Parker GJ, Lund KC, Taylor RP, McClain DA (2003) Insulin resistance of glycogen synthase mediated by O-linked N-acetylglucosamine. *J Biol Chem* 278:10022–10027. <https://doi.org/10.1074/jbc.M207787200>
63. Ashcroft FM, Rohm M, Clark A, Brereton MF (2017) Is type 2 diabetes a glycogen storage disease of pancreatic β cells? *Cell Metab* 26:17–23. <https://doi.org/10.1016/j.cmet.2017.05.014>
64. Miyamoto T, Amre H (2018) Neuronal gluconeogenesis regulate systemic glucose homeostasis. *SSRN Electron J*. <https://doi.org/10.2139/ssrn.3245217>
65. Jacob R, Fan X, Evans M et al (2002) Brain glucose levels are elevated in chronically hyperglycemic diabetic rats: no evidence for protective adaptation by the blood brain barrier. *Metabolism* 51(12):1522–1524. <https://doi.org/10.1053/meta.2002.36347>
66. Shah K, DeSilva S, Abbruscato T (2012) The role of glucose transporters in brain disease: diabetes and Alzheimer's disease. *Int J Mol Sci* 13:12629–12655. <https://doi.org/10.3390/ijms131012629>
67. Hwang JJ, Jiang L, Hamza M et al (2017) Blunted rise in brain glucose levels during hyperglycemia in adults with obesity and T2DM. *JCI Insight* 2(20):e95913. <https://doi.org/10.1172/jci.insight.95913>
68. Nichols CD (2006) *Drosophila melanogaster* neurobiology, neuropharmacology, and how the fly can inform central nervous system drug discovery. *Pharmacol Ther* 112:677–700. <https://doi.org/10.1016/j.pharmthera.2006.05.012>
69. Mehta A, Verma RS, Srivastava N (2005) Chlorpyrifos-induced alterations in rat brain acetylcholinesterase, lipid peroxidation and ATPases. *NOPR* 42(1):54–58. <https://hdl.handle.net/123456789/3499>
70. Gallo MA, Lawryk NJ (1991) Organic phosphorus pesticides. In: Hayes WJ, Laws ER (eds) *Handbook of pesticide toxicology*, vol 2. Academic Press, New York, pp 917–1123
71. Erukainure OL, Reddy R, Islam MS (2019) Raffia palm (*Raphia hookeri*) wine attenuates redox imbalance and modulates activities of glycolytic and cholinergic enzymes in hyperglycemia-induced testicular injury in type 2 diabetic rats. *J Food Biochem* 43:e12764. <https://doi.org/10.1111/jfbc.12764>
72. Moore A, Shindikar A, Fomison-Nurse I et al (2014) Rapid onset of cardiomyopathy in STZ-induced female diabetic mice involves the downregulation of pro-survival Pim-1. *Cardiovasc Diabetol* 13:68. <https://doi.org/10.1186/1475-2840-13-68>
73. Thulé PM, Liu J-M (2000) Regulated hepatic insulin gene therapy of STZ-diabetic rats. *Gene Ther* 7:1744–1752. <https://doi.org/10.1038/sj.gt.3301297>
74. Malaisse WJ, Zhang Y, Louchami K et al (2006) Brain phospholipid and triglyceride fatty acid content and pattern in Type 1 and Type 2 diabetic rats. *Neurosci Lett* 409:75–79. <https://doi.org/10.1016/j.neulet.2006.09.023>
75. Montilla P, Muñoz MC, Bujalance I et al (2005) Red wine prevents brain oxidative stress and nephropathy in streptozotocin-induced diabetic rats. *J Biochem Mol Biol* 38:539–544
76. Zhang H, Liu J, Li CR et al (2009) Deletion of *Drosophila* insulin-like peptide causes growth defects and metabolic abnormalities. *Proc Natl Acad Sci USA* 106:19617–19622. <https://doi.org/10.1073/pnas.0905083106>
77. Ghosh S, Chowdhury S, Das AK, Sil PC (2019) Taurine ameliorates oxidative stress induced inflammation and ER stress mediated testicular damage in STZ-induced diabetic Wistar rats. *Food Chem Toxicol* 124:64–80. <https://doi.org/10.1016/j.fct.2018.11.055>
78. Jimenez R, Toral M, Gómez-Guzmán M et al (2018) The role of Nrf2 signaling in PPAR β/δ -mediated vascular protection against hyperglycemia-induced oxidative stress. *Oxid Med Cell Longev* 2018:1–12. <https://doi.org/10.1155/2018/5852706>
79. Pickering RJ, Rosado CJ, Sharma A et al (2018) Recent novel approaches to limit oxidative stress and inflammation in diabetic complications. *Clin Transl Immunol* 7:e1016. <https://doi.org/10.1002/cti.21016>
80. Brownlee M (2001) Biochemistry and molecular cell biology of diabetic complications. *Nature* 414:813–820. <https://doi.org/10.1038/414813a>
81. Stitt AW, Li YM, Gardiner TA et al (1997) Advanced glycation end products (AGEs) co-localize with AGE receptors in the retinal vasculature of diabetic and of AGE-infused rats. *Am J Pathol* 150:523–531. <https://www.ncbi.nlm.nih.gov/pmc/articles/PMC1858286/>
82. Loboda A, Damulewicz M, Pyza E et al (2016) Role of Nrf2/HO-1 system in development, oxidative stress response and diseases: an evolutionarily conserved mechanism. *Cell Mol Life Sci* 73:3221–3247. <https://doi.org/10.1007/s00018-016-2223-0>
83. Mak DHF, Ip SP, Li PC et al (1996) Alterations in tissue glutathione antioxidant system in streptozotocin-induced diabetic rats. *Mol Cell Biochem* 162:153–158. <https://doi.org/10.1007/BF00227543>
84. Oliveira MF, Geihs MA, França TFA et al (2018) Is “Preparation for Oxidative Stress” a case of physiological conditioning hormesis? *Front Physiol* 9:945. <https://doi.org/10.3389/fphys.2018.00945>
85. Bartolini D, Comodi J, Piroddi M et al (2015) Glutathione S-transferase pi expression regulates the Nrf2-dependent response to hormone diselenides. *Free Radic Biol Med* 88:466–480. <https://doi.org/10.1016/j.freeradbiomed.2015.06.039>

86. Berridge MV, Herst PM, Tan AS (2005) Tetrazolium dyes as tools in cell biology: new insights into their cellular reduction. *Biotechnol Annu Rev* 11:127–152. [https://doi.org/10.1016/S1387-2656\(05\)11004-7](https://doi.org/10.1016/S1387-2656(05)11004-7)
87. Weiler A, Volkenhoff A, Hertenstein H, Schirmeier S (2017) Metabolic transport across the mammalian and insect brain diffusion barriers. *Neurobiol Dis* 107:15–31. <https://doi.org/10.1016/j.nbd.2017.02.008>
88. Peter Aadal Nielsen O, Gunnar Andersson R, Olga Andersson R (2015) Insect-based ex vivo model for testing blood-brain barrier penetration and method for exposing insect brain to chemical compounds. US9097706B2. <https://patents.google.com/patent/US9097706B2/en>
89. Stork T, Engelen D, Krudewig A et al (2008) Organization and function of the blood-brain barrier in *Drosophila*. *J Neurosci* 28:587–597. <https://doi.org/10.1523/JNEUROSCI.4367-07.2008>
90. Mayer F, Mayer N, Chinn L et al (2009) Evolutionary conservation of vertebrate blood-brain barrier chemoprotective mechanisms in *drosophila*. *J Neurosci* 29:3538–3550. <https://doi.org/10.1523/JNEUROSCI.5564-08.2009>
91. De Salvo MK, Hindle SJ, Rusan ZM et al (2014) The *Drosophila* surface glia transcriptome: evolutionary conserved blood-brain barrier processes. *Front Neurosci* 8:346. <https://doi.org/10.3389/fnins.2014.00346>
92. Dick APK, Harik SI (1986) Distribution of the glucose transporter in the mammalian brain. *J Neurochem* 46:1406–1411. <https://doi.org/10.1111/j.1471-4159.1986.tb01755.x>
93. Lei H, Gruetter R (2006) Effect of chronic hypoglycaemia on glucose concentration and glycogen content in rat brain: a localized ¹³C NMR study. *J Neurochem* 99:260–268. <https://doi.org/10.1111/j.1471-4159.2006.04115.x>

Publisher's Note Springer Nature remains neutral with regard to jurisdictional claims in published maps and institutional affiliations.

5.2. Article 2: Streptozotocin activates inflammation-associated signalling and antioxidant response in the lobster cockroach; *Nauphoeta cinerea*.

<https://doi.org/10.1016/j.cbi.2021.109563>.

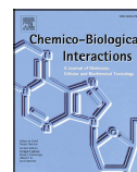
Chemico-Biological Interactions 345 (2021) 109563



Contents lists available at ScienceDirect

Chemico-Biological Interactions

journal homepage: www.elsevier.com/locate/chembioint



Streptozotocin activates inflammation-associated signalling and antioxidant response in the lobster cockroach; *Nauphoeta cinerea* (Blattodea: Blaberidae)

Olawande C. Olagoke^a, Ana L.A. Segatto^b, Blessing A. Afolabi^{a,c,d}, João B.T. Rocha^{a,*}

^a Departamento de Bioquímica e Biologia Molecular, Centro de Ciências Naturais e Exatas (CCNE), Universidade Federal de Santa Maria, 97105-900, Santa Maria, RS, Brazil

^b Instituto Federal de Educação, Ciência e Tecnologia do Rio Grande do Sul, RS, Brazil

^c Departamento de Bioquímica, Instituto de Ciências Básicas da Saúde, Universidade Federal do Rio Grande do Sul, 90035-003, Porto Alegre, RS, Brazil

^d Department of Biochemistry, Bowen University, Iwo, Osun State, Nigeria

Streptozotocin activates inflammation-associated signalling and antioxidant response in the lobster cockroach; *Nauphoeta cinerea* (Blattodea: Blaberidae).

Olawande C. Olagoke¹, Ana L. A. Segatto², Blessing A. Afolabi^{1,3,4}, João B. T. Rocha^{1*}

¹ Departamento de Bioquímica e Biologia Molecular, Centro de Ciências Naturais e Exatas (CCNE), Universidade Federal de Santa Maria, 97105-900 Santa Maria, RS, Brazil.

² Instituto Federal de Educação, Ciência e Tecnologia do Rio Grande do Sul, RS, Brasil.

³ Departamento de Bioquímica, Instituto de Ciências Básicas da Saúde, Universidade Federal do Rio Grande do Sul, 90035-003 Porto Alegre, RS, Brasil.

⁴ Department of Biochemistry, Bowen University, Iwo, Osun State, Nigeria.

*Corresponding Author

João B. T. Rocha,

Departamento de Bioquímica e Biologia Molecular, CCNE,

Universidade Federal de Santa Maria, 97105-900 Santa Maria, RS, Brazil.

Fax: +55 55 8104 0207.

E-mail: jbtrocha@gmail.com; jbtrocha@yahoo.com.br

ORCID

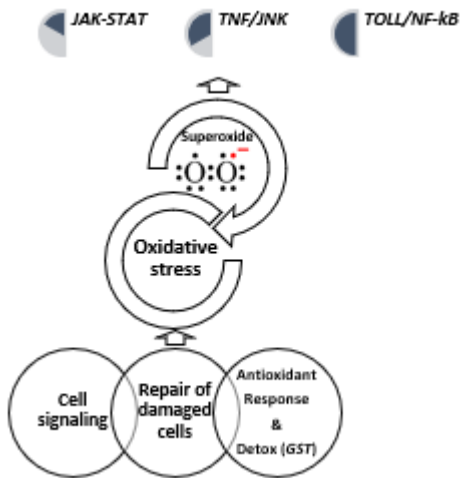
Olawande C. Olagoke: 0000-0001-9212-4948

Ana L. A. Segatto: 0000-0002-5044-1168

Blessing A. Afolabi: 0000-0003-4276-0123

João B. T. Rocha: 0000-0003-3829-0595

Graphical abstract.



Highlights

- Streptozotocin activates primary antioxidants genes of *Nauphoeta cinerea*.
- *JNK*, *TOLL/NF-kB* and *JAK/STAT* pathways are activated in STZ-treated *Nauphoeta cinerea*.
- *GST sigma* class secondary structure elements are conserved from *Nauphoeta cinerea* to mammals.
- This study buttressing support for Insect use in studying metabolic diseases like diabetes.

Abstract

Streptozotocin exhibits tropism to insulin-producing beta-cells in mammals and has been used to model diabetes-like phenotypes in insects. We have previously shown increased brain glucose levels and oxidative stress in STZ-treated nymphs of *Nauphoeta cinerea*. Here, we validate *Nauphoeta cinerea* as an experimental organism for studying STZ-induced metabolic disruptions by investigating the potential changes in the expression of inflammation and antioxidant related genes. Cockroaches were injected with 0.8% NaCl, 74 and 740 nmol of STZ. mRNA extracted from the head of cockroaches was used to estimate the RT-qPCR expression of inflammation and antioxidant genes. STZ-treatment upregulated the target genes of the *JNK* pathway (early growth factor response factor and reaper) but had no effect on *PDGF*-and *VEGF*-related factor 1. *TOLL 1*, the target gene of *TOLL / NF- κ B* pathway was up regulated, while both the activator and target gene of the *UPD3 / JAK / STAT* pathway [unpaired 3 and Suppressor of cytokine signalling at 36E] were upregulated. mRNA levels of primary antioxidants (superoxide dismutase and catalase) were increased in STZ treated nymphs but there was no effect on thioredoxins and Peroxiredoxin 4. Likewise, STZ treatment did not affect the expression of the *delta* class of the *glutathione S-transferase* gene family, but the *sigma* and *theta* classes of the *GST* family were upregulated. The STZ-induced *N. cinerea* gene expression modification demonstrates the involvement of primary antioxidants and the *GST* detoxification system in the cockroach oxidative stress response and buttresses the proposed crosstalk between inflammatory and redox pathways.

Keywords: *JNK* pathway; *TOLL/NF- κ B* pathway; *UPD3/JAK/ STAT* pathway; primary antioxidants; *GST* Phylogeny

1. Introduction

Gene expression studies have been established as useful tools for understanding reduction-oxidation (redox) and inflammatory changes in living systems, as there are recent indications of a cross-talk between inflammation and the regulation of redox pathways [1,2].

Reactive oxygen species (ROS) are generated in response to endogenous and exogenous stressors, including compounds like streptozotocin that have been linked with increased superoxide production in the mitochondrial electron transport [3–5]. The oxidative stress has been shown to activate insect pro-inflammatory pathways (**Scheme 1**) including: Janus kinase / Signal Transducer and Activator of Transcription [*JAK-STAT*]; Tumor necrosis factor alpha-induced activation of c-Jun N-terminal kinase [*TNF/JNK*]; and *TOLL*-like receptor 2-mediation of nuclear factor kappa-light-chain-enhancer of activated B cells [*TOLL/NF- κ B*], which are analogues of the mammalian Interleukin 6, Tumor necrosis factor, and *TOLL*-like receptors respectively [6–8].

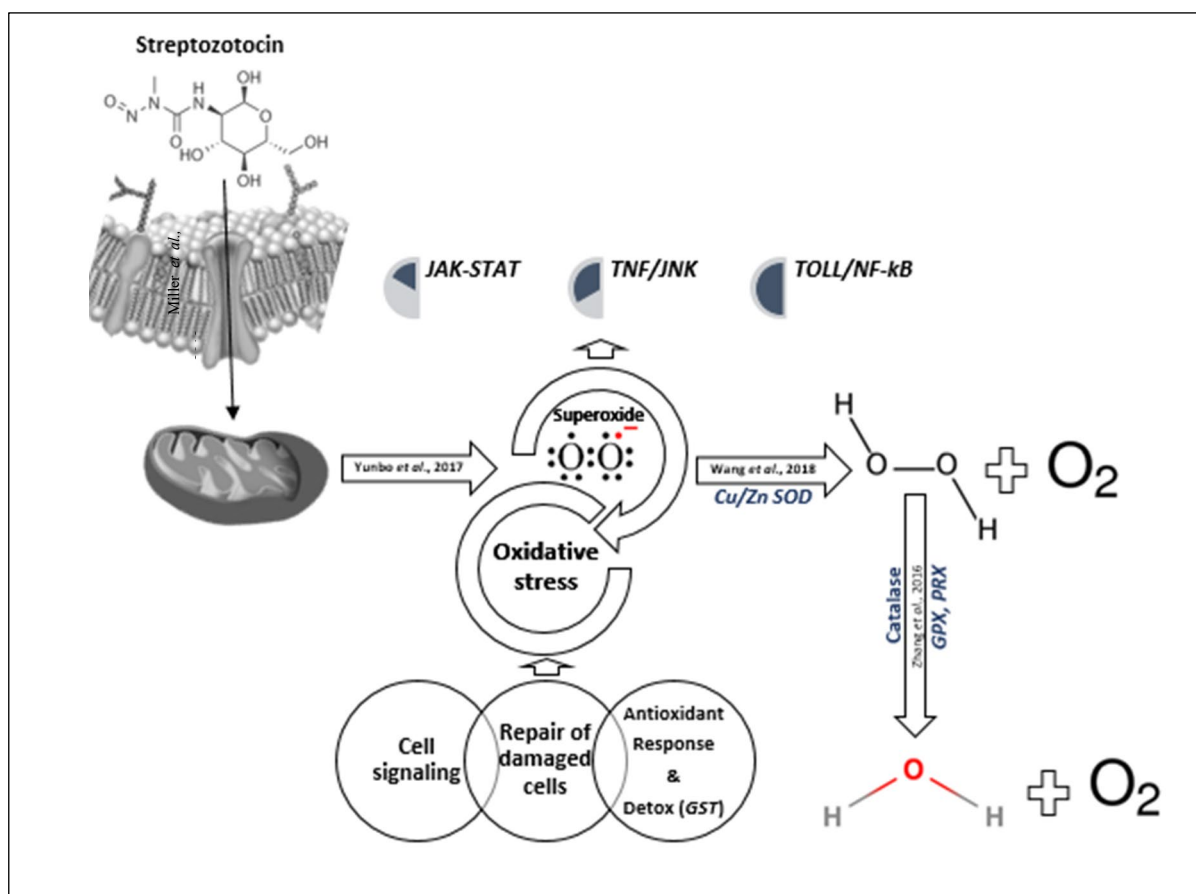
Three main mechanisms are employed by insects to counteract damages caused by reactive oxygen species: activation of cell signalling, use of antioxidant enzymes and free radical scavengers, and the repair of already damaged cells [9–11]. Antioxidant enzymes can be divided into primary antioxidants, second line defence systems and other enzymatic antioxidants [12]. Primary antioxidants are mostly enzymes that directly react with reactive species, for instance, superoxide dismutase enzymes (copper, zinc *Cu/Zn SOD* or manganese *MnSOD*) catalyse the dismutation of $2O_2^-$ to yield hydrogen peroxide (H_2O_2) and oxygen (O_2) [13]. Catalase (*CAT*) and peroxidase (*PRX*) then eliminates H_2O_2 by forming water ($2H_2O$) and oxygen (O_2) [14], but *PRX*'s depend on glutathione (*GSH*) and reduced thioredoxin (*TRX*) to reduce H_2O_2 [15] (**Scheme 1**).

The thioredoxin system consisting of thioredoxin, thioredoxin reductase and nicotinamide adenine dinucleotide phosphate is conserved from prokaryotes to eukaryotes. Albeit, while humans harness both flavoenzymes – glutathione reductase (*GR*) and thioredoxin reductase (*TrxR*) in dealing with oxidative challenge, many insects replace the *GR* glutathione reduction (**Reaction 1**) with the *TRX* system (**Reaction 2**) [16]. Similarly, the active sites of multi-functional enzymes like *glutathione S-transferases* that mainly detoxify xenobiotic electrophilic compounds via glutathione (GSH) conjugation are conserved (**Reaction 3**) [17]. *GST delta* (*GST d*) and *epsilon* (*GST e*) detoxify insecticides, *GST sigma* (*GST s*) protects metabolically active tissues from lipid peroxidation products, while *GST omega* (*GST o*), *theta* (*GST t*) and *zeta* (*GST z*) are primarily involved in metabolic processes [18,19]. The sigma class of *glutathione S-transferases* use a tyrosine as catalytic residue [20], and features a proline / alanine-rich N-terminal extension whose truncation does not affect the enzyme's kinetic parameters [19]. Structure-function relationships have been delineated for mammalian and fly *GST sigma* [20,21], we herein compare the amino acid sequence of *Nauphoeta cinerea GST sigma* with those of organisms with verified crystal structure, while analysing its phylogenetic relationship with other insect GSTs.



Lastly, the cell membrane and other biomolecules that are damaged by free radical exposure are repaired and reconstructed by *de novo* enzymes like polymerase, glycosylase, nuclease, proteinase, protease and peptidase [22]. We have previously reported the induction of oxidative stress and altered glucose metabolism in STZ-treated *Nauphoeta cinerea* [23]. Likewise,

Nauphoeta cinerea is increasingly been used to illustrate the interaction of xenobiotics with biological systems [24–26], as insects have proved effective in modelling metabolic alterations that characterize human diseases [27,28] We herein investigated the potential molecular mechanisms by which pro-inflammatory and antioxidant genes participate in STZ-induced metabolic disruptions in the head of cockroaches.



Scheme 1: Summary of possible mechanism for the antioxidant and inflammation-related response to streptozotocin-induced oxidative and cellular stress.

2. Materials and Methods

2.1. Chemicals

Streptozotocin was purchased from Sigma Aldrich, USA; TrizolTM reagent and platinum taq DNA polymerase were bought from ThermoFisher scientific, USA; DNase and GoScriptTM reverse transcriptase were purchased from Promega Corp, USA.

2.2. Insect experimental design

Male and female nymphs of *Nauphoeta cinerea* were obtained from Departamento de Bioquímica e Biologia Molecular, Universidade Federal de Santa Maria, Brasil. The insects were housed in 21.5cm x 21.5cm x 8.2cm; 2.5L translucent boxes in an observation room with a 12 hour dark-light cycle, average temperature of 24°C (minimum/maximum variation of about 3°C), humidity of 57 – 75%. The nymphs were allowed access to water and feed freely, and the feed constituents are as we have earlier shown [23]. Two hundred and sixteen (216) nymphs were acclimatized for one week, weighed and randomly designated to a triplicate of four groups (n=6), including: intact control; sham injection (0.8% NaCl); 74 and 740 nmol of STZ injection per cockroach. 20 µl of 74 nmol STZ injection had a concentration of 3.7 mM, while 20 µl of 740 nmol STZ injection had a concentration of 37 mM. Seven days after the single dose of STZ or sham injections, 3 heads per tube were homogenized with TrizolTM reagent, in six biological replicates per group and stored at -70°C pending RNA extraction. Normal saline (0.8% NaCl) was used as vehicle to dissolve the streptozotocin which was injected into the second right dorsal thoracic segment of each nymph. The dosage of treatment and duration of monitoring were based on earlier described pilot study and biochemical experiments [23].

2.3. Primer design, sequence alignment and phylogenetic analyses.

Gene sequences of insects within the Blattodea order were used to query our *Nauphoeta cinerea* transcriptome [29]. The ensuing sequences were confirmed on the NCBI blast platform (<https://blast.ncbi.nlm.nih.gov/Blast.cgi>) and used to design gene primers of interest on the Primer3input website (<http://primer3.ut.ee/>) which were verified with Oligoanalyzer (<https://www.idtdna.com/pages/tools/oligoanalyzer>). The gene sequences were also used as part of our phylogenetic workflow, alongside sequences from representative orders of the three Neoptera insect superclass (Polyneoptera, Paraneoptera and Holometabola). Molecular evolutionary genetics analysis (MEGA 5) [30] was utilized in the conduct of multiple sequence alignments via multiple sequence comparison by Log-expectation (MUSCLE) [31] with default gap penalties. Positions that were poorly aligned were cleaned up by Block Mapping and Gathering with Entropy (NGphylogeny.fr), and insect phylogenetic relationships were inferred by neighbour joining method [32] with 100 bootstrap replications as we have earlier described [23]

2.4. Real-time Polymerase chain reaction.

Total RNA from head of nymphs was isolated as described in the TrizolTM reagent protocol (ThermoFisher scientific, USA). DNase treatment (Promega Corp, USA) was used to ensure purity of the samples, and quality of the isolated RNA was ascertained by spectrophotometry (using NanoDropTM 2000 at 260/280nm) and agarose gel electrophoresis. Reverse transcription of 1µg Total RNA was performed using GoScriptTM protocol (Promega Corp, USA) with a T100TM Thermal Cycler (BIO-RAD, China). Real-time PCR was carried out using a QuantStudio 3 RT-qPCR System (ThermoFisher scientific, USA). Each well contained a final volume of 20 µl; 10 ng of cDNA and the reaction mix comprising of 0.2 µM of each primer (forward and reverse), 1 X buffer, 0.2 mM dNTP, 2 mM MgCl₂, 0.1 X SYBR green and 0.25 U of Platinum Taq DNA Polymerase (Invitrogen ®), made up with ultra-pure deionized water.

The cycling procedure used was: 94 °C for 5 min; 40 cycles of 94 °C for 15 s, 60 °C for 10 s and 72 °C for 30 s; and 1 cycle of 94 °C for 10 s, 55 °C for 60 s and 94 °C for 15 s as we have earlier explained [23]. The efficiency of each primer to bind to its target gene was evaluated using pools from all samples, five-point dilutions were made to obtain one standard curve for each primer. The results were analysed with the QuantStudio™ Design and Analysis software and only primers with 100% efficiency were used. The normalizer genes were tested using BestKeeper [33] and NormFinder [34] software. Among TATA-Box binding protein (*TBP*), glyceraldehyde-3-phosphate dehydrogenase (*GAPDH*), eukaryotic translation elongation factor 1 alpha 1 (*EF1A1*), glycerol-3-phosphate dehydrogenase (*GPDH*) and *Tubulin*, the most stable normalizer gene was *GAPDH*. Primer details are shown in **Table 1**.

Table 1: Primer Information for Nauphoeta Inflammation and redox genes.

Oligo name	Primer – Sequence (5' - 3')	Annealing Temperature	% Identity – Specie
<i>EGR</i>	F – CACTTGATGGCAGGTATTGGA R – GGATGAACACGATGTAAATGGA	60	67.03 – <i>C. secundus</i> 70.12 – <i>Z. nevadensis</i> 52.14 – <i>T. castaneum</i>
<i>PVFI</i>	F – AGCATTCCACAGCCTCGTAT R – GTTGACTGGGAGTCTGAGCA	60	51.30 – <i>B. germanica</i> 45.32 – <i>C. secundus</i> 46.08 – <i>Z. nevadensis</i>
<i>RPR</i>	F – CGAAGAGCGAGAGAGGATTG R – CAGGATGGTCTGCTGAAGGT	60	85.78 – <i>C. secundus</i> 83.07 – <i>Z. nevadensis</i> 55.28 – <i>T. castaneum</i>
<i>TOLL1</i>	F – TTGTGTTTCTGGACATCAGTCATAA R – CATGCAGATTGTTGTGTTCCA	60	58.44 – <i>B. germanica</i> 56.42 – <i>C. secundus</i> 56.33 – <i>Z. nevadensis</i>
<i>SOCS36E</i>	F – GGTGCTGGTGCATATTTGAAG R – TCTGCTGGAGATTGAACTGC	60	87.18 – <i>B. germanica</i> 82.65 – <i>C. secundus</i> 82.65 – <i>Z. nevadensis</i>

<i>UPD3</i>	F – GGAACATCCACCTCTGATCG R – TAGGAGGACCCGAGAATGTG	60	72.4 – <i>C. secundus</i> 61.8 – <i>T. castaneum</i>
<i>SOD</i> <i>[CU-ZN]</i>	F – GTATTCTGGTGGCTGCGAAA R – TAAACCCAACACAGAGCCTTG	60	71.73 – <i>C. secundus</i> 55.81 – <i>Z. nevadensis</i> 52.86 – <i>Thrips palmi</i>
<i>Catalase</i>	F – ACGAGATCCAGCATCTGACC R – CTCCACGGTTATCCACAGGT	60	89.37 – <i>C. secundus</i> 87.99 – <i>Z. nevadensis</i> 72.11 – <i>T. castaneum</i>
<i>PRX4</i>	F – GCTGTTCTATCCGCTGGACT R – CACTGAGCAAGCAACGACTT	60	85.71 – <i>C. secundus</i> 87.01 – <i>B. germanica</i> 86.44 – <i>C. formosanus</i>
<i>TRX1</i>	F – AGTATCCACGCGCCGTATT R – TGGGGTCTGCTCCTTGTATC	60	90.99 – <i>C. secundus</i> 90.09 – <i>Z. nevadensis</i> 72.52 – <i>B. germanica</i>
<i>TRX2</i>	F – TTATCAGCATTGGCACCAGA R – GCTGAATATCCGGCTGTCAT	60	77.88 – <i>C. secundus</i> 69.23 – <i>Z. nevadensis</i> 65.98 – <i>B. germanica</i>
<i>TRX5</i>	F – TCCTACCTGGGATGCTCTTG R – CCGAGCCTAGCATTCTACTT	60	77.27 – <i>C. secundus</i> 76.14 – <i>Z. nevadensis</i>
<i>GST s</i>	F – GGGACCTCTGAATGACGAAA R – CATGCCGTCCAAATAATCAA	60	75.98 – <i>B. germanica</i> 71.57 – <i>Z. nevadensis</i> 69.61 – <i>C. secundus</i>
<i>GST d</i>	F – AATCGGCGTTGATCTGAATC R – CGGCAAATAGCTCGACTTTC	60	69.30 – <i>P. americana</i> 56.46 – <i>C. secundus</i> 54.11 – <i>D. melonogaster</i>
<i>GST t</i>	F – AAGAAATGGGTTGCAGGAGA R – CATTGGGATGCTTGCTTACA	60	63.68 – <i>P. americana</i> 67.15 – <i>B. germanicagermanica</i> 56.46 – <i>C. Secundus</i>
<i>TBP</i>	F – GGTGCGAATGTGGAGTACAG R – TAGTGGCTCCAGTGCAAGTC	60	
<i>GAPDH</i>	F – CCGTGTCCCTGTTCCCTAATG R – GTCCAAGATGCCCTTCAGAG	60	
<i>EF1Aa1</i>	F – CGTGTCTGTTAAGGAACTGC R – CAAGCAATGTGAGCTGTATG	60	
<i>GPDH</i>	F – AGTTCATCAGGACGCTCTGC R – AGATCAATGCTGCCATCCTC		
<i>Tubulin</i>	F – TTGCCAGTGATGAGTTGCTC R – TAGTGGCTCCAGTGCAAGTC	60	

2.5. Statistical analysis.

GAPDH was chosen as reference gene for statistical analysis. The QuantStudio™ Design and Analysis software was used to generate cycle threshold (CT) values that were analysed by the comparative CT method ($2^{-\Delta\Delta CT}$ - Livak & Schmittgen, 2001). CT values were the evaluated with GraphPad Prism 6 and analysed using Kruskal-Wallis test followed by Dunn's multiple comparisons test options. Results appear as Mean \pm SEM. $P < 0.05$ was considered significant.

3. Results

3.1. Streptozotocin injection induces inflammation-associated signalling gene transcription in *Nauphoeta cinerea*.

We studied three target genes of JNK pathway in the *Nauphoeta cinerea* [Early growth response (*EGR1*), PDGF- and VEGF-related factor 1 (*PVFI*), and reaper (*RPR*)]. STZ injection (74 and 740 nmol/nymph) significantly upregulated *EGR1* [$H=19.52$, $P=0.0002$; Fig 1A] and *RPR* [$H=20.17$, $P=0.0002$; Fig 1B] mRNA levels. Albeit there was no significant difference in the mRNA levels of *PVFI* [$H=2.85$, $P=0.415$; Fig 1C] across groups. STZ injection (74 and 740 nmol/nymph) significantly upregulated mRNA levels of the *TOLL/NF- κ B* pathway target gene: *TOLLI* [$H=19.74$, $P=0.0002$; Fig 1D] and the activator of the *JAK/STAT* pathway; unpaired 3 (*UPD3*) [$H=19.98$, $P=0.0002$; Fig 1E]. Albeit there was no significant difference in expression of the target gene of the *JAK/STAT* pathway; Suppressor of cytokine signalling at 36E (*SCOS36E*) [$H=2.675$, $P=0.4445$; Fig 1F]

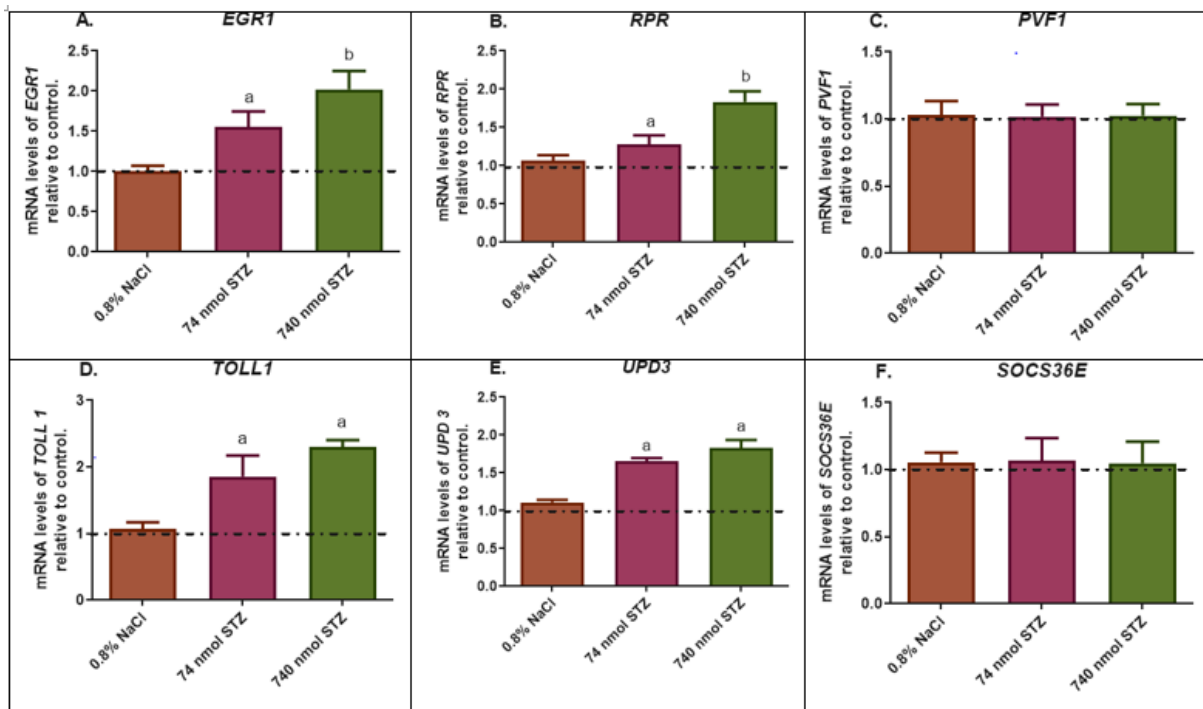


Figure 1. Streptozotocin injection induces inflammation-associated signalling in *Nauphoeta cinerea*. mRNA expression was assessed by RT-qPCR and analysed by Kruskal-Wallis test followed by Dunn's multiple comparisons test. $n = 6$. (A-C) Expression of target genes of the *JNK* pathway in *N. cinerea* 7 days after STZ injection (74 and 740 nmol/nymph). There was significant upregulation of *EGR* [$H=19.52$, $P=0.0002$] and *RPR* [$H=20.17$, $P=0.0002$], but there was no significant difference in mRNA level of *PVFI* [$H=2.85$, $P=0.415$] of STZ treated nymphs relative to control. (D). Expression of a target gene of the *TOLL/NF- κ B* pathway in *N. cinerea* 7 days after STZ injection (74 and 740 nmol/nymph). There was significant upregulation of *TOLL1* [$H=19.74$, $P=0.0002$]. (E-F). Expression of an activator and a target gene of the *UPD3/JAK/STAT* pathway in *N. cinerea* after 7 days after STZ injection (74 and 740 nmol/nymph). There was significant upregulation of *UPD3* [$H=19.98$, $P=0.0002$] and *SCOS36E* [$H=17.03$, $P=0.0007$]. All values are mean \pm SEM. Post hoc analysis by Tukey's test indicated differences among groups. Groups with different letters are significantly different from control group (shown as dotted lines) and from themselves at $p\leq 0.05$.

3.2. Streptozotocin injection activates primary antioxidant genes but has no effect on peroxiredoxin and thioredoxin genes of *Nauphoeta cinerea*.

We quantified the mRNA levels of primary antioxidant genes of *Nauphoeta cinerea* treated with streptozotocin. STZ injection (74 and 740 nmol/nymph) significantly upregulated *SOD* [H=19.74, P=0.0002; Fig 2A] and catalase [H=15.16, P=0.0001; Fig 2B] but there was no significant difference between *PRX4* mRNA levels [H=3.73, P=0.1572; Fig 2C] across groups. A hormetic response in which 74 nmol STZ injection upregulated mRNA levels of *SOD* and catalase more than 740 nmol STZ injection was recorded. We further quantified mRNA levels of second line antioxidant genes of *Nauphoeta cinerea* treated with streptozotocin. Three isoforms of *TRX* (*TRX1*, *TRX2* and *TRX5*) were measured and we found no significant difference in the mRNA levels of the *TRX*'s across groups [*TRX1* (H=2.322, P=0.5083; Fig 2D), *TRX2* [H=0.6976, P=0.8738; Fig 2E] and *TRX5* [H=1.808, P=0.6161; Fig 2F].

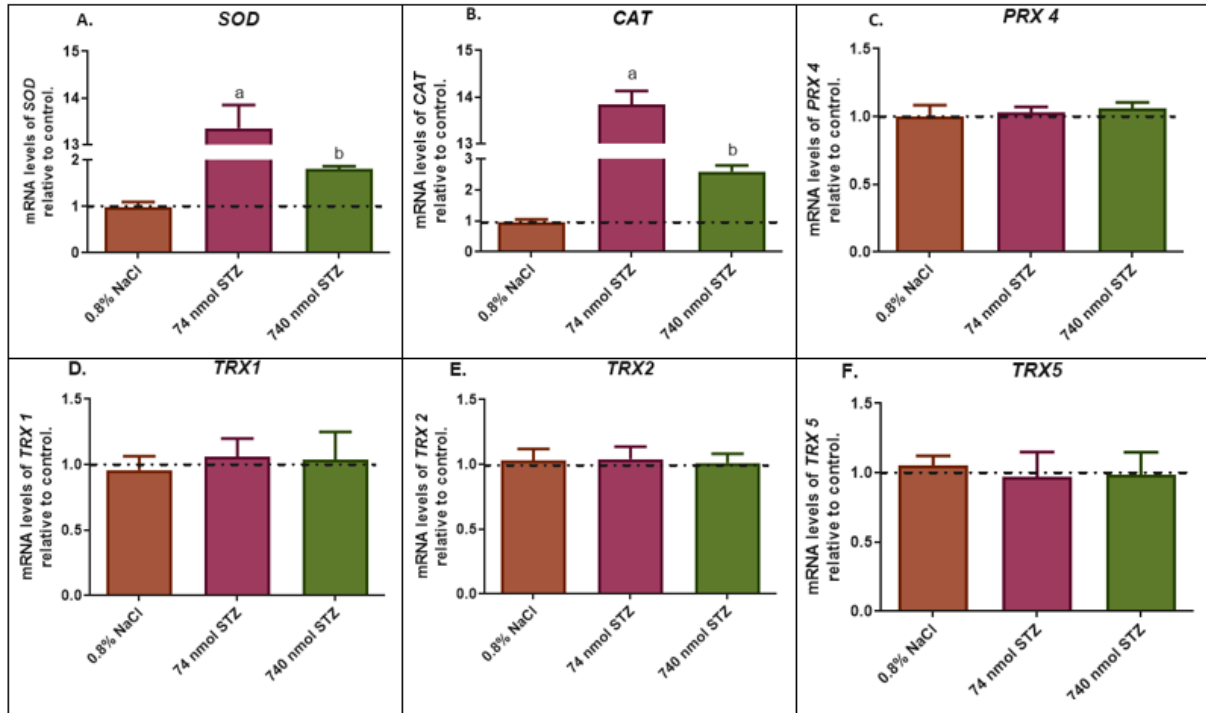


Figure 2: Streptozotocin injection activates primary antioxidant genes but has no effect on thioredoxin and peroxiredoxin genes of *Nauphoeta cinerea*. mRNA expression was assessed by RT-qPCR and analysed by Kruskal-Wallis test followed by Dunn's multiple comparisons test. n = 6. (A-C) Expression of primary antioxidants of *N. cinerea* 7 days after STZ injection (74 and 740 nmol/nymph). There was significant upregulation of significant upregulation of *SOD* [H=19.74, P=0.0002] and *CAT* [H=15.16, P=0.0001] but there was no significant difference between *PRX4* mRNA levels [H=3.73, P=0.1572] of control and STZ treated nymphs. (D-F). Expression of second line antioxidants of *N. cinerea* 7 days after STZ injection. STZ injection had so significant effect on mRNA levels of *TRX1* [H=2.322, P=0.5083], *TRX2* [H=0.6976, P=0.8738] and *TRX5* [H=1.808, P=0.6161] when compared with control. All values are mean±SEM. Post hoc analysis by Tukey's test indicated differences among groups. Groups with different letters are significantly different from control group (shown as dotted lines) and from themselves at $p \leq 0.05$.

3.3. Streptozotocin injection stimulates the *glutathione S-transferase* gene family of *Nauphoeta cinerea*.

We studied three *GST* classes (*GST sigma*, *GST delta* and *GST theta*) and found that *GST theta* had the most prominent response amongst STZ treated nymphs of *N. cinerea*. STZ injection (74 and 740 nmol/nymph) significantly upregulated *GST sigma* [H=15.16, P=0.0001; Fig 3A] and *GST theta* [H=20.72, P=0.0001; Fig 3C] but we found no significant difference in the mRNA levels of *GST delta* [H=2.032, P=0.5658] across groups. A hormetic response in which 74 nmol STZ injection upregulated mRNA levels of *GST sigma* and *GST theta* more than 740 nmol STZ injection was recorded.

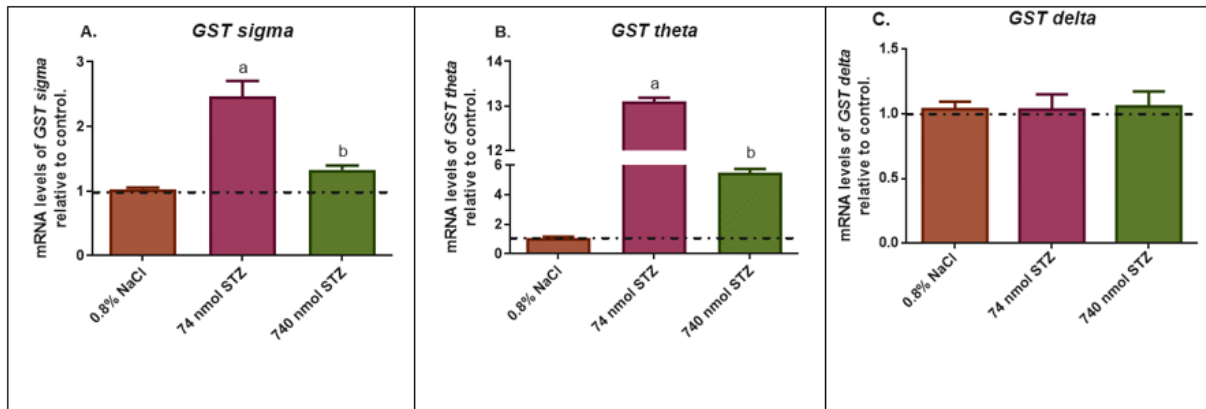


Figure 3: Relative mRNA levels of glutathione S-transferase gene family of *N. cinerea* 7 days after streptozotocin Injection (74 and 740 nmol/nymph). Kruskal-Wallis test followed by Dunn's multiple comparisons test (n=6) showed significant upregulation of *GST sigma* [H=20.72, P=0.0001] and *GST theta* [H=20.72, P=0.0001], but there was no significant difference in the expression of *GST delta* [H=2.032, P=0.5658]. All values are mean±SEM. Post hoc analysis by Tukey's test indicated differences among groups. Groups with different letters are significantly different from control group (shown as dotted lines) and from themselves at $p \leq 0.05$.

3.4. Multiple sequence alignment and evolutionary history *Neoptera cinerea* glutathione S-transferase sigma.

One hundred and twentyseven (127) glutathione S-transferase amino acid sequences were aligned to generate an unrooted neighbour joining tree for three cohorts (*polyneoptera*, *paraneoptera* and *holometabola*) of the Neoptera insect infraclass. We included all the transcripts variant available in the database. The tree showed a clear distinction of *Neoptera cinerea GST sigma* from other *GST* classes while confirming homology between Nauphoeta *GST sigma* and the sigma class of other insects (Fig 4A). A bootstrap test verified these results and the NCBI Blast platform showed a 75.98 % and 69.61 % identity between the Nauphoeta *GST sigma* and the *GST sigma* of *Blatella germanica* and *Cryptotermes secundus* respectively.

A structure-based amino acid sequence alignment between *Neoptera cinerea GST sigma* and the *GST sigma* of humans, rodents, worm and insects with known 3D-structure was done to delineate conserved secondary structure elements. *GST sigma* secondary structure elements were strongly conserved across the analysed amino acid sequences. They included the GSH binding sites and some putative electrophilic-binding sites.

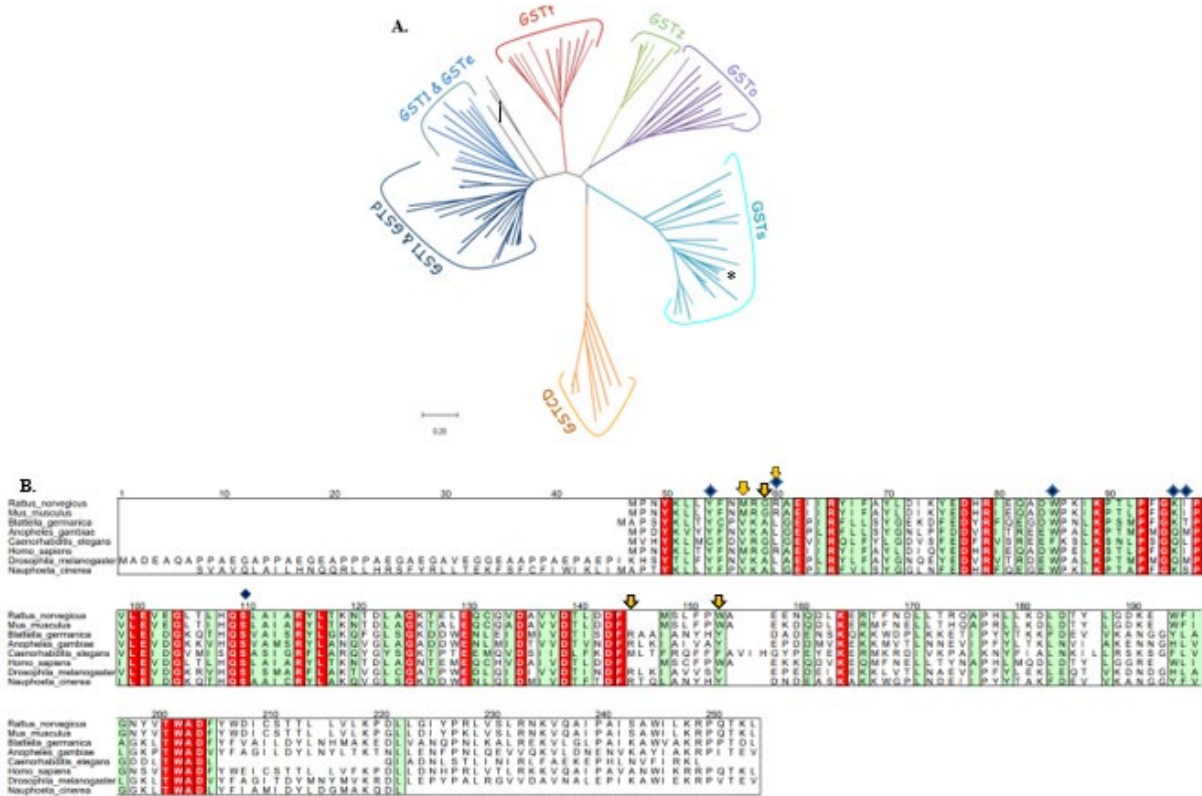


Figure 4: (A). An unrooted phylogenetic tree showing the relationship between the sigma class of *Nauphoeta cinerea* glutathione *S*-transferase (*) and representative members of other GST classes from the three cohorts (Polyneoptera, Paraneoptera, Holometabola) of the Neoptera Insect infraclass. (B). Structure-based sequence alignment of *Nauphoeta cinerea* glutathione *S*-transferase sigma and other organisms GST sigma with known tertiary structure. Regions of sequence conservation were estimated using the AMAS program built by Livingstone and Barton [36]. Strongly conserved sequences are highlighted in red, while weaker conservations are highlighted in light green, conserved sequences with known functional implications are marked in boxes. Secondary structure elements were obtained from the Protein Data Bank (<https://www.rcsb.org/>) and marked by blue diamonds to depict some putative GSH binding sites, yellow arrows to depict some putative electrophilic-binding sites. The GST sigma amino acid sequences included: Rat (*Rattus norvegicus*; O35543), Mouse (*Mus musculus*; Q9JHF7), Cockroach (*Blattella germanica*; O18598), Mosquito (*Anopheles*

gambiae; P46428), Worm (*Caenorhabditis elegans*; O16115), Human (*Homo sapiens*; O60760), Fly (*Drosophila melanogaster*; P41043), Cockroach (*Nauphoeta cinerea*; DN30377 – [29]).

Discussion

Exposure to stressors like streptozotocin, as well as the hyperglycaemic state they are known to cause may trigger the generation of reactive oxygen species [37,38], probably via the production of superoxide in the mitochondrial electron transport [39]. We herein examined the response of the lobster cockroach to increased brain glucose levels and ROS generation that we have earlier reported [23] and found significant increase in inflammation-like response via increased expression of some target genes of the *TOLL/NF- κ B*, *TNF/JNK* and *JAK/STAT* pathways. There was also a concomitant significant increase in relative mRNA levels of some primary antioxidants, and the *glutathione S-transferase* (*sigma* and *theta*) detoxification molecules, without subsequent increase in expression of secondary antioxidants. Furthermore, we delineated similarity between the *Nauphoeta cinerea GST sigma* and the *GST sigma* of other cockroaches and insects, signifying evolutionary conservation of the *GST* detoxification system.

The positive feedback control between ROS production by mitochondria and *TNF/JNK* signalling [40] may result in necrosis, but *JNK* may either repress *TNF*-induced apoptosis [41], or potentiate *TNF*-induced necrosis [42], depending on the cell type in which it is acting. We have earlier reported reduced quantifiable active cells, as well as increased ROS production in the head homogenates of cockroaches exposed to streptozotocin [23]. We herein show increased expression levels of early growth factor and reaper in STZ treated cockroaches, in consonance with findings of concurrent increase in oxidative stress and increased expression of target genes of the *TNF/JNK* pathway in *D. melanogaster*. [43,44].

The endogenous cytokine ligand, spätzle is the known *Drosophila* Toll receptor activator. The pro-protein (spätzle) is secreted as part of the insect immune response, and also in proportion to the level of ROS in the tissue [8,45]. Amongst other things, the *TOLL* pathway may mediate the elimination of unfit cells [46] through a process that has been tagged as cell competition [47]. Similarly, unpaired (*UPD*) - ligand of the *JAK/STAT* pathway is secreted in response to tissue damage [48], thereby activating macrophage-like cells to control wound repair and response to inflammation [49], with negative feedback regulation by cytokine signalling [*SOCS36E*] in the fruit fly [50,51]. We found increased mRNA levels of *TOLL1* and *UPD3* in nymphs treated with STZ, in line with studies showing activation of the *NF- κ B* and *JAK/STAT* pathways after disruption of cellular redox state of insects and mammals [52,53].

ROS generation is a natural consequence of energy metabolism in insects and mammals [54,55], It is also necessary for the functioning of crucial signalling pathways [56]. Albeit, unfettered ROS production possess significant disruption to normal metabolic processes within an organism [25,57–59]. We have earlier shown increased oxidative stress in head homogenates of STZ treated nymphs [23], suggesting that the *N. cinerea* brain is susceptible to increased ROS production after STZ treatment and is a viable model for studying disruption of energy metabolism and redox state in the brain..

We herein studied the stepwise recruitment of antioxidant enzymes by *N. cinerea* to counter ROS generation after exposure to the alkylating agent STZ and found significant increase in mRNA levels of the primary antioxidant genes; *SOD* and catalase, but there was no difference in expression levels of *PRX4*. Both the endogenous elevation of *SOD* levels and the exogenous introduction of *SOD* sources to *D. melanogaster* have been reported to mop-up free radicals and increase lifespan [60,61], while catalase is important for insect survival and fecundity

[62,63]. The basal expression of *PRX4* has been shown to be low in the mouse brain [64], and this may explain the nil difference in *PRX4* expression across our treatment groups. Insects depend on a high intracellular GSH concentration to counteract ROS formation, and a 2 GSH to GSSG ratio is an established in vivo marker of response to oxidative stress. [65]. The *TRX* system contributes to the maintenance of the required GSH concentration [16], but we found no significant difference in thioredoxin gene expression across groups, suggesting *N. cinerea*'s ability to handle some level of oxidative stress without engaging thioredoxins. Our previous finding of raised total thiol levels in STZ treated cockroaches may help explain the maintenance of cockroach GSH levels independent of thioredoxins [23].

Glutathione S-transferases are well researched because of their role in insecticide resistance [66]. Analogous to mammalian Alpha 4-4 *GST*, insect *GST sigma* catalyses the conjugation of GSH with 4-hydroxynonenal; a product of lipid peroxidation (**Reaction 3**) [19], thereby playing a crucial role in the detoxification process. *GSTs* are either located in the cytosol, mitochondria/peroxisome or microsome [67], and *GST* genes of microsomal origin have been detected in *D. melanogaster* and *Anopheles gambiae* [68,69], but most insect *GSTs* are cytosolic [66], which are either homo- or hetero-dimers ranging from 21-28kDa [70]. We found increased mRNA levels of two isoforms of the *N. cinerea* cytosolic *GST* (*sigma* and *theta*) in the treated nymphs, similar to our previous report of increased total GST enzyme activity in STZ-treated cockroaches [23]. Our results may imply that *GST s* and *GST t* are important detoxifying enzymes in *N. cinerea*.

Conclusion.

This study buttresses the use of *Nauphoeta cinerea* in the study of toxic substances, as our results are similar to inflammatory and antioxidant responses that have been recorded in mammals. We may then suppose that the toxic effect of STZ probably elicits a conserved response from insects to mammals.

Declarations:

Funding

This work is financially supported by FAPERGS/CNPq 12/2014-PRONEX: n° 16/2551-0000, FAPERGS/DOCFix-2018; CAPES/PROEX (n° 23038.004173/2019-93; n° 0493/2019; n° 88882.182125/2018-01; 88882.182123/2018-01), and INCT-EN: for Cerebral Diseases, Excitotoxicity, and Neuroprotection.

Conflicts of interest

The authors have no conflict of interest to declare.

Ethics approval

Not applicable

Availability of data and material

All data and materials used are available upon reasonable request made to the corresponding author.

Acknowledgements

Olawande C. Olagoke is a recipient of the 2017 CNPq-TWAS Postgraduate Fellowship (FR number: 3240299312).

References.

- [1] I. Lorenzen, L. Mullen, S. Bekeschus, E.M. Hanschmann, Redox Regulation of Inflammatory Processes Is Enzymatically Controlled, *Oxid. Med. Cell. Longev.* 2017 (2017). <https://doi.org/10.1155/2017/8459402>.
- [2] O.O. Oguntibeju, Type 2 diabetes mellitus, oxidative stress and inflammation: examining the links., *Int. J. Physiol. Pathophysiol. Pharmacol.* 11 (2019) 45–63. <http://www.ncbi.nlm.nih.gov/pubmed/31333808> (accessed February 22, 2020).
- [3] Y.H. Siddique, M.S. Ansari, Rahul, S. Jyoti, Effect of alloxan on the third instar larvae of transgenic *Drosophila melanogaster* (hsp70-lacZ)Bg9, *Toxin Rev.* (2018) 1–11. <https://doi.org/10.1080/15569543.2018.1472106>.
- [4] K.J. Kramer, R.M. Jacobs, R.D. Speirs, L.H. Hendmcks, Effect of vertebrate hypoglycemic and beta cell cytotoxic agents on insects, *Biochem. Physiol.* 61 (1978) 95–97. <https://pubag.nal.usda.gov/download/11675/PDF> (accessed February 23, 2020).
- [5] M.S. Cooke, M.D. Evans, M. Dizdaroglu, J. Lunec, Oxidative DNA damage: mechanisms, mutation, and disease, *FASEB J.* 17 (2003) 1195–1214. <https://doi.org/10.1096/fj.02-0752rev>.
- [6] A.R. Simon, U. Rai, B.L. Fanburg, B.H. Cochran, Activation of the JAK-STAT pathway by reactive oxygen species, *Am. J. Physiol. - Cell Physiol.* 275 (1998).

<https://doi.org/10.1152/ajpcell.1998.275.6.c1640>.

- [7] H. Blaser, C. Dostert, T.W. Mak, D. Brenner, TNF and ROS Crosstalk in Inflammation, *Trends Cell Biol.* 26 (2016) 249–261. <https://doi.org/10.1016/j.tcb.2015.12.002>.
- [8] I. Louradour, A. Sharma, I. Morin-Poulard, M. Letourneau, A. Vincent, M. Crozatier, N. Vanzo, Reactive oxygen species-dependent Toll/NF- κ B activation in the drosophila hematopoietic niche confers resistance to wasp parasitism, *Elife.* 6 (2017). <https://doi.org/10.7554/eLife.25496>.
- [9] L. Weissman, N.C. de Souza-Pinto, T. Stevnsner, V.A. Bohr, DNA repair, mitochondria, and neurodegeneration, *Neuroscience.* 145 (2007) 1318–1329. <https://doi.org/10.1016/j.neuroscience.2006.08.061>.
- [10] G.W. Felton, C.B. Summers, Antioxidant systems in insects, *Arch. Insect Biochem. Physiol.* 29 (1995) 187–197. <https://doi.org/10.1002/arch.940290208>.
- [11] P.D. Ray, B.W. Huang, Y. Tsuji, Reactive oxygen species (ROS) homeostasis and redox regulation in cellular signaling, *Cell. Signal.* 24 (2012) 981–990. <https://doi.org/10.1016/j.cellsig.2012.01.008>.
- [12] D.P. Blagojevic, G. Grubor-Lajsic, Multifunctionality of antioxidant system in insects, 2000.
- [13] Y. Wang, R. Branicky, A. Noë, S. Hekimi, Superoxide dismutases: Dual roles in controlling ROS damage and regulating ROS signaling, *J. Cell Biol.* 217 (2018) 1915–1928. <https://doi.org/10.1083/jcb.201708007>.
- [14] X. Zhang, Y. Li, J. Wang, T. Zhang, T. Li, W. Dong, E. Ma, J. Zhang, Identification and

characteristic analysis of the catalase gene from *Locusta migratoria*, *Pestic. Biochem. Physiol.* 132 (2016) 125–131. <https://doi.org/10.1016/j.pestbp.2016.03.010>.

- [15] G. Selvaggio, P.M.B.M. Coelho, A. Salvador, Mapping the phenotypic repertoire of the cytoplasmic 2-Cys peroxiredoxin – Thioredoxin system. 1. Understanding commonalities and differences among cell types, *Redox Biol.* 15 (2018) 297–315. <https://doi.org/10.1016/j.redox.2017.12.008>.
- [16] S.M. Kanzok, A. Fechner, H. Bauer, J.K. Ulschmid, H.M. Müller, J. Botella-Munoz, S. Schneuwly, R.H. Schirmer, K. Becker, Substitution of the thioredoxin system for glutathione reductase in *Drosophila melanogaster*, *Science* (80-.). 291 (2001) 643–646. <https://doi.org/10.1126/science.291.5504.643>.
- [17] M.C.J. Wilce, M.W. Parker, Structure and function of glutathione S-transferases, *Biochim. Biophys. Acta (BBA)/Protein Struct. Mol.* 1205 (1994) 1–18. [https://doi.org/10.1016/0167-4838\(94\)90086-8](https://doi.org/10.1016/0167-4838(94)90086-8).
- [18] P.G. Board, R.T. Baker, G. Chelvanayagam, L.S. Jermin, Zeta, a novel class of glutathione transferases in a range of species from plants to humans, *Biochem. J.* 328 (1997) 929–935. <https://doi.org/10.1042/bj3280929>.
- [19] S.P. Singh, J.A. Coronella, H. Beneš, B.J. Cochrane, P. Zimniak, Catalytic function of *Drosophila melanogaster* glutathione S-transferase DmGSTS1-1 (GST-2) in conjugation of lipid peroxidation end products, *Eur. J. Biochem.* 268 (2001) 2912–2923. <https://doi.org/10.1046/j.1432-1327.2001.02179.x>.
- [20] B. Agianian, P.A. Tucker, A. Schouten, K. Leonard, B. Bullard, P. Gros, Structure of a *Drosophila* sigma class glutathione S-transferase reveals a novel active site topography

- suites for lipid peroxidation products, *J. Mol. Biol.* 326 (2003) 151–165. [https://doi.org/10.1016/S0022-2836\(02\)01327-X](https://doi.org/10.1016/S0022-2836(02)01327-X).
- [21] D. Sheehan, G. Meade, V.M. Foley, C.A. Dowd, Structure, function and evolution of glutathione transferases: implications for classification of non-mammalian members of an ancient enzyme superfamily., *Biochem. J.* 360 (2001) 1–16. <https://doi.org/10.1042/0264-6021:3600001>.
- [22] M.B.S. Mota, M.A. Carvalho, A.N.A. Monteiro, R.D. Mesquita, DNA damage response and repair in perspective: *Aedes aegypti*, *Drosophila melanogaster* and *Homo sapiens*, *Parasites and Vectors.* 12 (2019) 1–20. <https://doi.org/10.1186/s13071-019-3792-1>.
- [23] O.C. Olagoke, B.A. Afolabi, J.B.T. Rocha, Streptozotocin induces brain glucose metabolic changes and alters glucose transporter expression in the Lobster cockroach ; *Nauphoeta cinerea* (*Blattodea* : *Blaberidae*), *Mol. Cell. Biochem.* (2020) 1–35. <https://doi.org/DOI: 10.1007/s11010-020-03976-4>.
- [24] B.C. Piccoli, J.C. Alvim, F.D. da Silva, P.A. Nogar, O.C. Olagoke, M. Aschner, C.S. Oliveira, J.B.T. Rocha, High level of methylmercury exposure causes persisted toxicity in *Nauphoeta cinerea*, *Environ. Sci. Pollut. Res.* (2019). <https://doi.org/10.1007/s11356-019-06989-9>.
- [25] B.A. Afolabi, O.C. Olagoke, D.O. Souza, M. Aschner, J.B.T. Rocha, A.L.A. Segatto, Modified expression of antioxidant genes in lobster cockroach, *Nauphoeta cinerea* exposed to methylmercury and monosodium glutamate, *Chem. Biol. Interact.* 318 (2020). <https://doi.org/10.1016/j.cbi.2020.108969>.
- [26] I.A. Adedara, I.O. Awogbindin, B.A. Afolabi, B.O. Ajayi, J.B.T. Rocha, E.O. Farombi,

Hazardous impact of diclofenac exposure on the behavior and antioxidant defense system in *Nauphoeta cinerea*, *Environ. Pollut.* 265 (2020) 115053. <https://doi.org/10.1016/j.envpol.2020.115053>.

[27] P. Graham, L. Pick, *Drosophila* as a Model for Diabetes and Diseases of Insulin Resistance, *Curr. Top. Dev. Biol.* 121 (2017) 1–4. <https://doi.org/10.1016/bs.ctdb.2016.07.011>.

[28] C.C. Rittschof, S. Schirmeier, Insect models of central nervous system energy metabolism and its links to behavior, *Glia.* 66 (2018) 1160–1175. <https://doi.org/10.1002/glia.23235>.

[29] A.L.A. Segatto, J.F. Diesel, E.L.S. Loreto, J.B.T. da Rocha, A.L.A. Segatto, J.F. Diesel, E.L.S. Loreto, J.B.T. da Rocha, De novo transcriptome assembly of the lobster cockroach *Nauphoeta cinerea* (Blaberidae), *Genet. Mol. Biol.* 41 (2018) 713–721. <https://doi.org/10.1590/1678-4685-gmb-2017-0264>.

[30] K. Tamura, D. Peterson, N. Peterson, G. Stecher, M. Nei, S. Kumar, MEGA5: Molecular evolutionary genetics analysis using maximum likelihood, evolutionary distance, and maximum parsimony methods, *Mol. Biol. Evol.* (2011). <https://doi.org/10.1093/molbev/msr121>.

[31] R.C. Edgar, MUSCLE: multiple sequence alignment with high accuracy and high throughput., *Nucleic Acids Res.* 32 (2004) 1792–7. <https://doi.org/10.1093/nar/gkh340>.

[32] N. Saitou, M. Nei, The neighbor-joining method: a new method for reconstructing phylogenetic trees., *Mol. Biol. Evol.* 4 (1987) 406–425. <https://doi.org/10.1093/oxfordjournals.molbev.a040454>.

- [33] M.W. Pfaffl, A. Tichopad, C. Prgomet, T.P. Neuvians, Determination of stable housekeeping genes, differentially regulated target genes and sample integrity: BestKeeper – Excel-based tool using pair-wise correlations, *Biotechnol. Lett.* 26 (2004) 509–515. <https://doi.org/10.1023/B:BILE.0000019559.84305.47>.
- [34] C.L. Andersen, J.L. Jensen, T.F. Ørntoft, Normalization of real-time quantitative reverse transcription-PCR data: A model-based variance estimation approach to identify genes suited for normalization, applied to bladder and colon cancer data sets, *Cancer Res.* 64 (2004) 5245–5250. <https://doi.org/10.1158/0008-5472.CAN-04-0496>.
- [35] K.J. Livak, T.D. Schmittgen, Analysis of relative gene expression data using real-time quantitative PCR and the $2^{-\Delta\Delta CT}$ method, *Methods.* 25 (2001) 402–408. <https://doi.org/10.1006/meth.2001.1262>.
- [36] C.D. Livingstone, G.J. Barton, Protein sequence alignments: A strategy for the hierarchical analysis of residue conservation, *Bioinformatics.* 9 (1993) 745–756. <https://doi.org/10.1093/bioinformatics/9.6.745>.
- [37] N.B.V. Barbosa, J.B.T. Rocha, D.C. Wondracek, J. Perottoni, G. Zeni, C.W. Nogueira, Diphenyl diselenide reduces temporarily hyperglycemia: Possible relationship with oxidative stress, *Chem. Biol. Interact.* 163 (2006) 230–238. <https://doi.org/10.1016/j.cbi.2006.08.004>.
- [38] M.A. Sodipo, S.I. Oyeleye, G. Oboh, J.O. Agbede, M.O. Oluwamukomi, Hypoglycemic effect of biscuits produced from flour blends of three medicinal foods on high-fat diet-streptozotocin-induced diabetic rats, *J. Food Biochem.* (2020). <https://doi.org/10.1111/jfbc.13334>.

- [39] R.L. Puntel, D.H. Roos, R.L. Seeger, J.B.T. Rocha, Mitochondrial electron transfer chain complexes inhibition by different organochalcogens, *Toxicol. Vitro*. 27 (2013) 59–70. <https://doi.org/10.1016/j.tiv.2012.10.011>.
- [40] R.J. Davis, Signal transduction by the JNK group of MAP kinases, in: *Inflamm. Process. Mol. Mech. Ther. Oppor.*, Birkhäuser Basel, 2000: pp. 13–21. https://doi.org/10.1007/978-3-0348-8468-6_2.
- [41] J.A. Lamb, J.J. Ventura, P. Hess, R.A. Flavell, R.J. Davis, JunD mediates survival signaling by the JNK signal transduction pathway, *Mol. Cell*. 11 (2003) 1479–1489. [https://doi.org/10.1016/S1097-2765\(03\)00203-X](https://doi.org/10.1016/S1097-2765(03)00203-X).
- [42] S. Papa, F. Zazzeroni, C. Bubici, S. Jayawardena, K. Alvarez, S. Matsuda, D.U. Nguyen, C.G. Pham, A.H. Nelsbach, T. Melis, E. De Smaele, W.J. Tang, L. D’Adamio, G. Franzoso, Gadd45 β mediates the NF- κ B suppression of JNK signalling by targeting MKK7/JNKK2, *Nat. Cell Biol.* 6 (2004) 146–153. <https://doi.org/10.1038/ncb1093>.
- [43] X. Wang, M. Chen, M. Zhong, Z. Hu, L. Qiu, S. Rajagopalan, N.G. Fossett, L.C. Chen, Z. Ying, Exposure to concentrated ambient PM_{2.5} shortens lifespan and induces inflammation-associated signaling and oxidative stress in *Drosophila*, *Toxicol. Sci.* 156 (2017) 199–207. <https://doi.org/10.1093/toxsci/kfw240>.
- [44] J.A. Sanchez, D. Mesquita, M.C. Ingaramo, F. Ariel, M. Milan, A. Dekanty, Eiger/TNF α -mediated Dilp8 and ROS production coordinate intra-organ growth in *drosophila*, *PLoS Genet.* 15 (2019) e1008133. <https://doi.org/10.1371/journal.pgen.1008133>.
- [45] B. Lemaitre, J. Hoffmann, The Host Defense of *Drosophila melanogaster*, *Annu. Rev.*

Immunol. 25 (2007) 697–743.

<https://doi.org/10.1146/annurev.immunol.25.022106.141615>.

- [46] S.N. Meyer, M. Amoyel, C. Bergantiños, C. De La Cova, C. Schertel, K. Basler, L.A. Johnston, An ancient defense system eliminates unfit cells from developing tissues during cell competition, *Science* (80-.). 346 (2014). <https://doi.org/10.1126/science.1258236>.
- [47] G. Morata, P. Ripoll, Minutes: Mutants of *Drosophila* autonomously affecting cell division rate, *Dev. Biol.* 42 (1975) 211–221. [https://doi.org/10.1016/0012-1606\(75\)90330-9](https://doi.org/10.1016/0012-1606(75)90330-9).
- [48] V.M. Wright, K.L. Vogt, E. Smythe, M.P. Zeidler, Differential activities of the *Drosophila* JAK/STAT pathway ligands Upd, Upd2 and Upd3, *Cell. Signal.* 23 (2011) 920–927. <https://doi.org/10.1016/j.cellsig.2011.01.020>.
- [49] R.P. Sorrentino, J.P. Melk, S. Govind, Genetic Analysis of Contributions of Dorsal Group and JAK-Stat92E Pathway Genes to Larval Hemocyte Concentration and the Egg Encapsulation Response in *Drosophila*, *Genetics.* 166 (2004) 1343–1356. <https://doi.org/10.1534/genetics.166.3.1343>.
- [50] P. Karsten, S. Häder, M.P. Zeidler, Cloning and expression of *Drosophila* SOCS36E and its potential regulation by the JAK/STAT pathway, *Mech. Dev.* 117 (2002) 343–346. [https://doi.org/10.1016/S0925-4773\(02\)00216-2](https://doi.org/10.1016/S0925-4773(02)00216-2).
- [51] A. Yoshimura, M. Suzuki, R. Sakaguchi, T. Hanada, H. Yasukawa, SOCS, inflammation, and autoimmunity, *Front. Immunol.* 3 (2012). <https://doi.org/10.3389/fimmu.2012.00020>.

- [52] R. Gill, A. Tsung, T. Billiar, Linking oxidative stress to inflammation: Toll-like receptors, *Free Radic. Biol. Med.* 48 (2010) 1121–1132. <https://doi.org/10.1016/j.freeradbiomed.2010.01.006>.
- [53] I. Kucinski, M. Dinan, G. Kolahgar, E. Piddini, Chronic activation of JNK JAK/STAT and oxidative stress signalling causes the loser cell status, *Nat. Commun.* 8 (2017) 1–13. <https://doi.org/10.1038/s41467-017-00145-y>.
- [54] D.F.S. Rolfe, G.C. Brown, Cellular energy utilization and molecular origin of standard metabolic rate in mammals, *Physiol. Rev.* 77 (1997) 731–758. <https://doi.org/10.1152/physrev.1997.77.3.731>.
- [55] L. Boardman, J.S. Terblanche, S.K. Hetz, E. Marais, S.L. Chown, Reactive oxygen species production and discontinuous gas exchange in insects, *Proc. R. Soc. B Biol. Sci.* 279 (2012) 893–901. <https://doi.org/10.1098/rspb.2011.1243>.
- [56] J. Zhang, X. Wang, V. Vikash, Q. Ye, D. Wu, Y. Liu, W. Dong, ROS and ROS-Mediated Cellular Signaling, *Oxid. Med. Cell. Longev.* 2016 (2016) 1–18. <https://doi.org/10.1155/2016/4350965>.
- [57] P. Newsholme, E.P. Haber, S.M. Hirabara, E.L.O. Rebelato, J. Procopio, D. Morgan, H.C. Oliveira-Emilio, A.R. Carpinelli, R. Curi, Diabetes associated cell stress and dysfunction: Role of mitochondrial and non-mitochondrial ROS production and activity, *J. Physiol.* 583 (2007) 9–24. <https://doi.org/10.1113/jphysiol.2007.135871>.
- [58] A.T. Salami, O.A. Odukanmi, C.O. Olagoke, T.O. Iyiola, S.B. Olaleye, Role of Nitric Oxide and Endogenous Antioxidants in Thyroxine Facilitated Healing of Ischemia-Reperfusion Induced Gastric Ulcers, *J. Pharm. Res.* 12 (2016) 189–206.

<http://www.nigjpharmres.com>.

- [59] B.A. Afolabi, O.C. Olagoke, High concentration of MSG alters antioxidant defence system in lobster cockroach *Nauphoeta cinerea* (Blattodea: Blaberidae), *BMC Res. Notes*. 13 (2020) 217. <https://doi.org/10.1186/s13104-020-05056-8>.
- [60] I. Reveillaud, A. Niedzwiecki, K.G. Bensch, J.E. Fleming, Expression of Bovine Superoxide Dismutase in *Drosophila melanogaster* Augments Resistance to Oxidative Stress, 1991. <http://mcb.asm.org/>.
- [61] W.C. Orr, R.S. Sohal, Does overexpression of Cu,Zn-SOD extend life span in *Drosophila melanogaster*?, 2003. www.elsevier.com/locate/expgero.
- [62] H. Diaz-Albiter, R. Mitford, F.A. Genta, M.R.V. Sant'Anna, R.J. Dillon, Reactive oxygen species scavenging by catalase is important for female *Lutzomyia longipalpis* fecundity and mortality, *PLoS One*. 6 (2011). <https://doi.org/10.1371/journal.pone.0017486>.
- [63] B. Rasool, B. Karpinska, J. Pascual, S. Kangasjärvi, C.H. Foyer, Catalase, glutathione, and protein phosphatase 2A-dependent organellar redox signalling regulate aphid fecundity under moderate and high irradiance, *Plant. Cell Environ*. 43 (2020) 209–222. <https://doi.org/10.1111/pce.13669>.
- [64] J. Goemaere, B. Knoop, Peroxiredoxin distribution in the mouse brain with emphasis on neuronal populations affected in neurodegenerative disorders, *J. Comp. Neurol*. 520 (2012) 258–280. <https://doi.org/10.1002/cne.22689>.
- [65] R.S. Sohal, L. Arnold, W.C. Orr, Effect of age on superoxide dismutase, catalase,

glutathione reductase, inorganic peroxides, TBA-reactive material, GSH/GSSG, NADPH/NADP⁺ and NADH/NAD⁺ in *Drosophila melanogaster*, *Mech. Ageing Dev.* 56 (1990) 223–235. [https://doi.org/10.1016/0047-6374\(90\)90084-S](https://doi.org/10.1016/0047-6374(90)90084-S).

[66] A.A. Enayati, H. Ranson, J. Hemingway, Insect glutathione transferases and insecticide resistance, *Insect Mol. Biol.* 14 (2005) 3–8. <https://doi.org/10.1111/j.1365-2583.2004.00529.x>.



[67] E. Birben, U.M. Sahiner, C. Sackesen, S. Erzurum, O. Kalayci, Oxidative stress and antioxidant defense, *World Allergy Organ. J.* 5 (2012) 9–19. <https://doi.org/10.1097/WOX.0b013e3182439613>.

[68] G. Toba, T. Aigaki, Disruption of the Microsomal glutathione S-transferase-like gene reduces life span of *Drosophila melanogaster*, *Gene.* 253 (2000) 179–187. [https://doi.org/10.1016/S0378-1119\(00\)00246-8](https://doi.org/10.1016/S0378-1119(00)00246-8).

[69] H. Ranson, C. Claudianos, F. Ortelli, C. Abgrall, J. Hemingway, M. V. Sharakhova, M.F. Unger, F.H. Collins, R. Feyereisen, Evolution of supergene families associated with insecticide resistance, *Science* (80-.). 298 (2002) 179–181. <https://doi.org/10.1126/science.1076781>.

[70] J.D. Hayes, J.U. Flanagan, I.R. Jowsey, Glutathione Transferases, *Annu. Rev. Pharmacol. Toxicol.* 45 (2005) 51–88. <https://doi.org/10.1146/annurev.pharmtox.45.120403.095857>.

5.3. Manuscript 1: Transcriptional signatures predictive of brain glucose metabolic alterations in streptozotocin-treated *Nauphoeta cinerea*.

 					
<small> LOGOUT • HELP • REGISTER • UPDATE MY INFORMATION • JOURNAL OVERVIEW MENU • CONTACT US • SUBMIT A MANUSCRIPT • INSTRUCTIONS FOR AUTHORS • PRIVACY </small>					
			Role: Author	Username: jbtrocha@yahoo.com.br	
Submissions Being Processed for Author JOAO BATISTA TEIXEIRA Teixeira ROCHA, PhD					
Page: 1 of 1 (1 total submissions)			Display 10 results per page.		
Action	Manuscript Number	Title	Initial Date Submitted	Status Date	Current Status
Action Links	BIOCHI-D-21-00138	Transcriptional signatures predictive of brain glucose metabolic alterations in streptozotocin-treated <i>Nauphoeta cinerea</i> .	13/02/2021	18/02/2021	With Editor

Transcriptional signatures predictive of brain glucose metabolic alterations in streptozotocin-treated *Nauphoeta cinerea*.

Olawande C. Olagoke¹, Ana L. A. Segatto², Blessing A. Afolabi³, Michael Aschner⁴, João B. T. Rocha^{1*}

¹Departamento de Bioquímica e Biologia Molecular, Centro de Ciências Naturais e Exatas (CCNE), Universidade Federal de Santa Maria, 97105-900 Santa Maria, RS, Brasil.

²Instituto Federal de Educação, Ciência e Tecnologia do Rio Grande do Sul, RS, Brasil.

³Department of Biochemistry, Bowen University, Iwo, Osun State, Nigeria.

⁴Department of Molecular Pharmacology, Albert Einstein College of Medicine, Bronx, NY, USA.

*Corresponding Author

João B. T. Rocha,

Departamento de Bioquímica e Biologia Molecular, CCNE,
Universidade Federal de Santa Maria, 97105-900 Santa Maria, RS, Brasil.

Fax: +55 55 8104 0207.

E-mail: jbtrocha@gmail.com; jbtrocha@yahoo.com.br

ORCID

Olawande C. Olagoke: 0000-0001-9212-4948

Ana L. A. Segatto: 0000-0002-5044-1168

Blessing A. Afolabi: 0000-0003-4276-0123

Michael Aschner: 0000-0002-2619-1656

João B. T. Rocha: 0000-0003-3829-0595

Abstract

The use of insects to model molecular events that characterize degenerative conditions such as diabetes was originally met with scepticism. However, the discovery of insect insulin-like peptides in the 1970's and the subsequent demonstration of evolutionary conservation of insulin-related signalling from insects to mammals have highlighted the importance and reduced cost of insect models in diabetes research. For example, *Drosophila melanogaster* has been used to screen genes that are implicated in glucose toxicity. Here, we expand on our earlier described modelling of streptozotocin-induced brain glucose metabolic disruption in *Nauphoeta cinerea* using RNA sequencing analysis to study transcriptional and genetic signatures of hyperglycemia in the lobster cockroach, in an attempt to provide a framework for future studies into the deregulation of brain energy metabolism in neurodegenerative conditions. Nymphs were randomly divided into three groups: Control (0.8 % NaCl), and two single streptozotocin injection doses (74 nmol and 740 nmol). The signatures of brain glucose metabolic alteration featured a deregulation of 226 genes at high dose STZ treatment and 278 genes at the low dose, including genes encoding ribosomal proteins and forkhead box (FoxO) that genome wide association studies (GWAS) have previously identified in relation to organ-specific diabetes modifications in mammals. Other significantly modified transcripts included genes encoding BAT 4 protein, pyruvate dehydrogenase protein, GTP cyclohydrolase 1 and cuticle protein 7, amongst others. Taken together, this study highlights the remarkable opportunity for *Nauphoeta cinerea* use as an experimental organism in diabetes research.

Keywords: Ribosomal protein; FoxO; Gene ontology; RNA-seq; Next-gen sequencing;

Transcriptome.

1. Introduction.

Streptozotocin (STZ) is an alkylating agent used to model diabetes or to treat metastatic pancreatic islet carcinoma in humans (National Center for Biotechnology Information, 2020). STZ specifically targets the mammalian beta cells, but there are evidences of both direct and indirect effects of STZ administration in other mammalian and insect organs (Knoll et al., 2005; Olagoke et al., 2020). Modelling of the systemic effects of STZ is helpful in deciphering therapeutic sites for pancreatic cancer treatment and enhance the development of models of diabetes and neurodegenerative diseases such as Alzheimer's disease (Abdollahi & Hosseini, 2014).

Chronic hyperglycaemic state is known to predispose to end organ damage via two major mechanisms, including a passive shunt of excess reducing sugar (glucose) through metabolic pathways (Giacco & Brownlee, 2010) and an active modification of neural gene expression profile in the central nervous system (Brownlee M, 2001). In this study, we used RNA-seq transcriptomic and bioinformatics approach to describe expression changes after STZ injection in the lobster cockroach in order to better understand the effects of STZ in the nervous system of insects.

High throughput next generation sequencing techniques like RNA-seq allow for characterizing complex molecular events like the qualitative and quantitative characterization of genetic materials that enable the organization of biological systems (Cembrowski & Menon, 2018; Costa-Silva et al., 2017). Considering that there is no requirement for a prior delineation of the genome sequence of the organism involved (Collins et al., 2008), this sequencing-by-synthesis method has been used in transcriptional profiling, differential gene expression analysis, RNA editing and single nucleotide polymorphism identification, amongst others

(Schuster, 2008). As such, RNA-seq has been invaluable in advancing novel hypotheses on the aetiology and progression of degenerative diseases, thereby highlighting pathophysiological mechanisms.(Costa et al., 2013; Dixit et al., 2016).

We herein describe STZ-induced changes to the entire head transcriptome of *Nauphoeta cinerea* nymphs in a bid to explore the underlying mechanisms of the diabetes-like phenotypes that we have earlier described (Olagoke et al., 2020). Even though there is currently no complete *Nauphoeta cinerea* genome sequence, our laboratory has previously published the transcriptome of *Nauphoeta cinerea* head and fat body (Segatto, Diesel, Loreto, & da Rocha, 2018). In this study, more than 157 million high quality reads were gotten from about 183 million total reads via the Illumina semiconductor sequencing method. The differential expression of genes between STZ-treated and control nymphs was analysed, and relative expression analyses were carried out to validate the most prominently deregulated protein-coding genes.

2. Materials and Methods.

2.1. Chemicals

All reagents used for these protocols were purchased from Thermo Fisher scientific Inc, USA, except otherwise stated.

2.2. Insect husbandry.

The lobster cockroach *Nauphoeta cinerea* was bred at the Biochemical Toxicology Laboratory of the Centre for Natural and Exact Sciences, Universidade Federal de Santa Maria, Brazil. Randomly selected nymphs weighing between 0.25 and 0.31 mg were acclimatized in white translucent cuboid containers measuring 21.5 cm by 21.5 cm by 8.2 cm.. Acclimatization lasted for one week under similar conditions as the treatment period, including: mean temperature of 24°C with minimum and maximum variation of about 3°C; minimum and maximum humidity of 57 and 75% respectively; light and dark cycle of 12 hours each; and unlimited access to water and feed (composed as described in (Olagoke et al., 2020)).

2.3. Streptozotocin treatment

One hundred and twenty nymphs (male and female) were assigned to three groups of forty (40) cockroaches each, namely: Control [20 µl 0.8% NaCl injection / nymph], and two groups of streptozotocin treatment [20 µl 74 nmol STZ injection / nymph and 20 µl 740 nmol STZ injection / nymph]. Powdery streptozotocin was dissolved in 0.8 % sodium chloride (NaCl). Furthermore, previous studies showed no significant difference between biochemical parameters of intact (non-injected) nymphs and nymphs injected with 0.8 % NaCl (Olagoke et al., 2020), therefore, the control group consisted of nymphs injected with 0.8 % NaCl. All injections were made in the second right dorsal thoracic segment of the nymphs.

2.4. RNA extraction and Illumina sequencing.

Nymphs were anesthetized on ice and their heads were excised for total RNA extraction with the Trizol™ (ThermoFisher scientific, USA) protocol. The quality of extracted RNA was measured by spectrophotometry (ThermoFisher scientific NanoDrop™ 2000 at 260/280 nm), agarose gel electrophoresis (electrophoresis power supply made by Loccus Biotecnologia, Brasil) and capillary electrophoresis (Agilent Technologies Bioanalyzer 2100 using the Agilent RNA 6000 Nano Kit). The quantification was made using fluorometry (ThermoFisher scientific Qubit™ 4 fluorometer, using the Qubit™ RNA assay kit protocol). Ten µg total RNA was purified with the ThermoFisher scientific Dynabeads™ mRNA purification kit protocol.

Purified RNA was used to prepare the requisite library using ThermoFisher scientific Ion Total RNA-Seq Kit v2. Library pools were quantified using Invitrogen Qubit™ dsDNA HS Assay Kit. The quality of pools was checked using Life Technologies Ion Sphere™ Quality Control Kit. Template preparation and sequencing was done using Thermo Fisher Scientific Ion 540™ Kit - OT2. The sequencing was performed on the Ion S5™ system (ThermoFisher scientific, USA) and the data were collected using Torrent Suite v4.0 software.

2.5. Quality verification and de novo transcriptome assembly

The quality of reads generated by the next gen sequencing system was ascertained on the FastQC platform <https://www.bioinformatics.babraham.ac.uk/projects/fastqc/> and Trimmomatic (Bolger et al., 2014) was used to trim low quality reads and adapters at default values. Given the unavailability of a reference genome for *Nauphoeta cinerea*, we made a de

novo transcriptome assembly from our RNA-seq data using Trinity (Grabherr et al., 2011; Segatto, Diesel, Loreto, & da Rocha, 2018). We analysed the quality of the assembled transcripts by computing contig Ex90N50 statistic and Ex90 transcript count (Grabherr et al., 2011), and assessed the transcriptome completeness by benchmarking universal single-copy orthologs (BUSCO) (Simão et al., 2015). The bioinformatic analyses were performed on the European Galaxy web platform <https://usegalaxy.eu/>.

2.6. Analysis of differentially expressed genes.

RNA-Seq data were pseudo-aligned to a reference transcriptome and counted using Kallisto quant (Bray et al., 2016) on Galaxy version 0.46.0.4 with an average fragmentation length of 100, standard deviation of fragmentation length of 20, and 100 bootstrap replications. Count data were analysed with Limma (Law et al., 2014; Smyth, 2005) on Galaxy Version 2.1 (<https://usegalaxy.org/>) and the transcripts were annotated on the Blast2Go platform (<https://www.blast2go.com>). A cut-off for adjusted p-value was set at <0.05, genes with positive logFC (difference between sample and baseline) were considered up regulated while genes with negative logFC were considered down regulated and sequence of each differentially expressed gene was extracted from the previously described Trinity assembled transcripts by filtering FASTA on headers and sequences in Galaxy Version 2.1. The GOs obtained from Blast2Go annotation were organized using REVIGO (Supek et al., 2011).

2.7. Identification of *Nauphoeta cinerea* genes and primer design.

Coding sequences of relevant Blattodea genes were downloaded from NCBI (National center for biotechnology information – <https://www.ncbi.nlm.nih.gov/>) and used to query our transcriptome (Segatto, Diesel, Loreto, da Rocha, et al., 2018) as we have earlier described

(Afolabi et al., 2020; Olagoke et al., 2020). The resulting *Nauphoeta cinerea* sequences were used to compute relative transcriptional expressions and mRNA levels of deregulated genes. Primers for RT-qPCR were designed on <https://primer3.ut.ee/> and verified using OligoAnalyzer (<https://www.idtdna.com/pages/tools/oligoanalyzer>). Primer details include: GaPDH sense CCGTGTCCCTGTTCCCTAATG, antisense GTCCAAGATGCCCTTCAGAG; GPDH sense AGTTCATCAGGACGCTCTGC, antisense AGATCAATGCTGCCATCCTC; EF1a1 sense CGTGTCTGTTAAGGAACTGC, antisense CAAGCAATGTGAGCTGTATG; Tubulin sense TTGCCAGTGATGAGTTGCTC, antisense TAGTGGCTCCAGTGCAAGTC; FoxO sense TCATTCACGGCACTCACCTA, antisense GGTGCTGAGTCACAAGTCCA.

2.8. Validation of differentially expressed genes by reverse transcription quantitative polymerase chain reaction (RT-qPCR)

The Trizol™ reagent protocol was used to extract total RNA from cockroach heads. Sample purity was ascertained by DNase treatment (Invitrogen™ protocol), spectrophotometry (NanoDrop™ 2000 at 260/280nm) and agarose gel electrophoresis. Complementary DNA was synthesized from 1 µg total RNA (Invitrogen™ protocol), using the T100™ Thermal Cycler (BIO-RAD, China). RT-qPCR was carried out using the QuantStudio 3 RT-qPCR System (ThermoFisher scientific, USA), with wells containing 10ng cDNA and 10µl reaction mix comprising [0.2µM of each primer, 1X buffer, 0.2mM dNTP, 2mM MgCl₂, 0.1X SYBR green, 0.25U Platinum Taq DNA Polymerase and ultra-pure deionized water]. The PCR cycling involved: 94oC for 5min; 40 cycles of 94oC for 15 s, 60oC for 10 s and 72oC for 30 s; and 1 cycle of 94oC for 10 s, 55oC for 1min and 94oC for 15 s. Primer efficacy was ascertained using pools from all samples as has been previously described (Olagoke et al., 2020).

2.9. Relative expression validation of differentially expressed genes.

Nucleotide sequences of relevant *Nauphoeta cinerea* genes were generated as described in section 2.7.. Results of trimmed transcripts [in section 2.5] of each group were then mapped to the nucleotide sequence of the target gene on the Geneious 9.1.8 platform (Biomatters, New Zealand) as we illustrated in Piccoli et al., 2020 (Piccoli et al., 2020). The relative expression of each target gene was then calculated using the equation:

$$\left(\frac{\text{No of mapped nucleotide in the sample} \div \text{No of coding sequence nucleotides in the target gene}}{\quad} \right)$$

The ensuing data were presented as Reads Per Kilobase Million (RPKM).

2.10. Statistical analysis.

Gene ontology domains were summarised using REVIGO and frequency of deregulation was presented as percentages. The specific deregulated genes were then annotated using LogFC on Blast2Go, with significant deregulation set at adjusted p value of 0.05.

RT-qPCR data was generated on the QuantStudio™ design and analysis software, evaluated with the comparative C_T method, and analysed with the GraphPad Prism 6 software using Kruskal-Wallis test, followed by Dunn's multiple comparisons test. mRNA levels were expressed as mean ± standard error of mean (SEM) and significance set at p≤0.05.

Differential expression of genes was verified on the Geneious 9.1.8 platform and analysed using two-way ANOVA [2 (rps3 and rps6) x 3 (0.8 % NaCl, 74 nmol STZ and 740 nmol STZ) factorial design] and Tukey's *post hoc* test on GraphPad Prism 6. Reads Per Kilobase

Million (RPKM) were expressed as mean \pm standard error of mean (SEM) and significance set at $p \leq 0.05$.

3. Results.

3.1. RNA-seq transcriptome characteristics.

The head RNA-seq transcriptional profile of *Nauphoeta cinerea* nymphs 7 days after 74 and 740 nmol STZ injection is summarised in **Table S1**. A total of 183,083,728 raw reads were sequenced, and there were 157,762,819 reads after low quality reads and adapters were trimmed with Trimmomatic. The trimmed reads were then used for further transcriptome assembly, annotation, and analysis. The quality of assembled transcripts that was ascertained by computing contig Ex90N50 statistic and Ex90 transcript count is shown in **Figure S1**. There were 504 highly expressed transcripts which made up 88% of total normalized expression data (Ex90N50). Furthermore, the completeness of assembled transcripts that was assessed by benchmarking universal single copy orthologs (BUSCO) is shown in **Figure S2**. The insecta orthologous gene library was employed and a total of 1367 BUSCO groups were searched, of which 789 (57.7%) were complete [complete and single-copy BUSCOs: 474 (34.7%); complete and duplicated BUSCOs: 315 (23.0%)]. There were 358 (26.2%) fragmented BUSCOs and 220 (16.1%) missing BUSCOs.

3.2. Functional annotation of assembled transcripts.

The Kallisto quantification summary of differentially expressed genes with $p < 0.05$ is shown as a Venn diagram in **Figure 1**. A total of 254 genes were up regulated in the 74 nmol STZ vs control group, 114 genes in the 740 nmol STZ vs the control group, and 68 genes in the 74 vs the 740 nmol STZ treatment groups. Conversely, 24 genes were down regulated in the 74 nmol STZ vs control group, 112 genes in the 740 nmol STZ vs the control group, and 24 genes in the 74 vs the 740 nmol STZ.

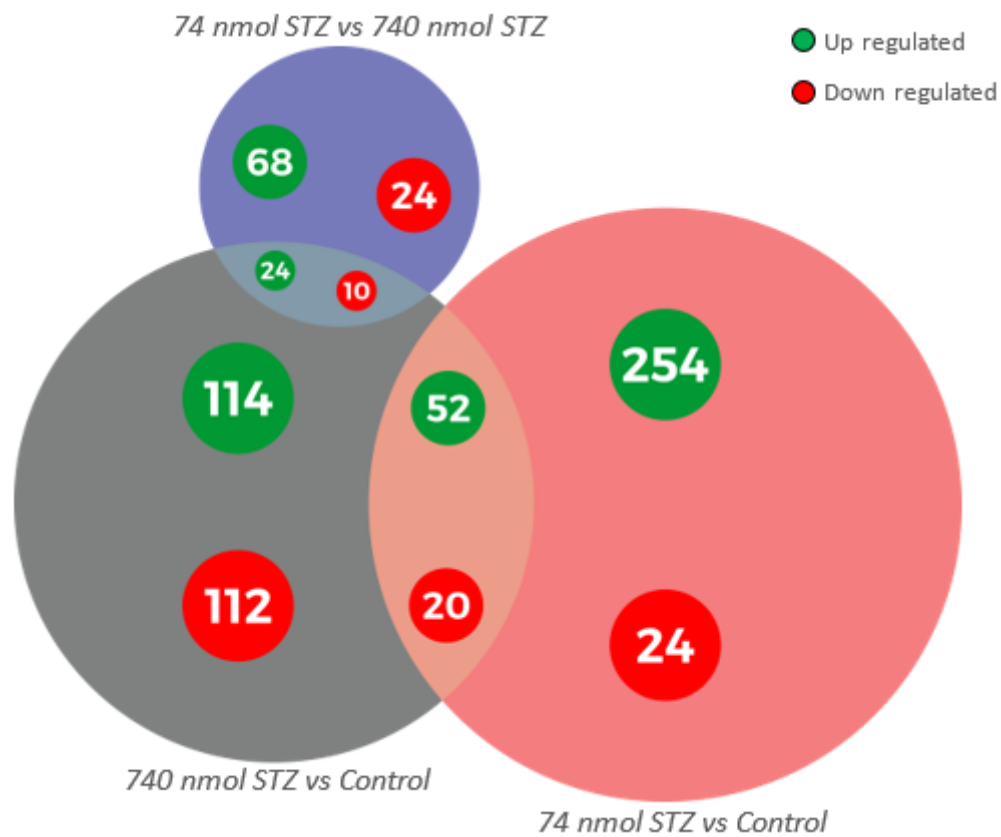


Figure 1. Venn diagram showing up (green) and down (red) regulated genes in *Nauphoeta cinerea* 7 days after single injection with 74 and 740 nmol STZ. Transcript isoform levels were quantified using Kallisto ($p \leq 0.05$) and the intersection between them was calculated on <http://bioinformatics.psb.ugent.be/webtools/Venn/>

3.3. Gene ontology domains of deregulated genes

The gene ontology domains modulated by STZ treatment are represented as: biological process, cellular component and molecular function, with the most predominantly affected domain been molecular function. **Figure 2** shows the comparison of 74 nmol STZ treatment with control. Metabolic process, oxidation-reduction process and regulation of transcription DNA-templated were the most predominant biological processes, while membrane, integral component of membrane and cytoplasm were the most predominant cellular components, and catalytic activity, hydrolase activity, nucleic acid binding were the most predominant molecular functions. **Figure 3** shows the comparison of 740 nmol STZ treatment with control. Oxidation-reduction process, transmembrane transport and proteolysis were the most predominant biological processes, while membrane, integral component of membrane and mitochondrion were the most predominant cellular components, and hydrolase activity, nucleic acid binding and transferase activity were the most predominant molecular functions. **Figure 4** shows the comparison of 74 nmol STZ treatment with 740 nmol STZ treatment. Cation transport, transmembrane transport and oxidation-reduction process were the most predominant biological processes, while membrane was the most predominant cellular components, and cation transmembrane transporter activity, carboxylic ester hydrolase activity and hydrolase activity were the most predominant molecular functions.

Blast2Go was used to annotate the specific deregulated genes in the gene ontology domains (biological process, cellular component, molecular function). Genes with positive logFC were considered up regulated while genes with negative logFC were considered down regulated. Ribosomal protein was the most prominent up regulated gene in both the 74 nmol STZ vs control and 740 nmol STZ vs control groups. In the 74 nmol vs control group, BAT4-like

protein and histone-lysine n-methyltransferase setmar-like protein had the highest up regulation while pyruvate dehydrogenase protein X component mitochondrial-like, nesprin-1 and Zinc transporter 9 had the most significant downregulation (**Figure 5**). Conversely, in the 740 nmol STZ vs control group, GTP cyclohydrolase 1, Annexin B9 and fibrillin-1-like had the highest up regulation, while cuticle protein 7, paramyosin and chromatin complexes had the most significant downregulation (**Figure 6**).

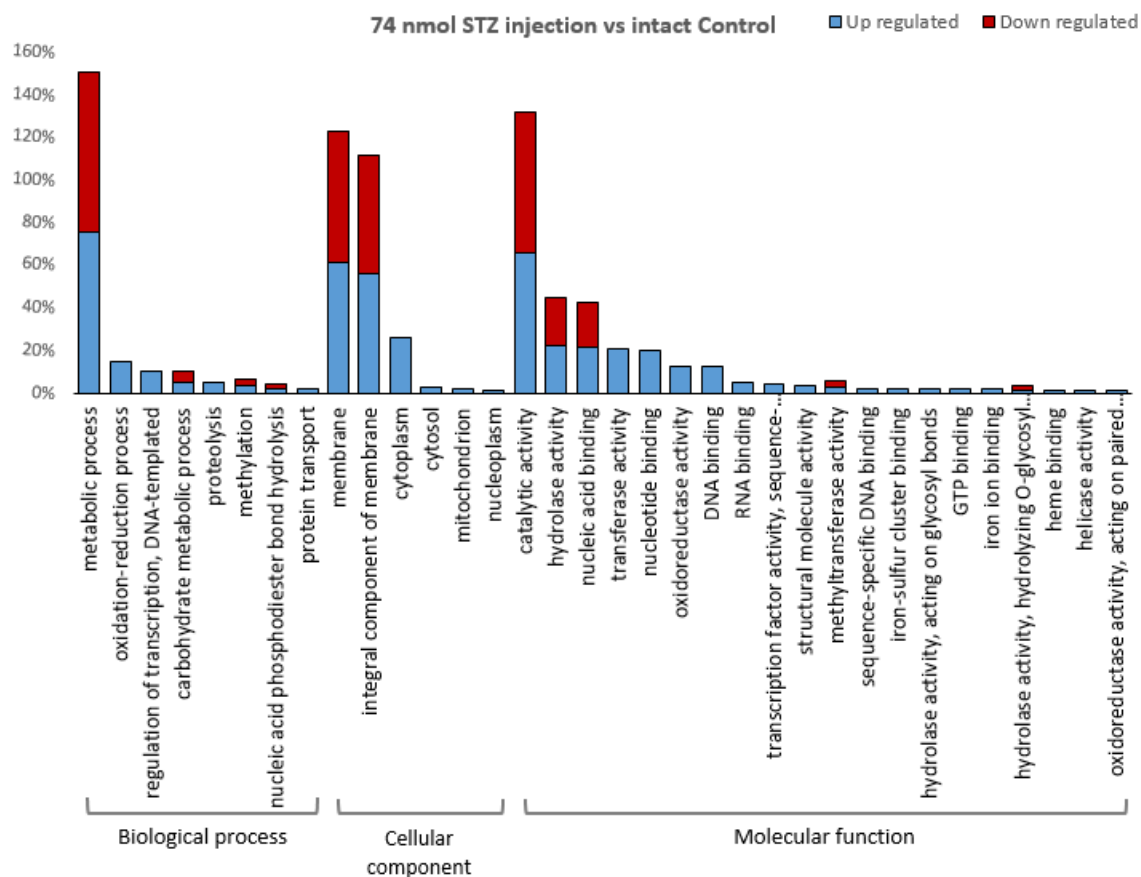


Figure 2: Gene ontology analysis of deregulated genes in STZ-treated *Nauphoeta cinerea*.

Graphs show the frequency of significantly deregulated genes when comparing 74 nmol STZ treatment with Control (0.8% NaCl) for molecular function, cellular component and biological process after 7 days. The full range of significantly deregulated genes is shown in Table S2.

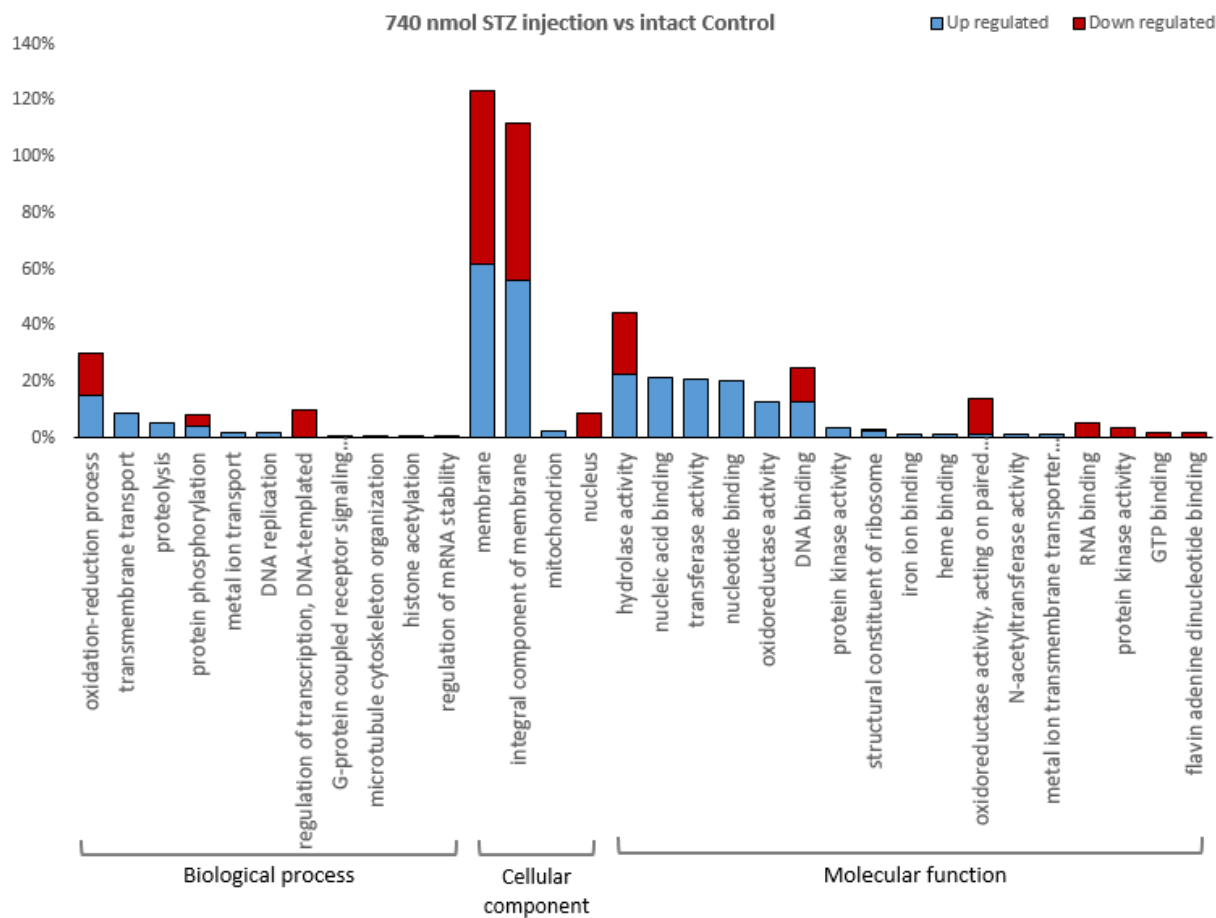


Figure 3: Gene ontology analysis of deregulated genes in STZ-treated *Nauphoeta cinerea*. Graphs show the frequency of significantly deregulated genes when comparing 740 nmol STZ treatment with Control (0.8% NaCl) for molecular function, cellular component and biological process after 7 days. The full range of significantly deregulated genes is shown in Table S2.

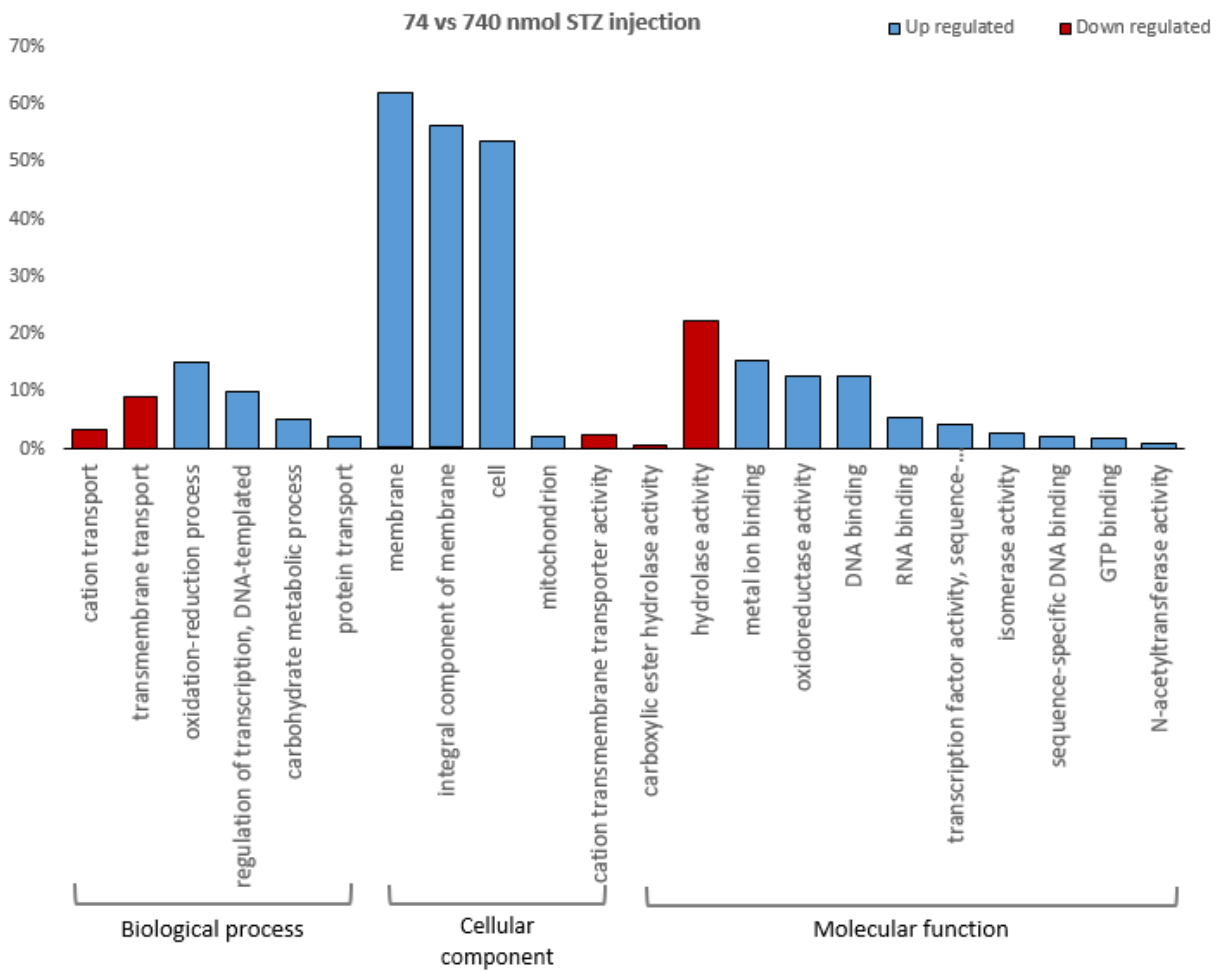


Figure 4: Gene ontology analysis of deregulated genes in STZ-treated *Nauphoeta cinerea*.

Graphs show the frequency of significantly deregulated genes when comparing 74 nmol STZ treatment with 740 nmol STZ treatment for molecular function, cellular component and biological process after 7 days. The full range of significantly deregulated genes is shown in Table S2.

3.4. Relative expression validation of deregulated genes.

A part of the therapeutic intervention for obesity, diabetes and cancer involves inhibiting the downstream effector of the rapamycin (mTOR) pathway; ribosomal protein S6. We have found translational up regulation of ribosomal protein, therefore we focused on the possible streptozotocin-induced deregulation of ribosomal proteins S3 and S6.

74 nmol STZ vs control

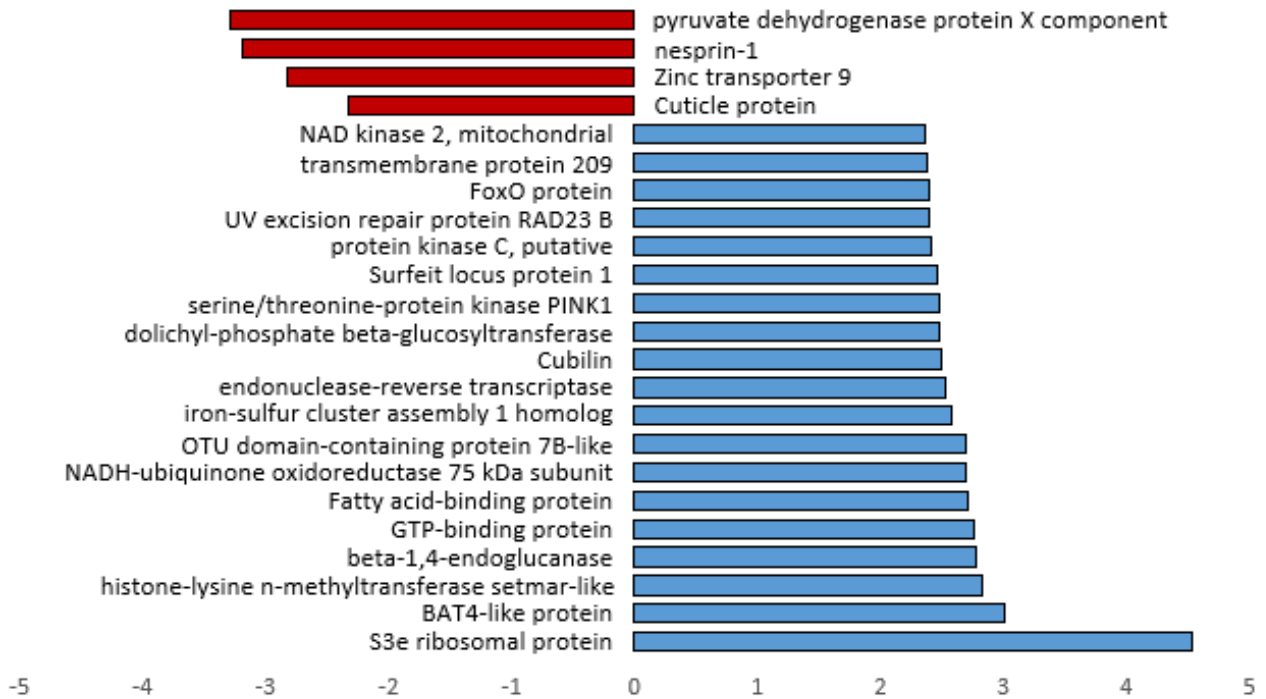


Figure 5: Significantly deregulated genes 7 days after 74 nmol STZ treatment in *Nauphoeta cinerea*. Blast2Go was used to compute the significant deregulation of genes by LogFC when comparing 74 nmol STZ treatment with control. Positive LogFC values denote up regulation (shown as blue bars) while negative logFC values denote down regulation (shown as red bars). Cut-off for up regulated genes shown here is set at 2.35 and the full range of significantly deregulated genes is shown in Table S3.

740 nmol STZ vs control

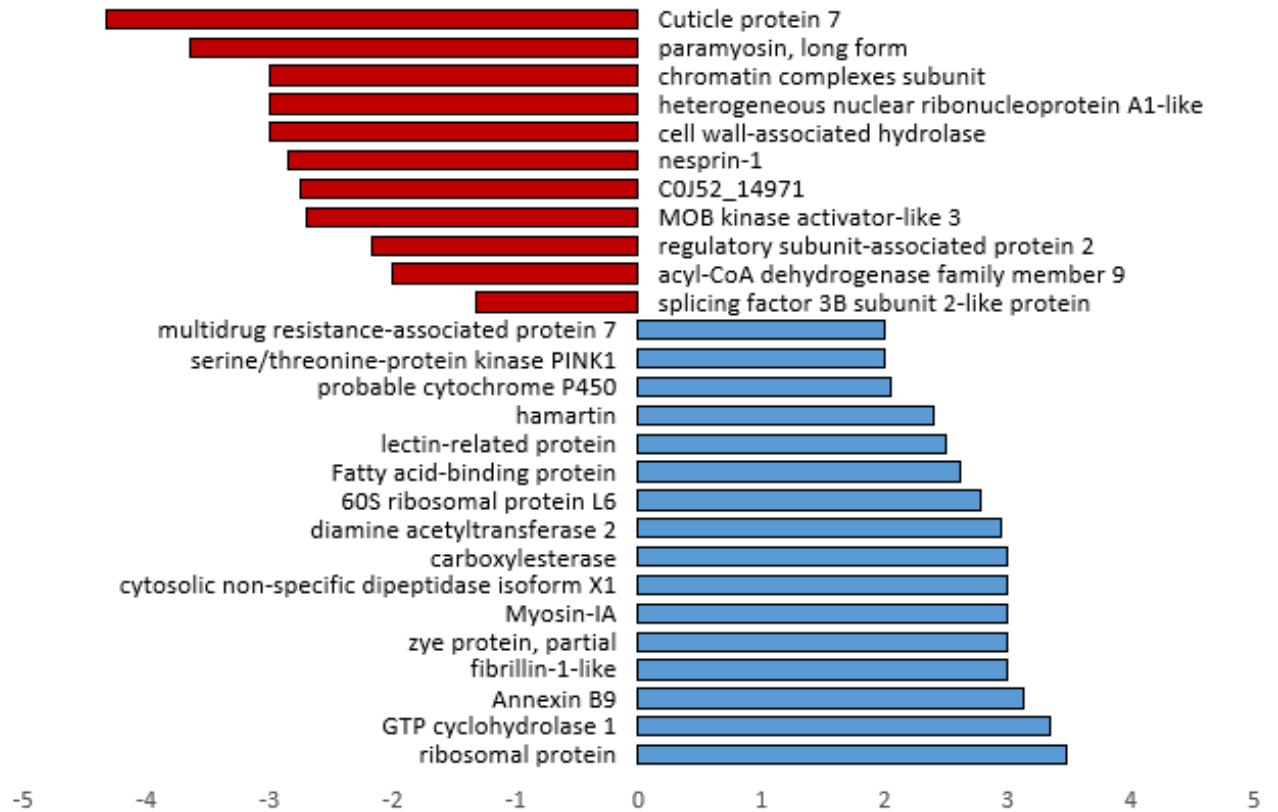


Figure 6: Significantly deregulated genes 7 days after 740 nmol STZ treatment in *Nauphoeta cinerea*. Blast2Go was used to compute the significant deregulation of genes by LogFC when comparing 740 nmol STZ treatment with control. Positive LogFC values denote up regulation (shown as blue bars) while negative logFC values denote down regulation (shown as red bars). The full data of significantly deregulated genes is shown in Table S3.

3.5. Relative expression validation of ribosomal proteins.

Ribosomal protein was the most significantly upregulated protein both in the 74 and 740 nmol vs control groups. The eukaryotic ribosome that synthesizes the cellular proteome is a ribonucleoprotein complex of about 80 proteins and four ribonucleic acids. Of the ribosomal proteins, the 40S ribosomal protein S6 has been implicated in degenerative diseases such as diabetes, and the 40S ribosomal protein S3 was strongly upregulated in our transcriptional profile of streptozotocin treated nymphs. We therefore evaluated the relative expression of the ribosomal proteins (**Figure 7**). Two-way ANOVA indicated a significant main effect of streptozotocin treatment [F (2, 18) = 5.660; P = 0.0124] as STZ upregulated rps3 (740 nmol STZ) and rps6 (both 74 and 740 nmol STZ).

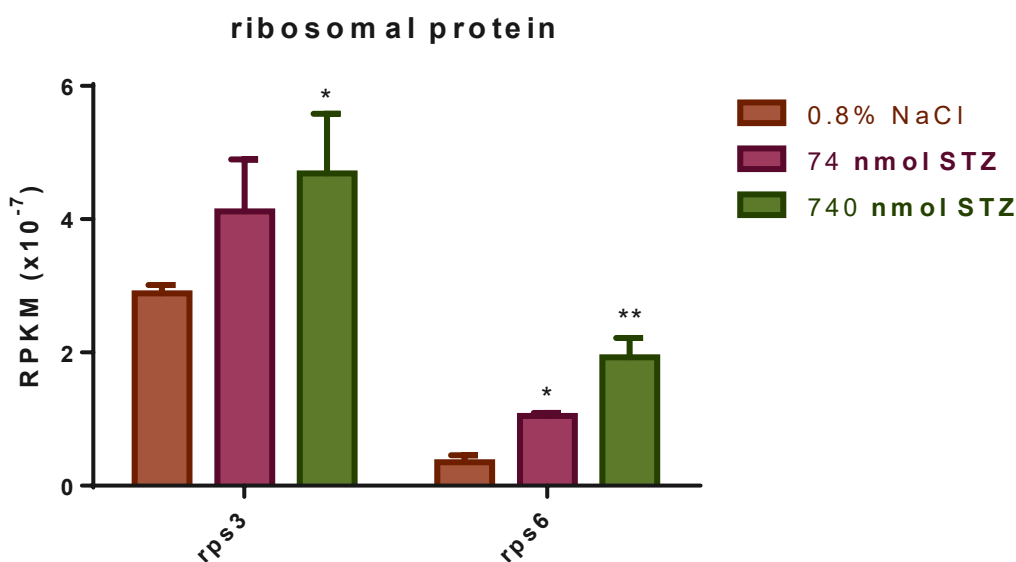


Figure 7. Relative expression of ribosomal protein-encoding genes (40S ribosomal protein S3 (rps3) and 40S ribosomal protein S6 (rps6)) of *Nauphoeta cinerea* 7 days after single streptozotocin injection. Two-way ANOVA indicated a significant main effect of streptozotocin

treatment [$F(2, 18) = 5.660$; $P = 0.0124$] as STZ upregulated rps3 (740 nmol STZ) and rps6 (both 74 and 740 nmol STZ). All values are mean \pm SEM. Tukey's post hoc test showed differences of $P \leq 0.05$ between groups indicated by * for significant vs sham injected group and ** for significant vs sham injected group and 74 nmol treatment.

3.6. Relative expression validation of FoxO deregulation.

The O class of forkhead box transcription factors (FoxO) is involved in a wide range of physiological and pathological processes that significantly impact neurodegenerative conditions like diabetes. We therefore validated the up regulation of FoxO in our STZ-treated transcripts. 74 and 740 nmol STZ treatment significantly upregulated mRNA levels of FOXO [$H=13.35$, $P=0.0001$; Figure 8].

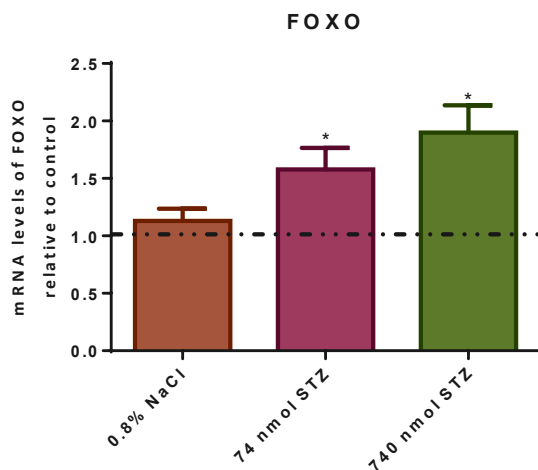


Figure 8: FoxO mRNA expression in *Nauphoeta cinerea* nymph heads, 7 days after single STZ injection. RT-qPCR mRNA expression was analysed using Kruskal-Wallis test and post-hoc test was carried out with Dunn's multiple comparisons test. n = 6. There was significant upregulation of FOXO [H=13.05, P=0.0001]. All values are mean±SEM. * indicate a difference of at least p<0.05 vs intact control (shown as dotted lines).

4. Discussion.

This study presents the transcriptional profile of *Nauphoeta cinerea* nymph heads after dorsal intrathoracic injection with doses of streptozotocin below an earlier determined mean lethal dose (LD50) (Olagoke et al., 2020). Indeed, low dose STZ treatment deregulated the expression of more genes than the high dose treatment, as 74 nmol treatment deregulated 278 genes (254 up regulated, 24 down regulated), while 740 nmol treatment deregulated 226 genes (114 up regulated, 112 down regulated). The gene ontology analysis of deregulated genes showed that molecular functions were the most deregulated across groups, followed by biological processes, and lastly cellular component. Ribosomal protein showed the highest level of up regulation (by LogFC) at both STZ doses, hence we examined the streptozotocin-induced deregulation of the ribosomal protein S3 (that was up regulated by the high dose treatment), and the ribosomal protein S6 (which is known for its role in diabetes pathogenesis (Lu et al., 2008; Zhang & Ma, 2020)).

Data from cryogenic electron microscopy and x ray analysis suggests that the ribosomal protein S3 (rpS3e) is situated at the mRNA entry site of the ribosomal 40S subunit (Anger et al., 2013; Armache et al., 2010) to initiate translation via start codon recognition and mRNA

interaction (Shivaya Valasek, 2012). Outside the ribosome, free rpS3e is involved in DNA repair (Deutsch et al., 1997), immune response and cellular proliferation via the NF- κ B pathway (Wan et al., 2007), inhibition of cancerous cells (Alam et al., 2020), apoptosis and the autoregulation of its own gene expression (Sykes et al., 2010). Given the recorded DNA alkylating and carcinogenic effect of streptozotocin in mammals (Bolzán & Bianchi, 2002), as well as the diminished MTT reduction that we have earlier shown in STZ-treated cockroach nymphs (Olagoke et al., 2020), it is plausible that rpS3e upregulation is an important mechanism to protect the *Nauphoeta cinerea* brain from the molecular manifestations of STZ proteotoxicity.

Similarly, the eukaryotic ribosome's main phosphoprotein – ribosomal protein S6 (rps6) – is found at the mRNA binding site of the ribosomal 40S subunit (Nygaard & Nilsson, 1990) and phosphorylates at five serine residues in the carboxy-terminal region for ribosomal biogenesis in the nucleolus and transcript translation in the cytoplasm of mammals and flies (Radimerski et al., 2000; Reinhard et al., 1994). Where, we report the up regulation of ribosomal protein S6 in streptozotocin-treated nymphs, similar to results of marked phosphorylation of rpS6 in rodent diabetes models (Gressner & Wool, 1976; Lu et al., 2008).

Subsequent to the ribosomal proteins, BAT4 protein and histone-lysine n-methyltransferase setmar-like protein were highly upregulated by the low dose treatment, while GTP cyclohydrolase 1, Annexin B9 and fibrillin-1 were up regulated at high dose STZ treatment. The BAT4 protein is coded for by a BAT4 gene that has been shown to be part of a major histocompatibility complex region in humans, pigs, monotremes and the zebrafish (Dohm et al., 2007; Renard et al., 2006; Sambrook et al., 2005; Spies et al., 1989). We have previously shown increased inflammation-like markers in STZ-treated *Nauphoeta cinerea* (),

but further studies would be needed to clarify if this increase is related to the up regulation of BAT4 in this study. Furthermore, the SETMAR gene that codes for the Histone-lysine n-methyltransferase SETMAR enzyme contain epigenetic activation tags for demethylation at double stranded breaks to enable protein repair via non-homologous end joining (NHEJ) (Fnu et al., 2011). The up regulation of SETMAR in streptozotocin treated nymphs suggests that STZ induces double strand breaks in *Nauphoeta cinerea* as has been recorded in mammalian models (Bedoya et al., 1996; Kaina, 1998).

GTP cyclohydrolase 1 is the rate limiting enzyme for *de novo* synthesis of tetrahydrobiopterin which facilitates melanin synthesis and is an important cofactor for nitric oxide synthase (Chen et al., 2015; Tie et al., 2009). Nitric oxide production has been reported in the Malpighian tubules of insects and there are suggestions of functional conservation from mammals to insects (Martínez, 1995). The STZ-induced up regulation of GTP cyclohydrolase 1 reported in this study suggests that STZ may affect *Nauphoeta cinerea* nitric oxide production as previously shown in mammals (Tie et al., 2009). Furthermore, the calcium dependent membrane binding protein – Annexin B9 – has been shown to be involved in endocytosis, leaving the process of protein transport susceptible to heat shock when knocked down (Tjota et al., 2011). Our result showing up regulation of Annexin B9 and the extracellular matrix glycoprotein component of calcium-binding microfibrils – fibrillin 1 may represent part of *Nauphoeta cinerea*'s defence against streptozotocin cytotoxicity.

Pyruvate dehydrogenase protein X component mitochondrial-like and nesprin-1 (nuclear envelope spectrin repeat proteins) showed the highest down regulation at the low STZ dose, while Structural components like cuticle protein 7, paramyosin and chromatin complexes were the most down regulated genes at the high STZ dose. Pyruvate

dehydrogenase protein X component, mitochondrial-like – also called the E3 binding protein – is evolutionarily conserved across many eukaryote species as it is necessary for the cellular respiratory process of catalysing pyruvate dehydration to acetyl-coA (Harris et al., 1997).

Mutations in the E3 binding protein have been linked with pyruvate dehydrogenase deficiency, lactic acid build up and neurological impairments in humans (Brown et al., 2007). The STZ-induced downregulation of E3 binding protein recorded in this study is similar to reports of reduced pyruvate dehydrogenase flux (Page et al., 2015) and increased proportion of inactive pyruvate dehydrogenase enzyme (Weinberg & Utter, 1980) in streptozotocin-induced diabetic rats. Likewise, nesprins are known emerin and lamina A vertebrate proteins of the striated muscle nuclear envelop (J. Zhang et al., 2009). Mutations of nesprin-1 has been linked with the pathogenesis of Emery-Dreifuss muscular dystrophy and orthologs of the nuclear membrane protein have been recorded in *Caenorhabditis elegans* and *Drosophila melanogaster* (Fraser et al., 2000; J. Zhang et al., 2009). The proposition that nesprin-1 acts as a nuclear dystrophin may indicate that our record of nesprin 1 downregulation is another cytotoxic implication of streptozotocin treatment.

The cuticle protein is an essential component of the insect exoskeleton, alongside chitin. Cuticle protein composition and degree of cross linking is dependent on the developmental stage of the insect and affects the physical property of the extracellular matrix (Charles, 2010). In the same vein, paramyosin – a rod-shaped component of the striated muscle thick filament with a central α helix flanked by 2 non α helix regions (Vinós et al., 1991) – modulates the assembly and function of the thick filament (Barany & Barany, 1980). Our report of STZ-induced downregulation of cuticle protein 7 and paramyosin may in part explain the disfigured exoskeleton that we noticed during moulting in the STZ treated groups. Furthermore,

chromatin complexes compact long DNA molecules to prevent damage during cell division. The STZ-induced downregulation of chromatin complexes recorded in this study may be a crucial part of the well documented DNA mutating effect of STZ in mammalian and insect cells (Bolzán et al., 1998; Bolzán & Bianchi, 2002).

Finally, the transactivation of FoxO orthologs via a DNA-binding domain, C-terminal domain, nuclear export sequence domain and nuclear localization signal domain is conserved from insects to mammals (Arden, 2008; Webb et al., 2016). Consequently, FoxO post translational modifications for the regulation of longevity and tumor suppression-related genes (Calnan & Brunet, 2008) is crucial in determining disease pathogenesis, as our record of FoxO upregulation in STZ-treated nymphs is similar to findings in STZ diabetic mice (Hulmi et al., 2012).

5. Conclusion

Summarily, we have shown the transcriptional response of *Nauphoeta cinerea* to low and high dose of single streptozotocin injection, with a higher rate of up regulation than down regulation, especially at the low dose. Of particular interest is the up regulation of ribosomal proteins at both doses, confirming the earlier reported involvement of ribosomal proteins in diabetes pathogenesis of rodents and humans. The relationship between increased expression of ribosomal proteins in insects treated with STZ and the deregulation of glucose homeostasis in *N. cinerea* will need further experimental data.

Declarations:**Acknowledgements**

Olawande C. Olagoke is a recipient of the 2017 CNPq-TWAS Postgraduate Fellowship (FR number: 3240299312).

Funding

This work is financially supported by Brazilian developmental agencies: FAPERGS/CNPq 12/2014-PRONEX: n° 16/2551-0000, CAPES/PROEX (n° 23038.004173/2019-93; n° 0493/2019; n° 88882.182125/2018-01; 88882.182123/2018-01), and INCT-EN: National Institute of Science and Technology for Cerebral Diseases, Excitotoxicity, and Neuroprotection.

Conflicts of interest

The authors have no conflict of interest to declare.

Ethics approval

Not applicable

Consent to participate.

Not applicable

Availability of data and material

All data and materials used are available upon reasonable request made to the corresponding author.

Code availability

Not applicable

References.

- Abdollahi, M., & Hosseini, A. (2014). Streptozotocin. In *Encyclopedia of Toxicology: Third Edition* (pp. 402–404). Elsevier. <https://doi.org/10.1016/B978-0-12-386454-3.01170-2>
- Afolabi, B. A., Olagoke, O. C., Souza, D. O., Aschner, M., Rocha, J. B. T., & Segatto, A. L. A. (2020). Modified expression of antioxidant genes in lobster cockroach, *Nauphoeta cinerea* exposed to methylmercury and monosodium glutamate. *Chemico-Biological Interactions*, 318. <https://doi.org/10.1016/j.cbi.2020.108969>
- Alam, E., Maaliki, L., & Nasr, Z. (2020). Ribosomal protein S3 selectively affects colon cancer growth by modulating the levels of p53 and lactate dehydrogenase. *Molecular Biology Reports*, 47(8), 6083–6090. <https://doi.org/10.1007/s11033-020-05683-1>
- Anger, A. M., Armache, J. P., Berninghausen, O., Habeck, M., Subklewe, M., Wilson, D. N., & Beckmann, R. (2013). Structures of the human and Drosophila 80S ribosome. *Nature*, 497(7447), 80–85. <https://doi.org/10.1038/nature12104>
- Arden, K. C. (2008). FOXO animal models reveal a variety of diverse roles for FOXO transcription factors. In *Oncogene* (Vol. 27, Issue 16, pp. 2345–2350). Nature Publishing Group. <https://doi.org/10.1038/onc.2008.27>
- Armache, J. P., Jarasch, A., Anger, A. M., Villa, E., Becker, T., Bhushan, S., Jossinet, F., Habeck, M., Dindar, G., Franckenberg, S., Marquez, V., Mielke, T., Thomm, M., Berninghausen, O., Beatrix, B., Söding, J., Westhof, E., Wilson, D. N., & Beckmann, R. (2010). Localization of eukaryote-specific ribosomal proteins in a 5.5-Å cryo-EM map of the 80S eukaryotic ribosome. *Proceedings of the National Academy of Sciences of the United States of America*, 107(46), 19754–19759. <https://doi.org/10.1073/pnas.1010005107>
- Barany, M., & Barany, K. (1980). *PHOSPHORYLATION OF THE MYOFIBRILLAR*

PROTEINS. www.annualreviews.org

- Bedoya, F. J., Solano, F., & Lucas, M. (1996). N-Monomethyl-arginine and nicotinamide prevent streptozotocin-induced double strand DNA break formation in pancreatic rat islets. *Experientia*, *52*(4), 344–347. <https://doi.org/10.1007/BF01919538>
- Bolger, A. M., Lohse, M., & Usadel, B. (2014). Trimmomatic: A flexible trimmer for Illumina sequence data. *Bioinformatics*, *30*(15), 2114–2120. <https://doi.org/10.1093/bioinformatics/btu170>
- Bolzán, A. D., & Bianchi, M. S. (2002). Genotoxicity of Streptozotocin. In *Mutation Research - Reviews in Mutation Research* (Vol. 512, Issues 2–3, pp. 121–134). Elsevier. [https://doi.org/10.1016/S1383-5742\(02\)00044-3](https://doi.org/10.1016/S1383-5742(02)00044-3)
- Bolzán, A. D., Bianchi, N. O., & Bianchi, M. S. (1998). Effects of antioxidants on streptozotocin-induced clastogenesis in mammalian and insect cells. *Mutation Research/Genetic Toxicology and Environmental Mutagenesis*, *418*(1), 35–42. [https://doi.org/10.1016/S1383-5718\(98\)00107-7](https://doi.org/10.1016/S1383-5718(98)00107-7)
- Bray, N. L., Pimentel, H., Melsted, P., & Pachter, L. (2016). Near-optimal probabilistic RNA-seq quantification. *Nature Biotechnology*, *34*(5), 525–527. <https://doi.org/10.1038/nbt.3519>
- Brown, R. M., Head, R. A., M, A. A., J, J. A., Walter, J. H., Whitehouse, W. P., & Brown, G. K. (2007). Pyruvate dehydrogenase E3 binding protein (protein X) deficiency. *Developmental Medicine & Child Neurology*, *48*(9), 756–760. <https://doi.org/10.1111/j.1469-8749.2006.tb01362.x>
- Brownlee M. (2001). Biochemistry and molecular cell biology of diabetic complications. *Nature*, *414*(December), 813–820.
- Calnan, D. R., & Brunet, A. (2008). The FoxO code. In *Oncogene* (Vol. 27, Issue 16, pp. 2276–2288). Nature Publishing Group. <https://doi.org/10.1038/onc.2008.21>

- Cembrowski, M. S., & Menon, V. (2018). Continuous Variation within Cell Types of the Nervous System. In *Trends in Neurosciences* (Vol. 41, Issue 6, pp. 337–348). Elsevier Ltd. <https://doi.org/10.1016/j.tins.2018.02.010>
- Charles, J. P. (2010). The regulation of expression of insect cuticle protein genes. In *Insect Biochemistry and Molecular Biology* (Vol. 40, Issue 3, pp. 205–213). Pergamon. <https://doi.org/10.1016/j.ibmb.2009.12.005>
- Chen, P., Wang, J., Li, H., Li, Y., Chen, P., Li, T., Chen, X., Xiao, J., & Zhang, L. (2015). Role of GTP-CHI links PAH and TH in melanin synthesis in silkworm, *Bombyx mori*. *Gene*, 567(2), 138–145. <https://doi.org/10.1016/j.gene.2015.03.043>
- Collins, L. J., Biggs, P. J., Voelckel, C., & Joly, S. (2008). An approach to transcriptome analysis of non-model organisms using short-read sequences. *Genome Informatics. International Conference on Genome Informatics*, 21, 3–14. https://doi.org/10.1142/9781848163324_0001
- Costa-Silva, J., Domingues, D., & Lopes, F. M. (2017). RNA-Seq differential expression analysis: An extended review and a software tool. *PLOS ONE*, 12(12), e0190152. <https://doi.org/10.1371/journal.pone.0190152>
- Costa, V., Aprile, M., Esposito, R., & Ciccodicola, A. (2013). RNA-Seq and human complex diseases: Recent accomplishments and future perspectives. In *European Journal of Human Genetics* (Vol. 21, Issue 2, pp. 134–142). Nature Publishing Group. <https://doi.org/10.1038/ejhg.2012.129>
- Deutsch, W. A., Yacoub, A., Jaruga, P., Zastawny, T. H., & Dizdaroglu, M. (1997). Characterization and mechanism of action of *Drosophila* ribosomal protein S3 DNA glycosylase activity for the removal of oxidatively damaged DNA bases. *Journal of Biological Chemistry*, 272(52), 32857–32860. <https://doi.org/10.1074/jbc.272.52.32857>
- Dixit, A. B., Banerjee, J., Srivastava, A., Tripathi, M., Sarkar, C., Kakkar, A., Jain, M., &

- Chandra, P. S. (2016). RNA-seq analysis of hippocampal tissues reveals novel candidate genes for drug refractory epilepsy in patients with MTLE-HS. *Genomics*, *107*(5), 178–188. <https://doi.org/10.1016/j.ygeno.2016.04.001>
- Dohm, J. C., Tsend-Ayush, E., Reinhardt, R., Grützner, F., & Himmelbauer, H. (2007). Disruption and pseudoautosomal localization of the major histocompatibility complex in monotremes. *Genome Biology*, *8*(8), R175. <https://doi.org/10.1186/gb-2007-8-8-r175>
- Fnu, S., Williamson, E. A., De Haro, L. P., Brenneman, M., Wray, J., Shaheen, M., Radhakrishnan, K., Lee, S. H., Nickoloff, J. A., & Hromas, R. (2011). Methylation of histone H3 lysine 36 enhances DNA repair by nonhomologous end-joining. *Proceedings of the National Academy of Sciences of the United States of America*, *108*(2), 540–545. <https://doi.org/10.1073/pnas.1013571108>
- Fraser, A. G., Kamath, R. S., Zipperlen, P., Martinez-Campos, M., Sohrmann, M., & Ahringer, J. (2000). Functional genomic analysis of *C. elegans* chromosome I by systematic RNA interference. *Nature*, *408*(6810), 325–330. <https://doi.org/10.1038/35042517>
- Giacco, F., & Brownlee, M. (2010). Oxidative stress and diabetic complications. In *Circulation Research* (Vol. 107, Issue 9, pp. 1058–1070). <https://doi.org/10.1161/CIRCRESAHA.110.223545>
- Grabherr, M. G., Haas, B. J., Yassour, M., Levin, J. Z., Thompson, D. A., Amit, I., Adiconis, X., Fan, L., Raychowdhury, R., Zeng, Q., Chen, Z., Mauceli, E., Hacohen, N., Gnirke, A., Rhind, N., Di Palma, F., Birren, B. W., Nusbaum, C., Lindblad-Toh, K., ... Regev, A. (2011). Full-length transcriptome assembly from RNA-Seq data without a reference genome. *Nature Biotechnology*, *29*(7), 644–652. <https://doi.org/10.1038/nbt.1883>
- Gressner, A. M., & Wool, I. G. (1976). Effect of experimental diabetes and insulin on phosphorylation of rat liver ribosomal protein S6. *Nature*, *259*(5539), 148–150.

<https://doi.org/10.1038/259148a0>

Harris, R. A., Bowker-Kinley, M. M., Wu, P., Jeng, J., & Popov, K. M. (1997).

Dihydrolipoamide dehydrogenase-binding protein of the human pyruvate dehydrogenase complex. DNA-derived amino acid sequence, expression, and reconstitution of the pyruvate dehydrogenase complex. *Journal of Biological Chemistry*, 272(32), 19746–19751. <https://doi.org/10.1074/jbc.272.32.19746>

Hulmi, J. J., Silvennoinen, M., Lehti, M., Kivelä, R., & Kainulainen, H. (2012). Altered REDD1, myostatin, and Akt/mTOR/FoxO/MAPK signaling in streptozotocin-induced diabetic muscle atrophy. *American Journal of Physiology-Endocrinology and Metabolism*, 302(3), E307–E315. <https://doi.org/10.1152/ajpendo.00398.2011>

Kaina, B. (1998). Critical steps in alkylation-induced aberration formation. *Mutation Research - Fundamental and Molecular Mechanisms of Mutagenesis*, 404(1–2), 119–124. [https://doi.org/10.1016/S0027-5107\(98\)00103-1](https://doi.org/10.1016/S0027-5107(98)00103-1)

Knoll, K. E., Pietrusz, J. L., & Liang, M. (2005). Tissue-specific transcriptome responses in rats with early streptozotocin-induced diabetes. *Physiological Genomics*, 21(2), 222–229. <https://doi.org/10.1152/physiolgenomics.00231.2004>

Law, C. W., Chen, Y., Shi, W., & Smyth, G. K. (2014). Voom: Precision weights unlock linear model analysis tools for RNA-seq read counts. *Genome Biology*, 15(2), 1–17. <https://doi.org/10.1186/gb-2014-15-2-r29>

Lu, H., Yang, Y., Allister, E. M., Wijesekara, N., & Wheeler, M. B. (2008). The identification of potential factors associated with the development of type 2 diabetes: A quantitative proteomics approach. *Molecular and Cellular Proteomics*, 7(8), 1434–1451. <https://doi.org/10.1074/mcp.M700478-MCP200>

Martínez, A. (1995). Nitric oxide synthase in invertebrates. *The Histochemical Journal*, 27(10), 770–776. <https://doi.org/10.1007/BF02388302>

National Center for Biotechnology Information. (2020). *PubChem Compound Summary for CID 7067772, Streptozotocin*.

<https://pubchem.ncbi.nlm.nih.gov/compound/Streptozotocin>

Nygaard, O., & Nilsson, L. (1990). Translational dynamics: Interactions between the translational factors, tRNA and ribosomes during eukaryotic protein synthesis. In *European Journal of Biochemistry* (Vol. 191, Issue 1, pp. 1–17). John Wiley & Sons, Ltd. <https://doi.org/10.1111/j.1432-1033.1990.tb19087.x>

Olagoke, O. C., Afolabi, B. A., & Rocha, J. B. T. (2020). Streptozotocin induces brain glucose metabolic changes and alters glucose transporter expression in the Lobster cockroach ; *Nauphoeta cinerea* (Blattodea : Blaberidae). *Molecular and Cellular Biochemistry*, 1–35. <https://doi.org/DOI: 10.1007/s11010-020-03976-4>

Page, L. M. L., Rider, O. J., Lewis, A. J., Ball, V., Clarke, K., Johansson, E., Carr, C. A., Heather, L. C., & Tyler, D. J. (2015). Increasing pyruvate dehydrogenase flux as a treatment for diabetic cardiomyopathy: A combined ¹³C hyperpolarized magnetic resonance and echocardiography study. *Diabetes*, 64(8), 2735–2743. <https://doi.org/10.2337/db14-1560>

Piccoli, B. C., Segatto, A. L. A., Loreto, É. L. S., Moreira, J. C. F., Ardisson-Araújo, D. M. P., & Rocha, J. B. T. (2020). Transcriptional analyses of acute per os exposure and co-exposure of 4-vinylcyclohexene and methylmercury-contaminated diet in adults of *Drosophila melanogaster*. *Environmental Pollution*, 263, 114632. <https://doi.org/10.1016/j.envpol.2020.114632>

Radimerski, T., Mini, T., Schneider, U., Wettenhall, R. E. H., Thomas, G., & Jenö, P. (2000). Identification of insulin-induced sites of ribosomal protein S6 phosphorylation in *Drosophila melanogaster*. *Biochemistry*, 39(19), 5766–5774. <https://doi.org/10.1021/bi9927484>

- Reinhard, C., Fernandez, A., Lamb, N. J. C., & Thomas, G. (1994). Nuclear localization of p85(s6k): Functional requirement for entry into S phase. *EMBO Journal*, *13*(7), 1557–1565. <https://doi.org/10.1002/j.1460-2075.1994.tb06418.x>
- Renard, C., Hart, E., Sehra, H., Beasley, H., Coggill, P., Howe, K., Harrow, J., Gilbert, J., Sims, S., Rogers, J., Ando, A., Shigenari, A., Shiina, T., Inoko, H., Chardon, P., & Beck, S. (2006). The genomic sequence and analysis of the swine major histocompatibility complex. *Genomics*, *88*(1), 96–110. <https://doi.org/10.1016/j.ygeno.2006.01.004>
- Sambrook, J. G., Figueroa, F., & Beck, S. (2005). A genome-wide survey of Major Histocompatibility Complex (MHC) genes and their paralogues in zebrafish. *BMC Genomics*, *6*(1), 1–10. <https://doi.org/10.1186/1471-2164-6-152>
- Schuster, S. C. (2008). Next-generation sequencing transforms today's biology. In *Nature Methods* (Vol. 5, Issue 1, pp. 16–18). <https://doi.org/10.1038/nmeth1156>
- Segatto, A. L. A., Diesel, J. F., Loreto, E. L. S., & da Rocha, J. B. T. (2018). De novo transcriptome assembly of the lobster cockroach *Nauphoeta cinerea* (Blaberidae). *Genetics and Molecular Biology*, *41*(3), 713–721. <https://doi.org/10.1590/1678-4685-gmb-2017-0264>
- Segatto, A. L. A., Diesel, J. F., Loreto, E. L. S., da Rocha, J. B. T., Segatto, A. L. A., Diesel, J. F., Loreto, E. L. S., & da Rocha, J. B. T. (2018). De novo transcriptome assembly of the lobster cockroach *Nauphoeta cinerea* (Blaberidae). *Genetics and Molecular Biology*, *41*(3), 713–721. <https://doi.org/10.1590/1678-4685-gmb-2017-0264>
- Shivaya Valasek, L. (2012). ‘Ribozomin’ – Translation Initiation from the Perspective of the Ribosome-bound Eukaryotic Initiation Factors (eIFs). *Current Protein & Peptide Science*, *13*(4), 305–330. <https://doi.org/10.2174/138920312801619385>
- Simão, F. A., Waterhouse, R. M., Ioannidis, P., Kriventseva, E. V., & Zdobnov, E. M. (2015). BUSCO: Assessing genome assembly and annotation completeness with single-copy

- orthologs. *Bioinformatics*, 31(19), 3210–3212.
<https://doi.org/10.1093/bioinformatics/btv351>
- Smyth, G. K. (2005). limma: Linear Models for Microarray Data. In *Bioinformatics and Computational Biology Solutions Using R and Bioconductor* (pp. 397–420). Springer-Verlag. https://doi.org/10.1007/0-387-29362-0_23
- Spies, T., Blanck, G., Bresnahan, M., Sands, J., & Strominger, J. L. (1989). A new cluster of genes within the human major histocompatibility complex. *Science*, 243(4888), 214–217. <https://doi.org/10.1126/science.2911734>
- Supek, F., Bošnjak, M., Škunca, N., & Šmuc, T. (2011). REVIGO Summarizes and Visualizes Long Lists of Gene Ontology Terms. *PLoS ONE*, 6(7), e21800.
<https://doi.org/10.1371/journal.pone.0021800>
- Sykes, M. T., Sperling, E., Chen, S. S., & Williamson, J. R. (2010). Quantitation of the ribosomal protein autoregulatory network using mass spectrometry. *Analytical Chemistry*, 82(12), 5038–5045. <https://doi.org/10.1021/ac9028664>
- Tie, L., Li, X.-J., Wang, X., Channon, K. M., & Chen, A. F. (2009). Endothelium-specific GTP cyclohydrolase I overexpression accelerates refractory wound healing by suppressing oxidative stress in diabetes. *American Journal of Physiology-Endocrinology and Metabolism*, 296(6), E1423–E1429. <https://doi.org/10.1152/ajpendo.00150.2009>
- Tjota, M., Lee, S. K., Wu, J., Williams, J. A., Khanna, M. R., & Thomas, G. H. (2011). Annexin B9 binds to β H-spectrin and is required for multivesicular body function in *Drosophila*. *Journal of Cell Science*, 124(17), 2914–2926.
<https://doi.org/10.1242/jcs.078667>
- Vinós, J., Domingo, A., Marco, R., & Cervera, M. (1991). Identification and characterization of *Drosophila melanogaster* paramyosin. *Journal of Molecular Biology*, 220(3), 687–700. [https://doi.org/10.1016/0022-2836\(91\)90110-R](https://doi.org/10.1016/0022-2836(91)90110-R)

- Wan, F., Anderson, D. E., Barnitz, R. A., Snow, A., Bidere, N., Zheng, L., Hegde, V., Lam, L. T., Staudt, L. M., Levens, D., Deutsch, W. A., & Lenardo, M. J. (2007). Ribosomal Protein S3: A KH Domain Subunit in NF- κ B Complexes that Mediates Selective Gene Regulation. *Cell*, *131*(5), 927–939. <https://doi.org/10.1016/j.cell.2007.10.009>
- Webb, A. E., Kundaje, A., & Brunet, A. (2016). Characterization of the direct targets of FOXO transcription factors throughout evolution. *Aging Cell*, *15*(4), 673–685. <https://doi.org/10.1111/accel.12479>
- Weinberg, M. B., & Utter, M. F. (1980). Effect of streptozotocin-induced diabetes mellitus on the turnover of rat liver pyruvate carboxylase and pyruvate dehydrogenase. *Biochemical Journal*, *188*(3), 601–608. <https://doi.org/10.1042/bj1880601>
- Zhang, J., Felder, A., Liu, Y., Guo, L. T., Lange, S., Dalton, N. D., Gu, Y., Peterson, K. L., Mizisin, A. P., Shelton, G. D., Lieber, R. L., & Chen, J. (2009). Nesprin 1 is critical for nuclear positioning and anchorage. *Human Molecular Genetics*, *19*(2), 329–341. <https://doi.org/10.1093/hmg/ddp499>
- Zhang, N., & Ma, S. (2020). Research Progress of 70 kDa Ribosomal Protein S6 Kinase (P70S6K) Inhibitors as Effective Therapeutic Tools for Obesity, Type II Diabetes and Cancer. *Current Medicinal Chemistry*, *27*(28), 4699–4719. <https://doi.org/10.2174/0929867327666200114113139>

5.4. Manuscript 2: Disruption of PI3K/AKT and MAPK insulin signalling in streptozotocin-treated *Nauphoeta cinerea*.

Disruption of *PI3K/AKT* and *MAPK* insulin signalling in streptozotocin-treated *Nauphoeta cinerea*.

Olawande C. Olagoke¹, Folorunso B. Oimage¹, Ana L. A. Segatto², João B. T. Rocha^{1*}

¹Departamento de Bioquímica e Biologia Molecular, Centro de Ciências Naturais e Exatas (CCNE), Universidade Federal de Santa Maria, 97105-900 Santa Maria, RS, Brazil.

² Instituto Federal de Educação, Ciência e Tecnologia do Rio Grande do Sul, RS, Brasil.

*Corresponding author

João B. T. Rocha,

Departamento de Bioquímica e Biologia Molecular, CCNE,

Universidade Federal de Santa Maria, 97105-900 Santa Maria, RS, Brazil.

Fax: +55 55 8104 0207.

E-mail: jbtrocha@gmail.com; jbtrocha@yahoo.com.br

ORCID

Olawande C. Olagoke: 0000-0001-9212-4948

Folorunso B. Oimage: 0000-0002-9750-5034

Ana L. A. Segatto: 0000-0002-5044-1168

João B. T. Rocha: 0000-0003-3829-0595

Abstract

Neurosecretory cells in the insect brain synthesize, store and release insulin-like peptide, similar to the insulin secretory function of the mammalian pancreatic beta cells. Consequently, the conservation of insulin-related signalling from insects to mammals makes it possible to study the molecular basis of impaired brain insulin signalling that have been reported in degenerative conditions like diabetes mellitus and Alzheimer's disease. Hence, we examined streptozotocin-induced modulations of the canonical *PI3K/AKT* and *RAS/MAPK* insulin signalling cascades in *Nauphoeta cinerea* and further explored structure-activity relationships of the target genes. The cockroaches were treated with a single injection of 0.8% NaCl, 74 and 740 nmol STZ and monitored for 7 days. RT-qPCR expression of *PI3K/AKT* target genes and relative transcriptional expression of *MAPK* genes was estimated from head mRNA. Streptozotocin treatment downregulated the insulin signalling pathway ligand *ILP* but had no significant effect on the receptor *INR*. Target genes of the *PI3K/AKT* cascade were also downregulated. The adaptor protein (*GRB2*), guanine exchange factor (*SOS*) and target genes (*RAS*, *RAF* and *ERK*) of the *RAS/MAPK* cascade were upregulated, though there was no significant difference in the expression of *MEK*. The upregulation of *RAS/MAPK* signalling was confirmed by the increased expression of stress and inflammation associated *P38* and *JNK* *MAPK* genes. The homology modelling of *N. cinerea* A,B,C further confirmed X,Y,Z, as *MAPK* structure-function elements were also conserved between *N. cinerea* and other eukaryotes, highlighting the suitability of the cockroach to model degenerative diseases.

Keywords: Neurosecretory cells; *PI3K/AKT* Cascade; *RAS/MAPK* signalling; *P38* *MAPK*; Homology modelling

1. Introduction

The first recorded detection of insulin in the rat brain and insulin-like peptide (*ILP*) in insect brain were in 1978 [1] and 1984 [2] respectively. Thereafter, methods ranging from in situ hybridization, immunohistochemistry and reverse transcription polymerase chain reaction (RT-PCR) have been used to detect brain insulin/insulin-like peptide mRNA at different developmental stages of animals. Insulin-related signalling establishes the necessary brain circuitries for energy allocation, modulates brain areas that control nutrient metabolism and regulates mechanisms of adaptive behaviour for energy homeostasis, consequently impacting brain cell proliferation and overall brain size [3]. A deranged brain insulin signalling is typical of degenerative conditions like diabetes mellitus and Alzheimer's disease [4], here, we model pathophysiological modulations of insulin-like peptide signalling in streptozotocin-treated *Nauphoeta cinerea*, in line with our previous report of altered brain glucose and redox homeostasis in cockroaches exposed to the alkylating agent [5]. We further explored relationships between the structure and activity of *N. cinerea* insulin signalling genes.

The presence of neurosecretory cells that synthesize, store and release insulin-like peptide in insect brain have been well demonstrated [6]. Some researchers have also argued that insulin can equally be synthesized [7] and stored [8] during development in the rodent brain, but it is more commonly agreed that insulin gets to the mammalian brain via circulation [9]. The phosphatidylinositol 3-kinase (*PI3K*) – protein kinase B (*AKT*) and mitogen activated protein kinase (*MAPK*) cascades are the main mechanisms of insulin action within the central nervous system [10]. Briefly, the fusion of insulin-like peptide to the insulin receptor α subunit auto phosphorylates the tyrosine residues located within the cytosolic facet of insulin receptor

β subunit [11]. The phosphorylated receptor then engages an adapter protein; Insulin receptor substrate (*IRS*) to present docking sites for signalling peptides of the *PI3K/AKT* and *RAS/MAPK* pathways [12]. While the *PI3K/AKT* cascade regulates metabolic homeostasis genes like Forkheadbox (*FoxO*), activation of *ERK/MAPK* at the TEY motif (tyrosine and threonine separated by a glutamate residue in their activation loop (**Figure 1**)) translocates *ERK* into the nucleus to phosphorylate transcription factors that are involved in cell cycle regulation.

Furthermore, stress stimuli activates the *p38* family of *MAPKs* namely, *p38 α* , *p38 β* , *p38 γ* and *p38 δ* by phosphorylation at the TGY motif (threonine and tyrosine residues separated by glycine in the activation loop (**Figure 1**)), while cytokines and environmental stressors activate the *JNK* family of protein kinases namely; *JNK1*, *JNK2* and *JNK3* by phosphorylation at the TPY motif (tyrosine and threonine residues separated by a proline residue in the activation loop (**Figure 1**)) [13]. Summarily, a serine/threonine kinase domain flanked by N- and C- terminal regions is a common feature to all *MAPKs*, but they differ in the length of the N- and C-terminal, as well as additional domains that some *MAPKs* possess [14]. The transcripts of streptozotocin-injected *Nauphoeta cinerea* may provide an effective experimental tool to understand *MAPK* structure-function relationships, while offering insights into their role in degenerative conditions like diabetes.

```

ERK2_Nauphoeta_cinerea      100 FLYQILRGLKYIHSANVLRD KPSNLLNNTTCDLKI DFGLARVADPDGFI TEY ATRIYRAPE MLNSKGYTKSIDINSVGCILAEMLSNRPIFPGKHYLDQLNHLIGLVGSPSTAE
ERK2_Zootermopsis_nevadensis 117 FLYQILRGLKYIHSANVLRD KPSNLLNNTTCDLKI DFGLARVADPDGFI TEY ATRIYRAPE MLNSKGYTKSIDINSVGCILAEMLSNRPIFPGKHYLDQLNHLIGLVGSPSTAE
ERK2_Drosophila_melanogaster 117 FLYQILRGLKYIHSANVLRD KPSNLLNNTTCDLKI DFGLARVADPDGFI TEY ATRIYRAPE MLNSKGYTKSIDINSVGCILAEMLSNRPIFPGKHYLDQLNHLIGLVGSPSRO
ERK2_Caenorhabditis_elegans 117 FLYQILRGLKYIHSANVLRD KPSNLLNNTTCDLKI DFGLARVADPDGFI TEY ATRIYRAPE MLNSKGYTKSIDINSVGCILAEMLSNRPIFPGKHYLDQLNHLIGLVGSPSNA
ERK2_Danio_erio            117 FLYQILRGLKYIHSANVLRD KPSNLLNNTTCDLKI DFGLARVADPDGFI TEY ATRIYRAPE MLNSKGYTKSIDINSVGCILAEMLSNRPIFPGKHYLDQLNHLIGLVGSPSQE
ERK2_Rattus_norvegicus     114 FLYQILRGLKYIHSANVLRD KPSNLLNNTTCDLKI DFGLARVADPDGFI TEY ATRIYRAPE MLNSKGYTKSIDINSVGCILAEMLSNRPIFPGKHYLDQLNHLIGLVGSPSQE
ERK2_Mus_musculus         114 FLYQILRGLKYIHSANVLRD KPSNLLNNTTCDLKI DFGLARVADPDGFI TEY ATRIYRAPE MLNSKGYTKSIDINSVGCILAEMLSNRPIFPGKHYLDQLNHLIGLVGSPSQE
ERK2_Homo_sapiens         114 FLYQILRGLKYIHSANVLRD KPSNLLNNTTCDLKI DFGLARVADPDGFI TEY ATRIYRAPE MLNSKGYTKSIDINSVGCILAEMLSNRPIFPGKHYLDQLNHLIGLVGSPSQE
P38B_Nauphoeta_cinerea     57  LLYQILRGLKYIHSAGIIRD KPSNIAVNEDCELKI DFGLARPTENE. ITGYATRIYR NY MLNWHYIQTVDINSVGCIMAE LLTGRTLFPGDTHIQQLNHLZMEILGTPHEE
P38B_Zootermopsis_nevadensis 119 LLYQILRGLKYIHSAGIIRD KPSNIAVNEDCELKI DFGLARPAESE. ITGYATRIYR NY MLNWHYIQTVDINSVGCIMAE LLTGRTLFPGDTHIQQLNHLZMEILGTPADE
P38B_Drosophila_melanogaster 119 LLYQILRGLKYIHSAGIIRD KPSNIAVNEDCELKI DFGLARPAESE. ITGYATRIYR NY MLNWHYIQTVDINSVGCIMAE LLTGRTLFPGDTHIQQLNHLZMEILGTPADE
P38B_Caenorhabditis_elegans 119 LLYQILRGLKYIHSAGIIRD KPSNIAVNERCEFKI DFGLARAQDAE. ITGYATRIYR NY MLNWHYIQTVDINSVGCIMAE LLTGRTLFPGDTHIQQLNHLZMEILGTPADE
P38B_Danio_erio           119 LLYQILRGLKYIHSAGIIRD KPSNIAVNEDCELKI DFGLARHTDDE. ITGYATRIYR NY MLNWHYIQTVDINSVGCIMAE LLTGRTLFPGDTHIQQLNHLZMEILGTPADE
P38B_Rattus_norvegicus     119 LLYQILRGLKYIHSAGIIRD KPSNIAVNEDCELKI DFGLARHTDDE. ITGYATRIYR NY MLNWHYIQTVDINSVGCIMAE LLTGRTLFPGDTHIQQLNHLZMEILGTPADE
P38B_Mus_musculus         119 LLYQILRGLKYIHSAGIIRD KPSNIAVNEDCELKI DFGLARHTDDE. ITGYATRIYR NY MLNWHYIQTVDINSVGCIMAE LLTGRTLFPGDTHIQQLNHLZMEILGTPADE
P38B_Homo_sapiens         119 LLYQILRGLKYIHSAGIIRD KPSNIAVNEDCELKI DFGLARHTDDE. ITGYATRIYR NY MLNWHYIQTVDINSVGCIMAE LLTGRTLFPGDTHIQQLNHLZMEILGTPADE
JNK_Nauphoeta_cinerea     118 LLYQMLCGIKHLSAGIIRD KPSNIVVKSDCITLKI DFGLARTAGTFMTPY VTRYYRAPE ILG.MGYKENVDINSVGCIMGEMIRGGVLPFGDTHIQQLNHLZMEILGTPSQQ
JNK_Zootermopsis_nevadensis 118 LLYQMLCGIKHLSAGIIRD KPSNIVVKSDCITLKI DFGLARTAGTFMTPY VTRYYRAPE ILG.MGYKENVDINSVGCIMGEMIRGGVLPFGDTHIQQLNHLZMEILGTPSQQ
JNK_Drosophila_melanogaster 118 LLYQMLCGIKHLSAGIIRD KPSNIVVKSDCITLKI DFGLARTAGTFMTPY VTRYYRAPE ILG.MGYKENVDINSVGCIMGEMIRGGVLPFGDTHIQQLNHLZMEILGTPSQQ
JNK_Caenorhabditis_elegans 118 LLYQMLCGIKHLSAGIIRD KPSNIVVKSDCITLKI DFGLARTAGTFMTPY VTRYYRAPE ILG.MGYKENVDINSVGCIMGEMIRGGVLPFGDTHIQQLNHLZMEILGTPSQQ
JNK_Danio_erio            118 LLYQMLCGIKHLSAGIIRD KPSNIVVKSDCITLKI DFGLARTAGTFMTPY VTRYYRAPE ILG.MGYKENVDINSVGCIMGEMIRGGVLPFGDTHIQQLNHLZMEILGTPSQQ
JNK_Rattus_norvegicus     118 LLYQMLCGIKHLSAGIIRD KPSNIVVKSDCITLKI DFGLARTAGTFMTPY VTRYYRAPE ILG.MGYKENVDINSVGCIMGEMIRGGVLPFGDTHIQQLNHLZMEILGTPSQQ
JNK_Mus_musculus         118 LLYQMLCGIKHLSAGIIRD KPSNIVVKSDCITLKI DFGLARTAGTFMTPY VTRYYRAPE ILG.MGYKENVDINSVGCIMGEMIRGGVLPFGDTHIQQLNHLZMEILGTPSQQ
JNK_Homo_sapiens         118 LLYQMLCGIKHLSAGIIRD KPSNIVVKSDCITLKI DFGLARTAGTFMTPY VTRYYRAPE ILG.MGYKENVDINSVGCIMGEMIRGGVLPFGDTHIQQLNHLZMEILGTPSQQ

```

Figure 1: Structure-based *MAPK* multiple sequence alignment of *Nauphoeta cinerea* and other eukaryotes.

The annotation of sequence conservation was performed in <http://www.bioinformatics.org/strap/aa/>. Strongly conserved parts of the alignment are shown in black bold font, while less conserved areas are faded in grey font. The conserved catalytic loop is boxed in red and the activation segment between and including the conserved tripeptide motifs; DFG and APE is boxed in purple. The conserved phosphorylation segments at the TEY motif for *ERK2*, TGY motif for *P38B* and TPY motif for *JNK* are boxed in green.

2. Materials and Methods

2.1. Chemicals and Insect stock.

Chemicals and reagents for RT-qPCR were purchased from Sigma Aldrich (St Lois, MO, USA), the exceptions are noted. Nymphs were housed at Departamento de Bioquímica e Biologia Molecular, Universidade Federal de Santa Maria, Brasil at temperature of 24 ± 3 , a 12-hour cycle of light and darkness, and humidity that ranged between 57% and 75%. Diet was compounded as earlier described [5] and water was accessible *ad libitum*.

2.2. Streptozotocin Treatment.

Nymphs were randomly allocated to four (4) treatment groups, including: Control; 0.8% NaCl; 74 nmol STZ and 740 nmol STZ. Single injections were administered into the right dorsal second thoracic segment and the nymphs were observed for 7 days, after which head segment were excised for total RNA extraction.

2.3. Identification of *Nauphoeta cinerea* insulin signalling genes, primer design and multiple sequence alignment.

Coding sequences of insect insulin signalling genes were downloaded from the NCBI platform (<https://www.ncbi.nlm.nih.gov/>) and used to query our *Nauphoeta* transcriptome [15]. Requisite *Nauphoeta* sequences were then used to design the primers of interest on the Primer3input website (<http://primer3.ut.ee/>) and multiple sequence alignment was performed using MEGA X as earlier described [5]. The primer sequences are shown in **Table S1**.

Table S1: Summary of Insulin signalling and normalizer primer sequences.

Oligo name.	Primer – Sequence (5'- 3').	Annealing Temperature.	% Identity - Specie
<i>INR</i>	F – TGGAGAGTGCACATCTGAC	60	89.31% – <i>Z. nevadensis</i>
	R – CCAGCAGCAATTTCTCAGC		87.79% – <i>C. secundus</i>
<i>ILP2</i>	F – GTGAATGACTCTGGCTTCTGG	60	41.27% – <i>D. melanogaster</i>
	R – AATGATCCCAGACAAGTGC		86.90% – <i>B. germanica</i>
<i>PI3K</i>	F – TTGCCGACAGACATTGAGC	60	77.44% – <i>Z. nevadensis</i>
	R – AATGGGACACGTTCTCTCG		28.04% – <i>D. melanogaster</i>
<i>AKT</i>	F – CGGATGATGCGAAAGAAATA	60	97.33% – <i>Z. nevadensis</i>
	R – CGTTACTTGTGGCTTGAAGG		95.33% – <i>C. secundus</i>
<i>Tubulin</i>	F – TTGCCAGTGATGAGTTGCTC	60	47.62% – <i>D. melanogaster</i>
	R – AGCATGTACCAAGGGCAGTT		
<i>TBP</i>	F – GGTGCGAATGTGGAGTACAG	60	
	R – TAGTGGCTCCAGTGCAAGTC		
<i>GAPDH</i>	F – CCGTGTCCCTGTTCTAATG	60	
	R – GTCCAAGATGCCCTTCAGAG		
<i>EF1α1</i>	F – CGTGTCTGTAAAGGAACTGC	60	
	R – CAAGCAATGTGAGCTGTATG		
<i>GPDH</i>	F – AGTTCATCAGGACGCTCTGC	60	
	R – AGATCAATGCTGCCATCCTC		

2.4. Total RNA Extraction, DNase Treatment, cDNA Synthesis and real-time q-PCR.

TRIZOL™ Reagent (ThermoFisher scientific, USA) was used to isolate total RNA, contaminating genomic DNA was removed by DNase treatment (Promega Corp, USA), RNA quality was estimated by spectrophotometry (NanoDrop™ 2000) and agarose gel electrophoresis, and total RNA was reverse transcribed to cDNA (GoScript™ Promega Corp, USA), in a T100™ Thermal Cycler (BIO-RAD, China). DNA amplification was performed by polymerase chain reaction of a 20µl volume made up of 10µl Mix and 10µl cDNA as earlier described ().

2.5. Relative expression analysis of MAPK target genes.

Transcriptional expression of *MAPK* genes was calculated as earlier described [16]. Transcript sequences of streptozotocin-treated *Nauphoeta cinerea* () were mapped to nucleotide sequences of the *MAPK* genes on the Geneious 9.1.8 platform (Biomatters, New Zealand), computed (equation 1), and expressed as Reads Per Kilobase Million (RPKM).

$$\left(\frac{\text{No of mapped nucleotide in the sample} \div \text{No of coding sequence nucleotides in the target gene}}{\quad} \right) \quad (1)$$

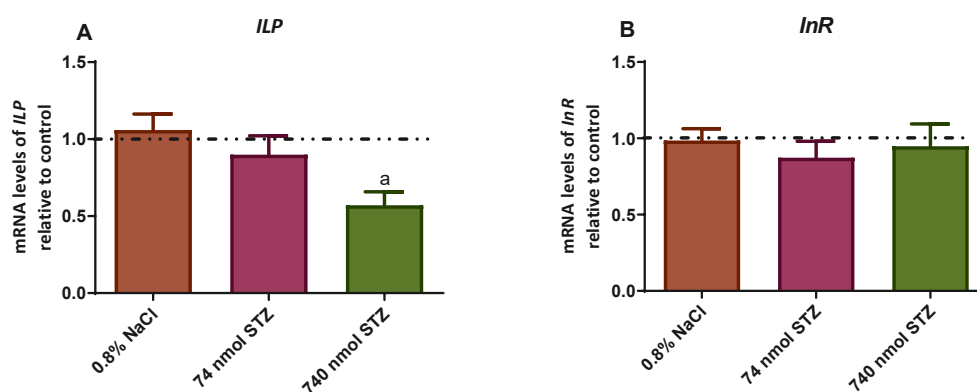
2.6. Statistical Analysis.

CT values for RT-qPCR data were generated with the QuantStudio™ Design and Analysis software and evaluated using the comparative C_T method. All data were analysed on GraphPad Prism 6, using Kruskal-Wallis test, followed by Dunn's multiple comparisons test. Significant difference between treated and control groups was set $P < 0.05$. Results were expressed as Mean \pm SEM.

3. Results

3.1. *Nauphoeta cinerea* PI3K/AKT response to STZ Treatment.

740 nmol STZ treatment significantly downregulated *ILP* [$H=13.05$, $P=0.0001$; Figure 2A] mRNA levels, but there was no significant difference in mRNA levels of the putative ligand *InR* [$H=4.643$, $P=0.0987$; Figure 2B]. Moreover, both 74 and 740 nmol STZ treatment significantly downregulated *PI3K* [$H=15.17$, $P=0.0001$; Figure 2C] and *AKT* [$H=12.93$, $P=0.0001$; Figure 2D] mRNA levels.



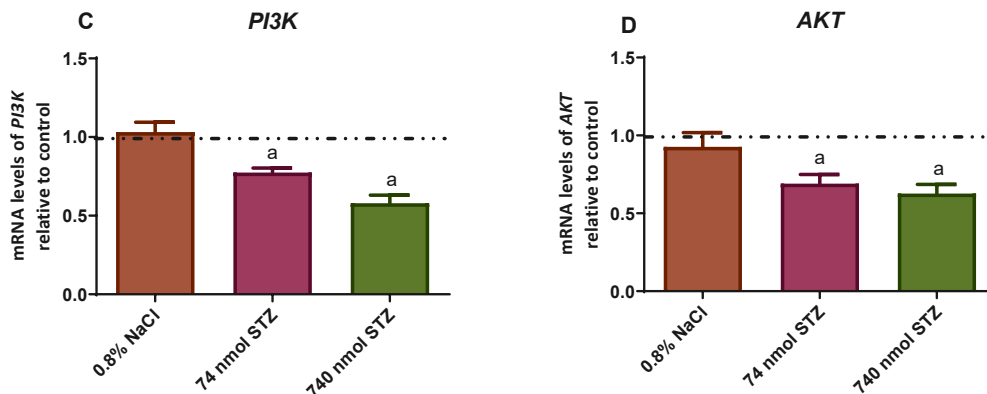
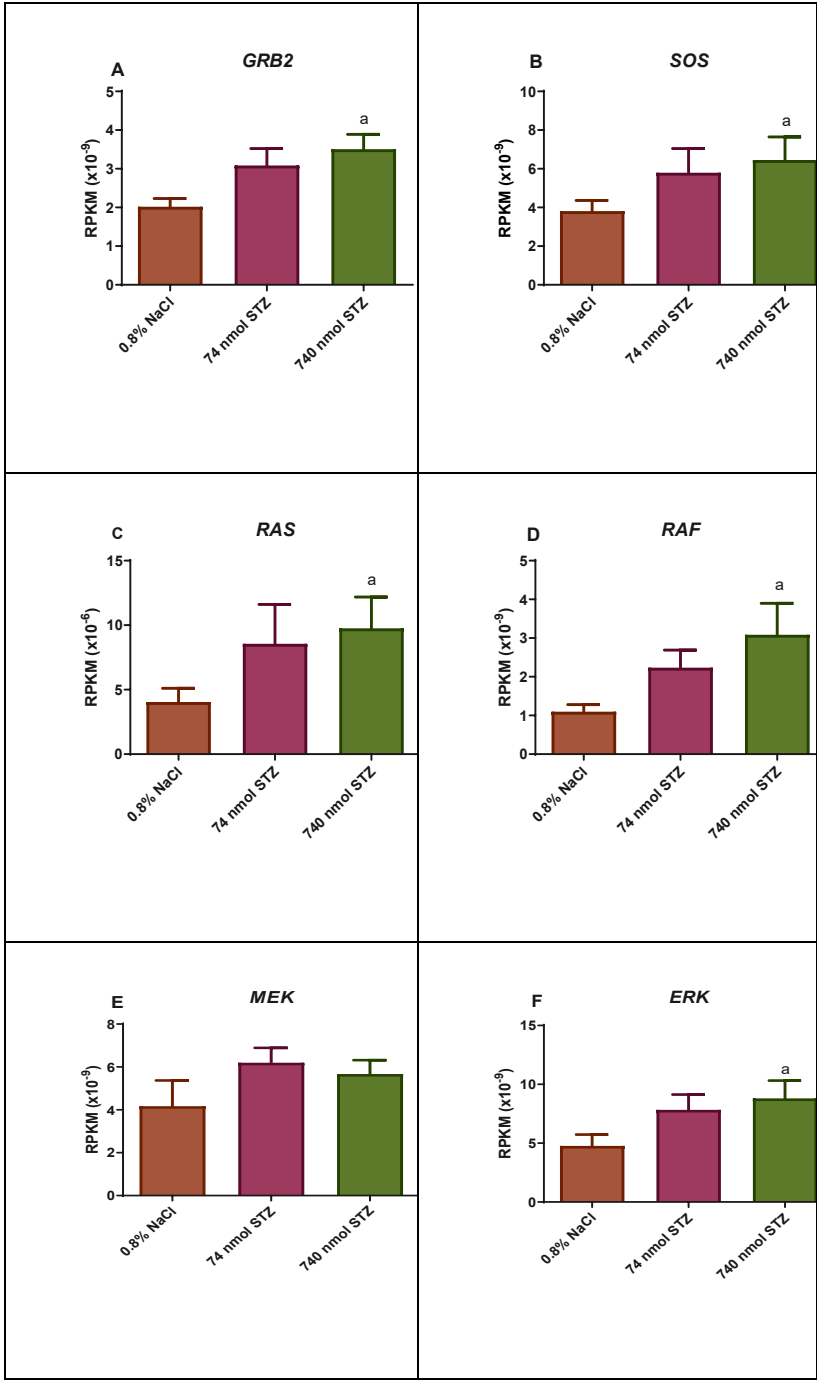


Figure 2: *PI3K/AKT* cascade mRNA levels in *Nauphoeta cinerea* nymph heads, 7 days after single STZ injection. (n = 6). There was significant downregulation of *ILP* [H=13.05, P=0.0001], but no significant difference in mRNA levels of *InR* [H=4.643, P=0.0987]. *PI3K* [H=15.17, P=0.0001] and *AKT* [H=12.93, P=0.0001] were also significantly downregulated. All values are mean±SEM. Significant difference at $p \leq 0.05$ is indicated by different letters.

3.2. *Nauphoeta cinerea* RAS, P38 and JNK MAPK response to STZ Treatment.

Kruskal-Wallis test followed by Dunn's multiple comparisons test showed significant upregulation of the adapter protein *GRB2* [H=7.538, P=0.0107; Figure 3A] and the guanine exchange factor protein *SOS* [H=7.731, P=0.0066; Figure 3B] in the 740 nmol STZ treatment group. 740 nmol STZ treatment further upregulated *RAS* [H=7.423, P=0.0132; Figure 3C], the *MAP3K*; *RAF* [H=8.769, P=0.0012; Figure 3D], but there was no significant difference in the transcriptional expression of the *MAP2K*; *MEK* [H=5.384, P=0.00573; Figure 3E]. Consequently, 740nmol STZ treatment significantly upregulated the *MAPK*; *ERK* [H=8.000, P=0.0048; Figure

3F]. There was also significant up regulation of *P38B* [H=8.769, P=0.0012; Figure 3G] and *JNK* [H=7.654, P=0.0076; Figure 3H] in the 740nmol STZ treatment group.



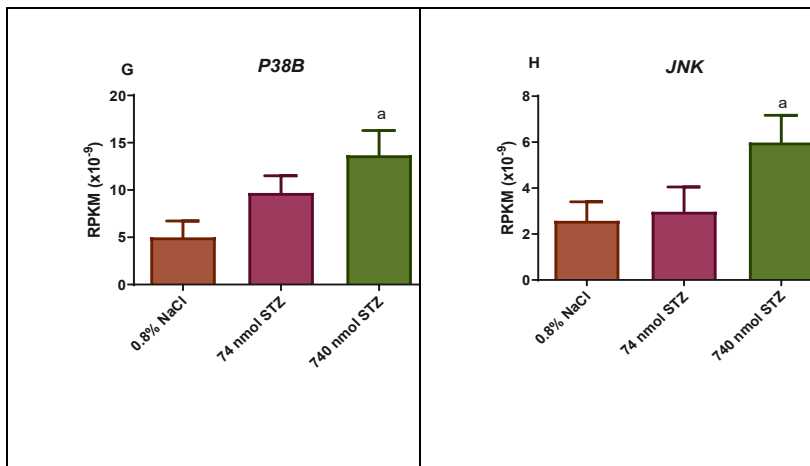


Figure 3: Relative expression of *RAS*, *P38* and *JNK* MAPK target genes in *Nauphoeta cinerea* nymph heads, 7 days after single STZ injection. (n = 6). 740 nmol STZ injection significantly upregulated *GRB2* [H=7.538, P=0.0107], *SOS* [H=7.731, P=0.0066], *RAS* [H=7.423, P=0.0132], *RAF* [H=8.769, P=0.0012] and *ERK* [H=8.000, P=0.0048], but there was no significant difference in transcriptional expression of *MEK* [H=5.384, P=0.00573]. 740 nmol STZ injection also significantly up regulated *P38B* [H=8.769, P=0.0012] and *JNK* [H=7.654, P=0.0076]. All values are mean±SEM. Significantly difference at $p \leq 0.05$ is indicated by different letters.

3.3. Primary and Secondary structure prediction of *Nauphoeta cinerea* MAPK target genes.

The protparam server predicts *GRB2* as stable with an instability index (II) of 35.80 (<50) and a grand average of hydropathicity (GRAVY) of -0.404, which indicates good protein-water interaction (hydrophilic). The protein contains 139 amino acids and weigh 15294.65 Daltons. Positively charged residues arginine and lysine and negatively charged residues aspartate and

glutamate in the sequence were found to be 18 and 20, respectively. None of the region was located in the transmembrane, as described by the TMHMM server (Figure-1).

4. Discussion

Data in mammals and insects have delineated insulin-signalling pathways and their downstream influence on transcription factors, gene and protein synthesis. Our focus in this study was to understand the molecular bases of the deranged brain glucose and redox homeostasis that we have earlier reported in STZ treated *N. cinerea* [5]. We built our hypothesis around the possible involvement of the *PI3K/AKT* and *RAS/MAPK* cascades and characterized for the first time, the insulin signalling response of *Nauphoeta cinerea* to the alkylating agent; streptozotocin.

The *PI3K/AKT* pathway – whose major activator is insulin [18] – is crucial for normal CNS functioning in mammals [19] and insects [20]. It is involved in neural processes like the regulation of growth and proliferation of neural stem cells [21], as well as, nerve potentiation [22]; which can be deranged by STZ's toxic effect on the cascade [23] to induce neuropathy [24], Alzheimer's disease [25], and other degenerative conditions. *ILPs* 2, 3 and 5 are putative ligands for the drosophila InR that triggers the brain *PI3K/AKT* pathway [26]. *ILP2* is released from paired clusters of neurosecretory cells in the pars intercerebralis (medial region) of the insect brain [27], to act on specific neuronal targets in larva and adults [28]. The release of *ILP* is controlled by glucose sensors that are independent of the neurosecretory cells [29], similar to insulin release from the mammalian beta cells of pancreas [30].

We found reduced mRNA levels of *ILP2* in head homogenates of STZ treated nymphs, similar to reports of decreased Insulin concentrations in brain of rats after intracerebroventricular STZ injection [31]. It is noteworthy that the knockout of *ILP2* in *Drosophila* is linked with decreased body weight, increased Trehalose levels and increased developmental time [32], similar to our earlier report of reduced body mass in this group of STZ-treated cockroaches [5]. Furthermore, the mRNA levels of *INR*, *AKT* and *PI3K* were significantly reduced, similar to findings in STZ-induced brain Insulin-resistance rats [33] and *D. melanogaster INR* that present defective insulin signalling [34].

Conversely, cell signalling via the *MAPK* pathway has been linked with the progression of degenerative diseases like Alzheimer's, diabetes and cancers both in Humans and rodent streptozotocin-models [35,36]. Our results demonstrate that up regulated *MAPK* signalling is a feature of streptozotocin induced metabolic disruptions in the cockroach head, indicating the possible relevance of *Nauphoeta cinerea* in studying human degenerative diseases, and suggesting the possibility of manipulating *MAPK* signalling in the cockroach brain for therapeutic advantage. We have previously shown upregulated inflammation-like response in streptozotocin-treated cockroaches (). Our current result of upregulated *P38* and *JNK MAPK* genes is in tandem with reports of the mediation of cellular response to xenobiotics via the *P38* and *JNK MAPK* stress activated protein kinase signalling [37].

Bioinformatics analysis of protein kinase crystal structure shows that the activation segment of *ERK/MAPK* range between two conserved tripeptide motifs (DFG and APE), and a catalytic loop comprising of a conserved aspartate residue immediately following an arginine residue (**Figure 1**) has been documented to precede the activation segment of conventional

kinases [38]. The conservation of *MAPK* structure-function elements that we have reported between *Nauphoeta cinerea* and other eukaryotes further highlights the suitability of the cockroach for modelling degenerative diseases.

References

- [1] J. Havrankova, D. Schmechel, J. Roth, M. Brownstein, Identification of insulin in rat brain., *Proc. Natl. Acad. Sci. U. S. A.* 75 (1978) 5737–41. <https://doi.org/10.1073/pnas.75.11.5737>.
- [2] H. Nagasawa, H. Kataoka, A. Isogai, S. Tamura, A. Suzuki, H. Ishizaki, A. Mizoguchi, Y. Fujiwara, A. Suzuki, Amino-terminal amino Acid sequence of the silkworm prothoracicotropic hormone: homology with insulin., *Science.* 226 (1984) 1344–5. <https://doi.org/10.1126/science.226.4680.1344>.
- [3] S.L. Chiu, C.M. Chen, H.T. Cline, Insulin Receptor Signaling Regulates Synapse Number, Dendritic Plasticity, and Circuit Function In Vivo, *Neuron.* 58 (2008) 708–719. <https://doi.org/10.1016/j.neuron.2008.04.014>.
- [4] S. Takeda, N. Sato, H. Rakugi, R. Morishita, Molecular mechanisms linking diabetes mellitus and Alzheimer disease: Beta-amyloid peptide, insulin signaling, and neuronal function, *Mol. Biosyst.* 7 (2011) 1822–1827. <https://doi.org/10.1039/c0mb00302f>.
- [5] O.C. Olagoke, B.A. Afolabi, J.B.T. Rocha, Streptozotocin induces brain glucose metabolic changes and alters glucose transporter expression in the Lobster cockroach ; *Nauphoeta cinerea* (*Blattodea* : *Blaberidae*), *Mol. Cell. Biochem.* (2020) 1–35. <https://doi.org/DOI: 10.1007/s11010-020-03976-4>.
- [6] E.J. Rulifson, S.K. Kim, R. Nusse, Ablation of insulin-producing neurons in flies: growth and diabetic phenotypes., *Science.* 296 (2002) 1118–20. <https://doi.org/10.1126/science.1070058>.
- [7] S.U. Devaskarss, S.J. Giddingsn, P.A. Rajakumars, L.R. Carnaghin, R.K. Menonll, D.S.

- Zahm, Insulin Gene Expression and Insulin Synthesis in Mammalian' Neuronal Cells, 1994. <http://www.jbc.org/content/269/11/8445.full.pdf> (accessed July 20, 2019).
- [8] E. Biazquez, E. Velázquez, V. Hurtado-Carneiro, J.M. Ruiz-Albusac, Insulin in the Brain: Its Pathophysiological Implications for States Related with Central Insulin Resistance, Type 2 Diabetes and Alzheimers Disease, *Front. Endocrinol. (Lausanne)*. 5 (2014) 161. <https://doi.org/10.3389/fendo.2014.00161>.
- [9] S.M. Gray, R.I. Meijer, E.J. Barrett, Insulin regulates brain function, but how does it get there?, *Diabetes*. 63 (2014) 3992–7. <https://doi.org/10.2337/db14-0340>.
- [10] W.A. Banks, J.B. Owen, M.A. Erickson, Insulin in the brain: There and back again, *Pharmacol. Ther.* 136 (2012) 82–93. <https://doi.org/10.1016/j.pharmthera.2012.07.006>.
- [11] Y. Antonova, A.J. Arik, W. Moore, M.A. Riehle, M.R. Brown, *Insulin-like Peptides: Structure, Signaling, and Function*, Elsevier, 2012. <https://doi.org/10.1016/B978-0-12-384749-2.10002-0>.
- [12] P. Hof, S. Pluskey, S. Dhe-Paganon, M. JEck, S. Shoelson, Crystal Structure of the Tyrosine Phosphatase SHP-2, *Nature*. 388 (1997) 539–547.
- [13] M. Cargnello, P.P. Roux, Activation and Function of the MAPKs and Their Substrates, the MAPK-Activated Protein Kinases, *Microbiol. Mol. Biol. Rev.* 75 (2011) 50–83. <https://doi.org/10.1128/mnbr.00031-10>.
- [14] A. V. Leopold, K.G. Chernov, V. V. Verkhusha, Optogenetically controlled protein kinases for regulation of cellular signaling, *Chem. Soc. Rev.* 47 (2018) 2454–2484. <https://doi.org/10.1039/c7cs00404d>.

- [15] A.L.A. Segatto, J.F. Diesel, E.L.S. Loreto, J.B.T. da Rocha, A.L.A. Segatto, J.F. Diesel, E.L.S. Loreto, J.B.T. da Rocha, De novo transcriptome assembly of the lobster cockroach *Nauphoeta cinerea* (Blaberidae), *Genet. Mol. Biol.* 41 (2018) 713–721. <https://doi.org/10.1590/1678-4685-gmb-2017-0264>.
- [16] B.C. Piccoli, A.L.A. Segatto, É.L.S. Loreto, J.C.F. Moreira, D.M.P. Ardisson-Araújo, J.B.T. Rocha, Transcriptional analyses of acute per os exposure and co-exposure of 4-vinylcyclohexene and methylmercury-contaminated diet in adults of *Drosophila melanogaster*, *Environ. Pollut.* 263 (2020) 114632. <https://doi.org/10.1016/j.envpol.2020.114632>.
- [17] B. Webb, A. Sali, Comparative protein structure modeling using MODELLER, *Curr. Protoc. Bioinforma.* (2016). <https://doi.org/10.1002/cpbi.3>.
- [18] V.A. Rafalski, A. Brunet, Energy metabolism in adult neural stem cell fate, *Prog. Neurobiol.* 93 (2011) 182–203. <https://doi.org/10.1016/j.pneurobio.2010.10.007>.
- [19] J. Sun, X. Yang, Y. Zhang, W. Zhang, J. Lu, Q. Hu, R. Liu, C. Zhou, C. Chen, Salvinatorin A attenuates early brain injury through PI3K/Akt pathway after subarachnoid hemorrhage in rat, *Brain Res.* 1719 (2019) 64–70. <https://doi.org/10.1016/j.brainres.2019.05.026>.
- [20] J.H. Kim, J.S. Choi, B.H. Lee, PI3K/Akt and MAPK pathways evoke activation of FoxO transcription factor to undergo neuronal apoptosis in brain of the silkworm *Bombyx mori* (Lepidoptera: Bombycidae), *Cell. Mol. Biol. (Noisy-Le-Grand)*. Suppl.58 (2012).
- [21] S.H. Koh, E.H. Lo, The role of the PI3K pathway in the regeneration of the damaged brain by neural stem cells after cerebral infarction, *J. Clin. Neurol.* 11 (2015) 297–304.

- <https://doi.org/10.3988/jcn.2015.11.4.297>.
- [22] H.Y. Man, Q. Wang, W.Y. Lu, W. Ju, G. Ahmadian, L. Liu, S. D'Souza, T.P. Wong, C. Taghibiglou, J. Lu, L.E. Becker, L. Pei, F. Liu, M.P. Wymann, J.F. MacDonald, Y.T. Wang, Activation of PI3-kinase is required for AMPA receptor insertion during LTP of mEPSCs in cultured hippocampal neurons, *Neuron*. 38 (2003) 611–624. [https://doi.org/10.1016/S0896-6273\(03\)00228-9](https://doi.org/10.1016/S0896-6273(03)00228-9).
- [23] S. Bathina, U.N. Das, Dysregulation of PI3K-Akt-mTOR pathway in brain of streptozotocin-induced type 2 diabetes mellitus in Wistar rats, *Lipids Health Dis*. 17 (2018) 1–11. <https://doi.org/10.1186/s12944-018-0809-2>.
- [24] H.M. Sickmann, H.S. Waagepetersen, Effects of diabetes on brain metabolism – is brain glycogen a significant player?, *Metab. Brain Dis*. 30 (2014) 335–343. <https://doi.org/10.1007/s11011-014-9546-z>.
- [25] M. Su, K. Naderi, N. Samson, I. Youssef, L. Fülöp, Z. Bozso, S. Laroche, B. Delatour, S. Davis, Mechanisms Associated with Type 2 Diabetes as a Risk Factor for Alzheimer-Related Pathology, *Mol. Neurobiol*. 56 (2019) 5815–5834. <https://doi.org/10.1007/s12035-019-1475-8>.
- [26] D.R. Nässel, Y. Liu, J. Luo, Insulin/IGF signaling and its regulation in *Drosophila*, *Gen. Comp. Endocrinol*. 221 (2015) 255–266. <https://doi.org/10.1016/j.ygcen.2014.11.021>.
- [27] B. de Velasco, T. Erclik, D. Shy, J. Sclafani, H. Lipshitz, R. McInnes, V. Hartenstein, Specification and development of the pars intercerebralis and pars lateralis, neuroendocrine command centers in the *Drosophila* brain, *Dev. Biol*. 302 (2007) 309–323. <https://doi.org/10.1016/j.ydbio.2006.09.035>.

- [28] R. Bader, L. Sarraf-Zadeh, M. Peters, N. Moderau, H. Stocker, K. Kö hler, M.J. Pankratz, E. Hafen, The IGFBP7 homolog Imp-L2 promotes insulin signaling in distinct neurons of the *Drosophila* brain, *J. Cell Sci.* 126 (2013) 2571–2576. <https://doi.org/10.1242/jcs.120261>.
- [29] S. Park, R.W. Alfa, S.M. Topper, G.E.S. Kim, L. Kockel, S.K. Kim, A Genetic Strategy to Measure Circulating *Drosophila* Insulin Reveals Genes Regulating Insulin Production and Secretion, *PLoS Genet.* 10 (2014). <https://doi.org/10.1371/journal.pgen.1004555>.
- [30] P. Rorsman, E. Renström, Insulin granule dynamics in pancreatic beta cells, *Diabetologia.* 46 (2003) 1029–1045. <https://doi.org/10.1007/s00125-003-1153-1>.
- [31] E. Grünblatt, M. Salkovic-Petrisic, J. Osmanovic, P. Riederer, S. Hoyer, Brain insulin system dysfunction in streptozotocin intracerebroventricularly treated rats generates hyperphosphorylated tau protein, *J. Neurochem.* 101 (2007) 757–770. <https://doi.org/10.1111/j.1471-4159.2006.04368.x>.
- [32] S. Grönke, D.F. Clarke, S. Broughton, T.D. Andrews, L. Partridge, Molecular evolution and functional characterization of *Drosophila* insulin-like peptides, *PLoS Genet.* 6 (2010). <https://doi.org/10.1371/journal.pgen.1000857>.
- [33] A. Knezovic, A. Loncar, J. Homolak, U. Smailovic, J. Osmanovic Barilar, L. Ganoci, N. Bozina, P. Riederer, M. Salkovic-Petrisic, Rat brain glucose transporter-2, insulin receptor and glial expression are acute targets of intracerebroventricular streptozotocin: risk factors for sporadic Alzheimer’s disease?, *J. Neural Transm.* 124 (2017) 695–708. <https://doi.org/10.1007/s00702-017-1727-6>.
- [34] M. Tatar, A. Kopelman, D. Epstein, M.P. Tu, C.M. Yin, R.S. Garofalo, A mutant

- Drosophila* insulin receptor homolog that extends life-span and impairs neuroendocrine function, *Science* (80-.). 292 (2001) 107–110. <https://doi.org/10.1126/science.1057987>.
- [35] L. Adhikary, F. Chow, D.J. Nikolic-Paterson, C. Stambe, J. Dowling, R.C. Atkins, G.H. Tesch, Abnormal p38 mitogen-activated protein kinase signalling in human and experimental diabetic nephropathy, *Diabetologia*. 47 (2004) 1210–1222. <https://doi.org/10.1007/s00125-004-1437-0>.
- [36] E.F. Wagner, Á.R. Nebreda, Signal integration by JNK and p38 MAPK pathways in cancer development, *Nat. Rev. Cancer*. 9 (2009) 537–549. <https://doi.org/10.1038/nrc2694>.
- [37] G. Sabio, R.J. Davis, TNF and MAP kinase signalling pathways, *Semin. Immunol.* 26 (2014) 237–245. <https://doi.org/10.1016/j.smim.2014.02.009>.
- [38] L.N. Johnson, M.E.M. Noble, D.J. Owen, Active and inactive protein kinases: Structural basis for regulation, *Cell*. 85 (1996) 149–158. [https://doi.org/10.1016/S0092-8674\(00\)81092-2](https://doi.org/10.1016/S0092-8674(00)81092-2).

5. DISCUSSION

The third sustainable development goal adopted by the United Nations is summarised as good health and wellbeing, as it seeks amongst other objectives to eradicate chronic non-communicable diseases which have been estimated to cause about 63% of global deaths (<https://sustainabledevelopment.un.org/sdg3>). Consequently, understanding the pathogenesis of these diseases is crucial to the establishment of appropriate prevention, management and treatment plans. Claude Bernard postulated that “*The problem of science will consist precisely in this, to seek the unitary character of physiological and pathological phenomena in the midst of the infinite variety of their particular manifestations*” [128], perfectly depicting the problems biomedical scientists face today with modeling pathophysiological conditions for therapeutic purposes. In spite of initial skepticism about the application of insects in biomedical studies, *Drosophila melanogaster* has been harnessed in the research for specialized cancer treatment [129,130], the screening of genes that are involved in glucose toxicity [113,131], and a host of other molecular studies into the etiology of neurodegenerative diseases. *Nauphoeta cinerea* is an established experimental organism for toxicity testing [132–135], we herein attempt to study the brain energy metabolic changes that ensue from glucose dyshomeostasis, by exposing the cockroach to a known alkylating agent – streptozotocin.

Our first experiment exposed *N. cinerea* nymphs to a single dose STZ injection (74 and 740 nmol) and monitored the cockroaches for 7 days. We found similar increase in glucose levels in head homogenates of the cockroaches as has been reported in the brain of hyperglycemic mammals [136,137]. Albeit, fat body glycogen levels were reduced in consonance with reports of negative feedback effect of hyperglycemia on glycogen synthase activity [138,139]. STZ is known to upregulate pro-apoptotic proteins and downregulate pro-survival proteins [140], this may explain our findings of reduced survival, total body mass and triglyceride content of head homogenates in the STZ-treated nymphs. We further found reduced AChE activity but increased TBARs levels in head homogenates of STZ treated nymphs, hyperglycemia triggers superoxide production which induces oxidative stress that activates nuclear factor erythroid 2-related factor to upregulate expression of antioxidant genes [141–143]. There was significant increase in the GST activity and GSH levels of STZ-treated nymphs, similar to data in STZ-treated rats and alloxan-treated *D. melanogaster* [104,144]. In both insects and mammals, the brain is “walled off” from circulation to prevent the toxic effect of circulatory solutes on the brain, glucose entry into the brain is therefore dependent on the expression of glucose

transporter 1 which is upregulated in the brain of STZ-treated rats [25,31,145]. We also found increased mRNA levels of GLUT 1 in head homogenates of *N. cinerea* treated with STZ.

Secondly, we examined the expression of inflammatory and antioxidant genes in response to the changes in glucose metabolism and oxidative stress that we have earlier reported in STZ-treated cockroaches. Raised levels of reactive oxygen species have been correlated with activation of the TNF/JNK and TOLL/NF- κ B pathways in *D. melanogaster* tissues [146,147], just as tissue damage triggers the JAK/STAT pathway to accomplish wound healing [148,149]. We found increased expression of target genes of the JNK, TOLL/NF- κ B and JAK/STAT pathways in head homogenates of STZ-treated *N. cinerea*. Antioxidant systems are essential for protection against ROS-mediated tissues damage [150,151]. We recorded increased expression of SOD and Catalase but no significant difference in mRNA levels PRX4 and TRX1,2 and 5, suggesting capacity of the cockroach to handle the level of oxidative stress we have earlier recorded only with primary antioxidants and with no need for the peroxiredoxin system. On the other hand, GST sigma and theta were upregulated in STZ-treated nymphs, but there was no significant difference in GST delta expression, signifying the importance of GST *s and t* as *N. cinerea* detoxification enzymes as have been earlier recorded [133,134]. We further highlighted the evolutionary conservation between the GST toxification system of *Nauphoeta cinerea* and other insects.

Third, we used RNA sequencing transcriptomic technique to investigate brain-specific molecular events that characterize our earlier described streptozotocin-induced glucose metabolic changes in the lobster cockroach. 226 genes were deregulated at low dose STZ treatment, while 278 genes were deregulated at high dose treatment. There were more up regulated than down regulated genes at both doses of injection, as ribosomal proteins were the most up regulated at both low and high dose streptozotocin treatment in line with reports of increased phosphorylation of the 40S ribosomal protein S6 in rodent models of diabetes and hyperglycemic humans [152] Finally, we used RT-qPCR and in silico methods to explore the modulation of insulin signaling the lobster cockroach. Target genes of the phosphatidylinositol 3-kinase (*PI3K*)/protein kinase B (*AKT*) insulin signaling were down regulated while a downstream effector of the pathway; forkhead box (FOXO) was up regulated, this is similar to reports of brain insulin resistance in streptozotocin-treated rats [153], impaired PI3K/AKT signaling in insulin receptor mutant rats [154], and negative feedback response of FOXO to

PI3K/AKT signaling [155]. The ‘second arm’ of the insulin signaling pathway; RAS/MAPK (mitogen-activated protein kinase) is associated with the progression of diabetes. Our result of up regulated RAS/MAPK signalling, alongside increased P38 and c-Jun N-terminal kinase (JNK) MAPK inflammation-like response mirrors the reported pathogenesis of diabetes mellitus in humans and rodents [156,157] as bioinformatic analysis further showed conservation of MAPK structure-function elements between *Nauphoeta cinerea* and other animals.

6. CONCLUSION

Evidences from the studies presented herein suggest that streptozotocin toxicity is conserved from insects to mammals and the mammalian β -cell cytotoxic glucose analogue may impair glucose metabolism in insects, making *Nauphoeta cinerea* a potential viable organism for studying hyperglycaemia-associated genetic and biochemical perturbations.

In a similar manner to biochemical changes in rodents, head glucose, *GLUT1* and TBARS levels were raised. Interestingly, the cockroach seemed capable of detoxifying the dosage of STZ used and attaining redox balance as enzyme and mRNA levels of antioxidants / detoxifying molecules (*GST*, *GSH*, *SOD*, *Catalase*, *GST sigma* and *GST theta*) and inflammation-related genes (*JNK*, *TOLL/NF-kB* and *UPD3/JAK/STAT* pathway genes) were increased. The corresponding up regulation of both antioxidant and inflammation-related genes further buttresses the proposed crosstalk between redox and inflammation signaling. Consequently fat body glycogen content, head triglyceride, AChE and MTT reducing ability were reduced. Indeed the RNA seq transcriptomic result of up regulated ribosomal proteins in STZ-treated nymphs requires in depth study as the 40S ribosomal protein S6 has been implicated in the pathogenesis of diabetes in mammals. Moreover, the conserved PI3K/AKT and ERK/MAPK insulin-like signaling of *N. cinerea* is modified by streptozotocin injection.

The conservation of mammalian pancreatic beta cell function in the insulin-like peptide producing cells of the insect brain, as well as our report of similar effect of STZ injection in *N. cinerea* compared with results in mammalian models makes the cockroach a likely experimental organism for studying hyperglycaemia-linked metabolic changes, especially in the brain.

7. PERSPECTIVES

The availability of a full genome sequence is generally considered as a prerequisite for the establishment of a model organism for biomedical research. Our current transcriptomic approach gives useful insight into time and treatment-specific molecular events, but the use of *Nauphoeta cinerea* in researching human diseases would benefit greatly from a full genomic data that offers indebt knowledge of the areas of homology between the cockroach and mammals. Furthermore, our study may benefit from data of mitochondrial analysis, as well as electrophysiological and behavioral recordings in STZ-treated cockroaches (especially with direct injections to the head) as it may present pathophysiological information that would be significant to understanding human neurodegenerative diseases, thereby adding to knowledge of the relationship between hyperglycemia and Alzheimer's disease.

8. References.

- [1] M. Ghamari, V. Hosseiniaveh, A. Darvishzadeh, N.P. Chougule, carbohydrases in the digestive system of the spined soldier bug, *podisus maculiventris* (say) (hemiptera: pentatomidae), Arch. Insect Biochem. Physiol. 85 (2014) 195–215. <https://doi.org/10.1002/arch.21153>.
- [2] S. Ramzi, V. Hosseiniaveh, Biochemical characterization of digestive α -amylase, α -glucosidase and β -glucosidase in pistachio green stink bug, *Brachynema germari* Kolenati (Hemiptera: Pentatomidae), J. Asia. Pac. Entomol. 13 (2010) 215–219. <https://doi.org/10.1016/j.aspen.2010.03.009>.
- [3] James L. Nation, Insect Physiology and Biochemistry, 2016. <https://doi.org/10.1038/267754a0>.
- [4] Y. Dong Wei, K. Sik Lee, Z. Zheng Gui, H. Joo Yoon, I. Kim, G. Zheng Zhang, X. Guo, H. Dae Sohn, B. Rae Jin, Molecular cloning, expression, and enzymatic activity of a novel endogenous cellulase from the mulberry longicorn beetle, *Apriona germari*, Comp. Biochem. Physiol. - B Biochem. Mol. Biol. 145 (2006) 220–229.

<https://doi.org/10.1016/j.cbpb.2006.07.007>.

- [5] Y.D. Wei, K.S. Lee, Z.Z. Gui, H.J. Yoon, I. Kim, Y.H. Je, S.M. Lee, G.Z. Zhang, X. Guo, H.D. Sohn, B.R. Jin, N-linked glycosylation of a beetle (*Apriona germari*) cellulase Ag-EGase II is necessary for enzymatic activity, *Insect Biochem. Mol. Biol.* 36 (2006) 435–441. <https://doi.org/10.1016/j.ibmb.2006.03.007>.
- [6] T. Kunieda, M. Beye, H. Takeuchi, A. Kamikouchi, R. Maleszka, T. Fujiyuki, A.L. Toth, E. Kage, S. Foret, T. Kubo, M. Morioka, G.E. Robinson, K. Ohashi, S.A. Ament, R. Kucharski, Carbohydrate metabolism genes and pathways in insects: insights from the honey bee genome, *Insect Mol. Biol.* 15 (2006) 563–576. <https://doi.org/10.1111/j.1365-2583.2006.00677.x>.
- [7] A. Becker, P. Schlöder, J.E. Steele, G. Wegener, The regulation of trehalose metabolism in insects, *Experientia.* 52 (1996) 433–439. <https://doi.org/10.1007/BF01919312>.
- [8] G.R. Wyatt, G.F. Kale, The chemistry of insect hemolymph. II. Trehalose and other carbohydrates., *J. Gen. Physiol.* 40 (1957) 833–847. <https://doi.org/10.1085/jgp.40.6.833>.
- [9] S.. Thompson, Trehalose-The Insect 'Blood' sugar, in: S.. Simpson (Ed.), *Adv. In Insect Phys.*, Elsevier Academic Press, 2003: pp. 206–261. [https://doi.org/10.1016/S0065-2806\(03\)31004-5](https://doi.org/10.1016/S0065-2806(03)31004-5).
- [10] R. Gruetter, Glycogen: The forgotten cerebral energy store, *J. Neurosci. Res.* 74 (2003) 179–183. <https://doi.org/10.1002/jnr.10785>.
- [11] S.J. Hindle, R.J. Bainton, Barrier mechanisms in the *Drosophila* blood-brain barrier, *Front. Neurosci.* 8 (2014) 1–12. <https://doi.org/10.3389/fnins.2014.00414>.
- [12] A.A.K. Patabendige, D.E.M. Dolman, N.J. Abbott, D.J. Begley, S.R. Yusof, Structure and function of the blood–brain barrier, *Neurobiol. Dis.* 37 (2009) 13–25. <https://doi.org/10.1016/j.nbd.2009.07.030>.
- [13] S. Park, R.W. Alfa, S.M. Topper, G.E.S. Kim, L. Kockel, S.K. Kim, A Genetic Strategy to Measure Circulating *Drosophila* Insulin Reveals Genes Regulating Insulin Production and Secretion, *PLoS Genet.* 10 (2014). <https://doi.org/10.1371/journal.pgen.1004555>.

- [14] Y.-W.C. Fridell, M. Hoh, O. Kréneisz, S. Hosier, C. Chang, D. Scantling, D.K. Mulkey, S.L. Helfand, Increased uncoupling protein (UCP) activity in *Drosophila* insulin-producing neurons attenuates insulin signaling and extends lifespan, *Aging* (Albany, NY). 1 (2009) 699–713. <https://doi.org/10.18632/aging.100067>.
- [15] O. Kréneisz, X. Chen, Y.W.C. Fridell, D.K. Mulkey, Glucose increases activity and Ca²⁺ in insulin-producing cells of adult *Drosophila*, *Neuroreport*. 21 (2010) 1116–1120. <https://doi.org/10.1097/WNR.0b013e3283409200>.
- [16] H.G. Joost, B. Thorens, The extended GLUT-family of sugar/polyol transport facilitators: Nomenclature, sequence characteristics, and potential function of its novel members, *Mol. Membr. Biol.* 18 (2001) 247–256. <https://doi.org/10.1080/09687680110090456>.
- [17] G.A. Rutter, T.J. Pullen, D.J. Hodson, A. Martinez-Sanchez, Pancreatic β -cell identity, glucose sensing and the control of insulin secretion, *Biochem. J.* 466 (2015) 203–218. <https://doi.org/10.1042/BJ20141384>.
- [18] D.R. Nässel, J. Vanden Broeck, Insulin/IGF signaling in *Drosophila* and other insects: Factors that regulate production, release and post-release action of the insulin-like peptides, *Cell. Mol. Life Sci.* 73 (2016) 271–290. <https://doi.org/10.1007/s00018-015-2063-3>.
- [19] K. Takata, T. Kasahara, M. Kasahara, O. Ezaki, H. Hirano, Erythrocyte/HEPG2-type glucose transporter is concentrated in cells of blood-tissue barriers, *Biochem. Biophys. Res. Commun.* (1990). [https://doi.org/10.1016/S0006-291X\(05\)81022-8](https://doi.org/10.1016/S0006-291X(05)81022-8).
- [20] S. Obici, Z. Feng, G. Karkanias, D.G. Baskin, L. Rossetti, Decreasing hypothalamic insulin receptors causes hyperphagia and insulin resistance in rats, *Nat. Neurosci.* 5 (2002) 566–572. <https://doi.org/10.1038/nn0602-861>.
- [21] E. Biazquez, E. Velázquez, V. Hurtado-Carneiro, J.M. Ruiz-Albusac, Insulin in the Brain: Its Pathophysiological Implications for States Related with Central Insulin Resistance, Type 2 Diabetes and Alzheimers Disease, *Front. Endocrinol. (Lausanne)*. 5 (2014) 161. <https://doi.org/10.3389/fendo.2014.00161>.
- [22] A.P.K. Dick, S.I. Harik, A. Klip, D.M. Walker, Identification and characterization of the

glucose transporter of the blood-brain barrier by cytochalasin B binding and immunological reactivity, *Proc. Natl. Acad. Sci. U. S. A.* 81 (1984) 7233–7237. <https://doi.org/10.1073/pnas.81.22.7233>.

- [23] A.P.K. Dick, S.I. Harik, Distribution of the Glucose Transporter in the Mammalian Brain, *J. Neurochem.* 46 (1986) 1406–1411. <https://doi.org/10.1111/j.1471-4159.1986.tb01755.x>.
- [24] B.E. Levin, A.A. Dunn-Meynell, V.H. Routh, Brain glucose sensing and body energy homeostasis: role in obesity and diabetes, *Am. J. Physiol. Integr. Comp. Physiol.* 276 (1999) R1223–R1231. <https://doi.org/10.1152/ajpregu.1999.276.5.R1223>.
- [25] D.-J. Kim, J.H. Yu, M.-S. Shin, Y.-W. Shin, M.-S. Kim, Hyperglycemia Reduces Efficiency of Brain Networks in Subjects with Type 2 Diabetes, *PLoS One.* 11 (2016) e0157268. <https://doi.org/10.1371/journal.pone.0157268>.
- [26] J. Shi, B. Dong, Y. Mao, W. Guan, J. Cao, R. Zhu, S. Wang, Review: Traumatic brain injury and hyperglycemia, a potentially modifiable risk factor., *Oncotarget.* 7 (2016) 71052–71061. <https://doi.org/10.18632/oncotarget.11958>.
- [27] A. Weiler, A. Volkenhoff, H. Hertenstein, S. Schirmeier, Metabolite transport across the mammalian and insect brain diffusion barriers, *Neurobiol. Dis.* 107 (2017) 15–31. <https://doi.org/10.1016/j.nbd.2017.02.008>.
- [28] O. Peter Aadal Nielsen, R. Gunnar Andersson, R. Olga Andersson, Insect-based ex vivo model for testing blood-brain barrier penetration and method for exposing insect brain to chemical compounds, US009097706B2, 2015. <https://patents.google.com/patent/US20150072369A1/en>.
- [29] O. Peter Aadal Nielsen, R. Gunnar Andersson, Screening methods employing insects with blood brain barrier, US009 194864B2, 2015. <https://patents.google.com/patent/US9194864B2/en>.
- [30] T. Stork, D. Engelen, A. Krudewig, M. Silies, R.J. Bainton, C. Klämbt, Organization and function of the blood-brain barrier in *Drosophila*, *J. Neurosci.* 28 (2008) 587–597. <https://doi.org/10.1523/JNEUROSCI.4367-07.2008>.

- [31] F. Mayer, N. Mayer, L. Chinn, R.L. Pinsonneault, D. Kroetz, R.J. Bainton, Evolutionary conservation of vertebrate blood-brain barrier chemoprotective mechanisms in *Drosophila*, *J. Neurosci.* 29 (2009) 3538–3550. <https://doi.org/10.1523/jneurosci.5564-08.2009>.
- [32] T. Schwabe, R.J. Bainton, R.D. Fetter, U. Heberlein, U. Gaul, GPCR signaling is required for blood-brain barrier formation in *Drosophila*, *Cell.* 123 (2005) 133–144. <https://doi.org/10.1016/j.cell.2005.08.037>.
- [33] M.K. DeSalvo, S.J. Hindle, Z.M. Rusan, S. Orng, M. Eddison, K. Halliwill, R.J. Bainton, The *Drosophila* surface glia transcriptome: Evolutionary conserved blood-brain barrier processes, *Front. Neurosci.* 8 (2014). <https://doi.org/10.3389/fnins.2014.00346>.
- [34] J. Havrankova, D. Schmechel, J. Roth, M. Brownstein, Identification of insulin in rat brain., *Proc. Natl. Acad. Sci. U. S. A.* 75 (1978) 5737–41. <https://doi.org/10.1073/pnas.75.11.5737>.
- [35] H. Nagasawa, H. Kataoka, A. Isogai, S. Tamura, A. Suzuki, H. Ishizaki, A. Mizoguchi, Y. Fujiwara, A. Suzuki, Amino-terminal amino Acid sequence of the silkworm prothoracicotropic hormone: homology with insulin., *Science.* 226 (1984) 1344–5. <https://doi.org/10.1126/science.226.4680.1344>.
- [36] N. Okamoto, *Insect Insulin-Like Peptides*, *Handb. Horm.* (2016) 368–370. <https://doi.org/10.1016/B978-0-12-801028-0.00207-5>.
- [37] E.J. Rulifson, S.K. Kim, R. Nusse, Ablation of insulin-producing neurons in flies: growth and diabetic phenotypes., *Science.* 296 (2002) 1118–20. <https://doi.org/10.1126/science.1070058>.
- [38] T. Ikeya, M. Galic, P. Belawat, K. Nairz, E. Hafen, Nutrient-Dependent Expression of Insulin-like Peptides from Neuroendocrine Cells in the CNS Contributes to Growth Regulation in *Drosophila*, *Curr. Biol.* 12 (2002) 1293–1300. [https://doi.org/10.1016/S0960-9822\(02\)01043-6](https://doi.org/10.1016/S0960-9822(02)01043-6).
- [39] A.B. Nuss, M.R. Brown, Isolation of an insulin-like peptide from the Asian malaria mosquito, *Anopheles stephensi*, that acts as a steroidogenic gonadotropin across diverse mosquito taxa, *Gen. Comp. Endocrinol.* 258 (2018) 140–148.

<https://doi.org/10.1016/J.YGCEN.2017.05.007>.

- [40] D.W. Clarke, L. Mudd, F.T. Boyd, M. Fields, M.K. Raizada, Insulin Is Released from Rat Brain Neuronal Cells in Culture, *J. Neurochem.* 47 (1986) 831–836. <https://doi.org/10.1111/j.1471-4159.1986.tb00686.x>.
- [41] L. Wei, H. Matsumoto, D.E. Rhoads, Release of Immunoreactive Insulin from Rat Brain Synaptosomes Under Depolarizing Conditions, *J. Neurochem.* 54 (1990) 1661–1662. <https://doi.org/10.1111/j.1471-4159.1990.tb01219.x>.
- [42] W.S. Young, Periventricular hypothalamic cells in the rat brain contain insulin mRNA, *Neuropeptides.* 8 (1986) 93–97. [https://doi.org/10.1016/0143-4179\(86\)90035-1](https://doi.org/10.1016/0143-4179(86)90035-1).
- [43] R. Schechter, L. Holtzclaw, F. Sadiq, A. Kahn, S. Devaskar, Insulin Synthesis by Isolated Rabbit Neurons, *Endocrinology.* 123 (1988) 505–513. <https://doi.org/10.1210/endo-123-1-505>.
- [44] S.U. Devaskarss, S.J. Giddingsn, P.A. Rajakumars, L.R. Carnaghin, R.K. Menonll, D.S. Zahm, Insulin Gene Expression and Insulin Synthesis in Mammalian' Neuronal Cells, 1994. <http://www.jbc.org/content/269/11/8445.full.pdf> (accessed July 20, 2019).
- [45] W.A. Banks, J.B. Jaspan, A.J. Kastin, Effect of Diabetes Mellitus on the Permeability of the Blood–Brain Barrier to Insulin, *Peptides.* 18 (1997) 1577–1584. [https://doi.org/10.1016/S0196-9781\(97\)00238-6](https://doi.org/10.1016/S0196-9781(97)00238-6).
- [46] B.J. Wallum, G.J. Taborsky, D. Porte, D.P. Figlewicz, L. Jacobson, J.C. Beard, W.K. Ward, D. Dorsa, Cerebrospinal Fluid Insulin Levels Increase During Intravenous Insulin Infusions in Man*, *J. Clin. Endocrinol. Metab.* 64 (1987) 190–194. <https://doi.org/10.1210/jcem-64-1-190>.
- [47] T. Yamada, O. Habara, H. Kubo, T. Nishimura, Correction: Fat body glycogen serves as a metabolic safeguard for the maintenance of sugar levels in *Drosophila* (doi:10.1242/dev.158865) , *Development.* 145 (2018) dev165910. <https://doi.org/10.1242/dev.165910>.
- [48] S.M. Gray, R.I. Meijer, E.J. Barrett, Insulin regulates brain function, but how does it get there?, *Diabetes.* 63 (2014) 3992–7. <https://doi.org/10.2337/db14-0340>.

- [49] S. Grönke, D.F. Clarke, S. Broughton, T.D. Andrews, L. Partridge, Molecular evolution and functional characterization of *Drosophila* insulin-like peptides, *PLoS Genet.* 6 (2010). <https://doi.org/10.1371/journal.pgen.1000857>.
- [50] I. Yoshida, K. Moto, S. Sakurai, M. Iwami, A novel member of the bombyxin gene family: structure and expression of bombyxin G1 gene, an insulin-related peptide gene of the silkworm *Bombyx mori*, *Dev. Genes Evol.* 208 (1998) 407–410. <https://doi.org/10.1007/s004270050197>.
- [51] E. Świdarska, J. Strycharz, A. Wróblewski, J. Szemraj, J. Drzewoski, A. Śliwińska, Role of PI3K/AKT Pathway in Insulin-Mediated Glucose Uptake, in: *Glucose Transp. [Working Title]*, IntechOpen, 2018. <https://doi.org/10.5772/intechopen.80402>.
- [52] C. Kenyon, J. Chang, E. Gensch, A. Rudner, R. Tabtiang, A *C. elegans* mutant that lives twice as long as wild type, *Nature.* 366 (1993) 461–464. <https://doi.org/10.1038/366461a0>.
- [53] L. Fontana, L. Partridge, V.D. Longo, Extending healthy life span--from yeast to humans., *Science.* 328 (2010) 321–6. <https://doi.org/10.1126/science.1172539>.
- [54] D.J. Clancy, D. Gems, L.G. Harshman, S. Oldham, H. Stocker, E. Hafen, S.J. Leivers, L. Partridge, Extension of life-span by loss of CHICO, a *Drosophila* insulin receptor substrate protein., *Science.* 292 (2001) 104–6. <https://doi.org/10.1126/science.1057991>.
- [55] C. Kenyon, The Plasticity of Aging: Insights from Long-Lived Mutants, *Cell.* 120 (2005) 449–460. <https://doi.org/10.1016/J.CELL.2005.02.002>.
- [56] L.P. van der Heide, M.F.M. Hoekman, M.P. Smidt, The ins and outs of FoxO shuttling: mechanisms of FoxO translocation and transcriptional regulation, *Biochem. J.* 380 (2004) 297–309. <https://doi.org/10.1042/BJ20040167>.
- [57] X. Huang, G. Liu, J. Guo, Z. Su, The PI3K/AKT pathway in obesity and type 2 diabetes., *Int. J. Biol. Sci.* 14 (2018) 1483–1496. <https://doi.org/10.7150/ijbs.27173>.
- [58] Y. Antonova, A.J. Arik, W. Moore, M.A. Riehle, M.R. Brown, *Insulin-like Peptides: Structure, Signaling, and Function*, Elsevier, 2012. <https://doi.org/10.1016/B978-0-12-384749-2.10002-0>.

- [59] Bernard C., *Leçons de Physiologie Experimentale Applique a la Medicine Faites au College de France*. Paris, Baillière et fils, 1855.
https://books.google.com.br/books?hl=en&lr=&id=8rzKCq24woC&oi=fnd&pg=PR5&ots=5LlGjeiPH&sig=SZiVzqIq29irHrc2r0eB7Emyxk&redir_esc=y#v=onepage&q&f=false (accessed July 22, 2019).
- [60] R.. Schulingkamp, T.. Pagano, D. Hung, R.. Raffa, Insulin receptors and insulin action in the brain: review and clinical implications, *Neurosci. Biobehav. Rev.* 24 (2000) 855–872. [https://doi.org/10.1016/S0149-7634\(00\)00040-3](https://doi.org/10.1016/S0149-7634(00)00040-3).
- [61] N. Marty, M. Dallaporta, B. Thorens, Brain Glucose Sensing, Counterregulation, and Energy Homeostasis, *Physiology.* 22 (2007) 241–251. <https://doi.org/10.1152/physiol.00010.2007>.
- [62] A.I. Duarte, M.S. Santos, R. Seïça, C.R. de Oliveira, Insulin affects synaptosomal GABA and glutamate transport under oxidative stress conditions, *Brain Res.* 977 (2003) 23–30. [https://doi.org/10.1016/S0006-8993\(03\)02679-9](https://doi.org/10.1016/S0006-8993(03)02679-9).
- [63] A.I. Duarte, T. Proença, C.R. Oliveira, M.S. Santos, A.C. Rego, Insulin restores metabolic function in cultured cortical neurons subjected to oxidative stress., *Diabetes.* 55 (2006) 2863–70. <https://doi.org/10.2337/db06-0030>.
- [64] A.A.M. Rensink, I. Otte-Höller, R. de Boer, R.R. Bosch, H.J. ten Donkelaar, R.M.W. de Waal, M.M. Verbeek, B. Kremer, Insulin inhibits amyloid β -induced cell death in cultured human brain pericytes, *Neurobiol. Aging.* 25 (2004) 93–103. [https://doi.org/10.1016/S0197-4580\(03\)00039-3](https://doi.org/10.1016/S0197-4580(03)00039-3).
- [65] R. Ghasemi, A. Haeri, L. Dargahi, Z. Mohamed, A. Ahmadiani, Insulin in the Brain: Sources, Localization and Functions, *Mol. Neurobiol.* 47 (2013) 145–171. <https://doi.org/10.1007/s12035-012-8339-9>.
- [66] M. Schubert, D.P. Brazil, D.J. Burks, J.A. Kushner, J. Ye, C.L. Flint, J. Farhang-Fallah, P. Dikkes, X.M. Warot, C. Rio, G. Corfas, M.F. White, Insulin receptor substrate-2 deficiency impairs brain growth and promotes tau phosphorylation., *J. Neurosci.* 23 (2003) 7084–92. <https://doi.org/10.1523/JNEUROSCI.23-18-07084.2003>.
- [67] Q.-G. Xu, X.-Q. Li, S.A. Kotecha, C. Cheng, H.S. Sun, D.W. Zochodne, Insulin as an in

- vivo growth factor, *Exp. Neurol.* 188 (2004) 43–51.
<https://doi.org/10.1016/J.EXPNEUROL.2004.03.008>.
- [68] D.W. Clarke, F.T. Boyd, M.S. Kappys, M.K. Raizadatjj, The Journal Of Biological Chemistry Insulin Binds to Specific Receptors and Stimulates Deoxyglucose Uptake in Cultured Glial Cells from Rat Brain, 1984.
<http://www.jbc.org/content/259/19/11672.full.pdf> (accessed July 21, 2019).
- [69] E.M. Bingham, D. Hopkins, D. Smith, A. Pernet, W. Hallett, L. Reed, P.K. Marsden, S.A. Amiel, The Role of Insulin in Human Brain Glucose Metabolism, *Diabetes*. 51 (2002) 3384–3390. <https://doi.org/10.2337/DIABETES.51.12.3384>.
- [70] C. García-Cáceres, C. Quarta, L. Varela, Y. Gao, T. Gruber, B. Legutko, M. Jastroch, P. Johansson, J. Ninkovic, C.-X. Yi, O. Le Thuc, K. Szigeti-Buck, W. Cai, C.W. Meyer, P.T. Pfluger, A.M. Fernandez, S. Luquet, S.C. Woods, I. Torres-Alemán, C.R. Kahn, M. Götz, T.L. Horvath, M.H. Tschöp, Astrocytic Insulin Signaling Couples Brain Glucose Uptake with Nutrient Availability, *Cell*. 166 (2016) 867–880.
<https://doi.org/10.1016/J.CELL.2016.07.028>.
- [71] A. Kleinridders, H.A. Ferris, W. Cai, C.R. Kahn, Insulin action in brain regulates systemic metabolism and brain function., *Diabetes*. 63 (2014) 2232–43.
<https://doi.org/10.2337/db14-0568>.
- [72] G. Bedse, F. Di Domenico, G. Serviddio, T. Cassano, Aberrant insulin signaling in Alzheimer’s disease: current knowledge, *Front. Neurosci.* 9 (2015) 204.
<https://doi.org/10.3389/fnins.2015.00204>.
- [73] A.D. Association, 2. Classification and diagnosis of diabetes: Standards of medical care in diabetesd2019, *Diabetes Care*. 42 (2019) S13–S28. <https://doi.org/10.2337/dc19-S002>.
- [74] T.J. Wilkin, The accelerator hypothesis: A review of the evidence for insulin resistance as the basis for type i as well as type II diabetes, *Int. J. Obes.* 33 (2009) 716–726.
<https://doi.org/10.1038/ijo.2009.97>.
- [75] A. King, A. Austin, Animal Models of Type 1 and Type 2 Diabetes Mellitus, in: P.M. Conn (Ed.), *Anim. Model. Study Hum. Dis.*, Second, Elsevier Inc., 2017: pp. 245–265.

<https://www.sciencedirect.com/book/9780128094686/animal-models-for-the-study-of-human-disease> (accessed November 21, 2020).

- [76] P. Graham, L. Pick, *Drosophila* as a Model for Diabetes and Diseases of Insulin Resistance, in: *Curr. Top. Dev. Biol.*, Academic Press Inc., 2017: pp. 397–419. <https://doi.org/10.1016/bs.ctdb.2016.07.011>.
- [77] E.J. Rulifson, S.K. Kim, R. Nusse, Ablation of insulin-producing neurons in flies: Growth and diabetic phenotypes, *Science* (80-.). 296 (2002) 1118–1120. <https://doi.org/10.1126/science.1070058>.
- [78] P. Pournaghi, R.-A. Sadrkhanlou, S. Hasanzadeh, A. Foroughi, An investigation on body weights, blood glucose levels and pituitary-gonadal axis hormones in diabetic and metformin-treated diabetic female rats., *Vet. Res. Forum an Int. Q. J.* 3 (2012) 79–84. <http://www.ncbi.nlm.nih.gov/pubmed/25653751> (accessed November 21, 2020).
- [79] L.P. Musselman, J.L. Fink, T.J. Baranski, Similar effects of high-fructose and high-glucose feeding in a *Drosophila* model of obesity and diabetes, *PLoS One.* 14 (2019). <https://doi.org/10.1371/journal.pone.0217096>.
- [80] J.B. Majithiya, R. Balaraman, Metformin reduces blood pressure and restores endothelial function in aorta of streptozotocin-induced diabetic rats, *Life Sci.* 78 (2006) 2615–2624. <https://doi.org/10.1016/j.lfs.2005.10.020>.
- [81] K.L.D. De Angelis, A.R. Oliveira, P. Dall’Ago, L.R.A. Peixoto, G. Gadonski, S. Lacchini, T.G. Fernandes, M.C. Irigoyen, Effects of exercise training on autonomic and myocardial dysfunction in streptozotocin-diabetic rats, in: *Brazilian J. Med. Biol. Res., Associacao Brasileira de Divulgacao Cientifica*, 2000: pp. 635–641. <https://doi.org/10.1590/S0100-879X2000000600004>.
- [82] B.L. Furman, Streptozotocin-Induced Diabetic Models in Mice and Rats, *Curr. Protoc. Pharmacol.* 70 (2015) 5.47.1-5.47.20. <https://doi.org/10.1002/0471141755.ph0547s70>.
- [83] K. Shah, S. DeSilva, T. Abbruscato, The role of glucose transporters in brain disease: Diabetes and Alzheimer’s disease, *Int. J. Mol. Sci.* 13 (2012) 12629–12655. <https://doi.org/10.3390/ijms131012629>.

- [84] O.C. Olagoke, B.A. Afolabi, J.B.T. Rocha, Streptozotocin induces brain glucose metabolic changes and alters glucose transporter expression in the Lobster cockroach ; *Nauphoeta cinerea* (Blattodea : Blaberidae), *Mol. Cell. Biochem.* (2020) 1–35. <https://doi.org/DOI: 10.1007/s11010-020-03976-4>.
- [85] W. Zhang, A. Welihinda, J. Mechanic, H. Ding, L. Zhu, Y. Lu, Z. Deng, Z. Sheng, B. Lv, Y. Chen, J.Y. Roberge, B. Seed, Y.X. Wang, EGT1442, a potent and selective SGLT2 inhibitor, attenuates blood glucose and HbA1c levels in db/db mice and prolongs the survival of stroke-prone rats, *Pharmacol. Res.* 63 (2011) 284–293. <https://doi.org/10.1016/j.phrs.2011.01.001>.
- [86] H. Si, Z. Fu, P.V.A. Babu, W. Zhen, T. LeRoith, M.P. Meaney, K.A. Voelker, Z. Jia, R.W. Grange, D. Liu, Dietary Epicatechin Promotes Survival of Obese Diabetic Mice and *Drosophila melanogaster*, *J. Nutr.* 141 (2011) 1095–1100. <https://doi.org/10.3945/jn.110.134270>.
- [87] T.J. Huang, S.A. Price, L. Chilton, N.A. Calcutt, D.R. Tomlinson, A. Verkhatsky, P. Fernyhough, Insulin prevents depolarization of the mitochondrial inner membrane in sensory neurons of type 1 diabetic rats in the presence of sustained hyperglycemia, *Diabetes.* 52 (2003) 2129–2136. <https://doi.org/10.2337/diabetes.52.8.2129>.
- [88] W.E. Barry, C.S. Thummel, The *Drosophila* HNF4 nuclear receptor promotes glucose-stimulated insulin secretion and mitochondrial function in adults, *Elife.* 5 (2016). <https://doi.org/10.7554/eLife.111183>.
- [89] J.R.B. Newman, A. Conesa, M. Mika, F.N. New, S. Onengut-Gumuscu, M.A. Atkinson, S.S. Rich, L.M. McIntyre, P. Concannon, Disease-specific biases in alternative splicing and tissue-specific dysregulation revealed by multitissue profiling of lymphocyte gene expression in type 1 diabetes, *Genome Res.* 27 (2017) 1807–1815. <https://doi.org/10.1101/gr.217984.116>.
- [90] M.B. Zimering, M. Grinberg, J. Burton, K.C.H. Pang, Circulating Agonist Autoantibody to 5-Hydroxytryptamine 2A Receptor in Lean and Diabetic Fatty Zucker Rat Strains., *Endocrinol. Diabetes Metab. J.* 4 (2020). [/pmc/articles/PMC7550200/?report=abstract](https://pubmed.ncbi.nlm.nih.gov/38811111/) (accessed November 22, 2020).

- [91] S.K. Raut, M. Khullar, The big entity of new RNA world: Long non-coding RNAs in microvascular complications of diabetes, *Front. Endocrinol. (Lausanne)*. 9 (2018) 1. <https://doi.org/10.3389/fendo.2018.00300>.
- [92] S.P. Patel, Toward A Genome-Wide Association Study Of Diet Related Mortality In *Drosophila Melanogaster*: High Sugar Diet, 2020. <https://search.proquest.com/openview/2497f867fe2d9e8d7c7b2cfd79de75b4/1?cbl=18750&diss=y&pq-origsite=gscholar> (accessed November 22, 2020).
- [93] H. Ikegami, T. Maegawa, T. Ohno, F. Horio, N. Babaya, M. Takahashi, Y. Miyasaka, M. Kobayashi, Congenic mapping and candidate gene analysis for streptozotocin-induced diabetes susceptibility locus on mouse chromosome 11, *Mamm. Genome*. 29 (2018) 273–280. <https://doi.org/10.1007/s00335-018-9742-y>.
- [94] M. Barthez, M. Poplineau, M. Elrefaey, N. Caruso, Y. Graba, A.J. Saurin, Human ZKSCAN3 and *Drosophila* M1BP are functionally homologous transcription factors in autophagy regulation, *Sci. Rep.* 10 (2020) 9653. <https://doi.org/10.1038/s41598-020-66377-z>.
- [95] K.J. Kramer, R.M. Jacobs, R.D. Speirs, L.H. Hendmcks, Effect of vertebrate hypoglycemic and beta cell cytotoxic agents on insects, *Biochem. Physiol.* 61 (1978) 95–97. <https://pubag.nal.usda.gov/download/11675/PDF> (accessed February 23, 2020).
- [96] R. Valencia, J.M. Mason, R.C. Woodruff, S. Zimmering, Chemical mutagenesis testing in *Drosophila*. III. Results of 48 coded compounds tested for the national toxicology program, *Environ. Mutagen.* 7 (1985) 325–348. <https://doi.org/10.1002/em.2860070309>.
- [97] Y.H. Siddique, M.S. Ansari, Rahul, S. Jyoti, Effect of alloxan on the third instar larvae of transgenic *Drosophila melanogaster* (hsp70-lacZ)Bg9, *Toxin Rev.* (2018) 1–11. <https://doi.org/10.1080/15569543.2018.1472106>.
- [98] R. Agrawal, E. Tyagi, R. Shukla, C. Nath, Insulin receptor signaling in rat hippocampus: A study in STZ (ICV) induced memory deficit model, *Eur. Neuropsychopharmacol.* 21 (2011) 261–273. <https://doi.org/10.1016/j.euroneuro.2010.11.009>.
- [99] A. Knezovic, A. Loncar, J. Homolak, U. Smailovic, J. Osmanovic Barilar, L. Ganoci, N. Bozina, P. Riederer, M. Salkovic-Petrisic, Rat brain glucose transporter-2, insulin

- receptor and glial expression are acute targets of intracerebroventricular streptozotocin: risk factors for sporadic Alzheimer's disease?, *J. Neural Transm.* 124 (2017) 695–708. <https://doi.org/10.1007/s00702-017-1727-6>.
- [100] W.J. Schnedl, S. Ferber, J.H. Johnson, C.B. Newgard, STZ transport and cytotoxicity. Specific enhancement in GLUT2-expressing cells., *Diabetes.* 43 (1994) 1326–33. <https://doi.org/10.2337/DIAB.43.11.1326>.
- [101] R.A. Bennett, A.E. Pegg, Alkylation of DNA in Rat Tissues following Administration of Streptozotocin, 41 (1981) 2786–2791.
- [102] J.M. Berthiaume, J.G. Kurdys, D.M. Muntean, M.G. Rosca, Mitochondrial NAD + /NADH Redox State and Diabetic Cardiomyopathy , *Antioxid. Redox Signal.* 30 (2017) 375–398. <https://doi.org/10.1089/ars.2017.7415>.
- [103] Y. He, C. Martinez-Fleites, A. Bubb, T.M. Gloster, G.J. Davies, Structural insight into the mechanism of streptozotocin inhibition of O-GlcNAcase, *Carbohydr. Res.* 344 (2009) 627–631. <https://doi.org/10.1016/j.carres.2008.12.007>.
- [104] N.B.V. Barbosa, J.B.T. Rocha, J.C.M. Soares, D.C. Wondracek, J.F. Gonçalves, M.R.C. Schetinger, C.W. Nogueira, Dietary diphenyl diselenide reduces the STZ-induced toxicity, *Food Chem. Toxicol.* 46 (2008) 186–194. <https://doi.org/10.1016/J.FCT.2007.07.014>.
- [105] S. Miwa, J. St-Pierre, L. Partridge, M.D. Brand, Superoxide and hydrogen peroxide production by *Drosophila* mitochondria, *Free Radic. Biol. Med.* 35 (2003) 938–948. [https://doi.org/10.1016/S0891-5849\(03\)00464-7](https://doi.org/10.1016/S0891-5849(03)00464-7).
- [106] Y.H. Siddique, M.S. Ansari, Rahul, S. Jyoti, Effect of alloxan on the third instar larvae of transgenic *Drosophila melanogaster* (*hsp70-lacZ*)Bg9, *Toxin Rev.* 39 (2020) 41–51. <https://doi.org/10.1080/15569543.2018.1472106>.
- [107] K.J. Kramer, R.M. Jacobs, R.D. Speirs, L.H. Hendricks, Effect of vertebrate hypoglycemic and β -cell cytotoxic agents on insects, *Comp. Biochem. Physiol. Part C Comp. Pharmacol.* 61 (1978) 95–97. [https://doi.org/10.1016/0306-4492\(78\)90117-X](https://doi.org/10.1016/0306-4492(78)90117-X).
- [108] R. Das, L.L. Dobens, Conservation of gene and tissue networks regulating insulin

signalling in flies and vertebrates, *Biochem. Soc. Trans.* 43 (2015) 1057–1062.
<https://doi.org/10.1042/BST20150078>.

- [109] K. Kannan, Y.-W.C. Fridell, Functional implications of *Drosophila* insulin-like peptides in metabolism, aging, and dietary restriction, *Front. Physiol.* 4 (2013) 288.
<https://doi.org/10.3389/fphys.2013.00288>.
- [110] K.D. Baker, C.S. Thummel, Diabetic Larvae and Obese Flies-Emerging Studies of Metabolism in *Drosophila*, *Cell Metab.* 6 (2007) 257–266.
<https://doi.org/10.1016/j.cmet.2007.09.002>.
- [111] S. Huang, M.P. Czech, The GLUT4 Glucose Transporter, *Cell Metab.* 5 (2007) 237–252. <https://doi.org/10.1016/j.cmet.2007.03.006>.
- [112] V. Parra, H.E. Verdejo, M. Iglewski, A. Del Campo, R. Troncoso, D. Jones, Y. Zhu, J. Kuzmicic, C. Pennanen, C. Lopez-Crisosto, F. Jaña, J. Ferreira, E. Noguera, M. Chiong, D.A. Bernlohr, A. Klip, J.A. Hill, B.A. Rothermel, E.D. Abel, A. Zorzano, S. Lavandero, Insulin stimulates mitochondrial fusion and function in cardiomyocytes via the AktmTOR-NFkB-Opa-1 signaling pathway, *Diabetes.* 63 (2014) 75–88.
<https://doi.org/10.2337/db13-0340>.
- [113] G. Lee, J.H. Park, Hemolymph sugar homeostasis and starvation-induced hyperactivity affected by genetic manipulations of the adipokinetic hormone-encoding gene in *Drosophila melanogaster*, *Genetics.* 167 (2004) 311–323.
<https://doi.org/10.1534/genetics.167.1.311>.
- [114] A.T. Haselton, Y.W.C. Fridell, Adult *Drosophila melanogaster* as a model for the study of glucose homeostasis, *Aging (Albany. NY).* 2 (2010) 523–526.
<https://doi.org/10.18632/aging.100185>.
- [115] R. Ugrankar, E. Berglund, F. Akdemir, C. Tran, M.S. Kim, J. Noh, R. Schneider, B. Ebert, J.M. Graff, *Drosophila* glucone screening identifies Ck1alpha as a regulator of mammalian glucose metabolism, *Nat. Commun.* 6 (2015).
<https://doi.org/10.1038/ncomms8102>.
- [116] S.N. Thompson, D.B. Borchardt, L.W. Wang, Dietary nutrient levels regulate protein and carbohydrate intake, gluconeogenic/glycolytic flux and blood trehalose level in the

- insect *Manduca sexta* L, *J. Comp. Physiol. B Biochem. Syst. Environ. Physiol.* 173 (2003) 149–163. <https://doi.org/10.1007/s00360-002-0322-8>.
- [117] D.J. Candy, A. Becker, G. Wegener, Coordination and integration of metabolism in insect flight, in: *Comp. Biochem. Physiol. - B Biochem. Mol. Biol.*, Pergamon, 1997: pp. 497–512. [https://doi.org/10.1016/S0305-0491\(97\)00212-5](https://doi.org/10.1016/S0305-0491(97)00212-5).
- [118] J. Blatt, F. Roces, Haemolymph sugar levels in foraging honeybees (*Apis mellifera carnica*): Dependence on metabolic rate and in vivo measurement of maximal rates of trehalose synthesis, *J. Exp. Biol.* 204 (2001) 2709–2716.
- [119] S.J. Broughton, M.D.W. Piper, T. Ikeya, T.M. Bass, J. Jacobson, Y. Driege, P. Martinez, E. Hafen, D.J. Withers, S.J. Leivers, L. Partridge, Longer lifespan, altered metabolism, and stress resistance in *Drosophila* from ablation of cells making insulin-like ligands, *Proc. Natl. Acad. Sci. U. S. A.* 102 (2005) 3105–3110. <https://doi.org/10.1073/pnas.0405775102>.
- [120] A. Haselton, E. Sharmin, J. Schrader, M. Sah, P. Poon, Y.W.C. Fridell, Partial ablation of adult *drosophila* insulin-producing neurons modulates glucose homeostasis and extends life span without insulin resistance, *Cell Cycle.* 9 (2010) 3135–3143. <https://doi.org/10.4161/cc.9.15.12458>.
- [121] H. Zhang, J. Liu, C.R. Li, B. Momen, R.A. Kohanski, L. Pick, Deletion of *Drosophila* insulin-like peptides causes growth defects and metabolic abnormalities, *Proc. Natl. Acad. Sci. U. S. A.* 106 (2009) 19617–19622. <https://doi.org/10.1073/pnas.0905083106>.
- [122] L.P. Musselman, J.L. Fink, K. Narzinski, P.V. Ramachandran, S.S. Hathiramani, R.L. Cagan, T.J. Baranski, A high-sugar diet produces obesity and insulin resistance in wild-type *Drosophila*, *DMM Dis. Model. Mech.* 4 (2011) 842–849. <https://doi.org/10.1242/dmm.007948>.
- [123] M.Y. Pasco, P. Léopold, High sugar-induced insulin resistance in *Drosophila* relies on the Lipocalin Neural Lazarillo, *PLoS One.* 7 (2012) e36583. <https://doi.org/10.1371/journal.pone.0036583>.
- [124] L.P. Musselman, J.L. Fink, P.V. Ramachandran, B.W. Patterson, A.L. Okunade, E. Maier, M.R. Brent, J. Turk, T.J. Baranski, Role of fat body lipogenesis in protection

against the effects of caloric overload in drosophila, *J. Biol. Chem.* 288 (2013) 8028–8042. <https://doi.org/10.1074/jbc.M112.371047>.

- [125] Invasive Species and Human Health - Google Books, (n.d.). https://books.google.com.br/books?id=2YtIDwAAQBAJ&pg=PA70&lpg=PA70&dq=SPECKLED+FEEDER+ROACHES+-+Fact+Sheet+Nauphoeta+cinerea&source=bl&ots=HU5_Wx3c1D&sig=ACfU3U28q0cjzbzkUzdVIQZ_M41S9kWyNA&hl=en&sa=X&ved=2ahUKEwi3oduw05joAhXoGbkGHcXVB9YQ6AEwF3oECAkQAQ#v=onepage&q=SPECKLED FEEDER ROACHES - Fact Sheet Nauphoeta cinerea&f=false (accessed March 13, 2020).
- [126] L.S. Corley, A.J. Moore, Fitness of alternative modes of reproduction: Developmental constraints and the evolutionary maintenance of sex, *Proc. R. Soc. B Biol. Sci.* 266 (1999) 471–476. <https://doi.org/10.1098/rspb.1999.0661>.
- [127] L.S. Corley, J.R. Blankenship, A.J. Moore, P.J. Moore, Developmental constraints on the mode of reproduction in the facultatively parthenogenetic cockroach *Nauphoeta cinerea*, *Evol. Dev.* 1 (1999) 90–99. <https://doi.org/10.1046/j.1525-142x.1999.99001.x>.
- [128] W.J. Bell, L.M. Roth, C.A. Nalepa, *Cockroaches ecology, behaviour, and natural history.*, The Johns Hopkins University Press, 2007. https://www.zin.ru/Animalia/Coleoptera/ADDPAGES/Andrey_Ukrainsky_Library/References_files/Bell07.pdf.
- [129] Nicholas J Strausfeld, *Atlas of an Insect Brain*, Springer Berlin Heidelberg, 1976. <https://doi.org/10.1007/978-3-642-66179-2>.
- [130] C. Bernard, *An introduction to the study of experimental medicine.* - PsycNET, (1927). <https://psycnet.apa.org/record/1928-01714-000> (accessed June 12, 2020).
- [131] T.K. Das, R.L. Cagan, A *Drosophila* approach to thyroid cancer therapeutics, *Drug Discov. Today Technol.* 10 (2013) e65–e71. <https://doi.org/10.1016/j.ddtec.2012.09.004>.
- [132] V.A. Rudrapatna, R.L. Cagan, T.K. Das, *Drosophila* cancer models, *Dev. Dyn.* 241 (2012) 107–118. <https://doi.org/10.1002/dvdy.22771>.

- [133] J. Pendse, P. V. Ramachandran, J. Na, N. Narisu, J.L. Fink, R.L. Cagan, F.S. Collins, T.J. Baranski, A *Drosophila* functional evaluation of candidates from human genome-wide association studies of type 2 diabetes and related metabolic traits identifies tissue-specific roles for dHHEX, *BMC Genomics*. 14 (2013). <https://doi.org/10.1186/1471-2164-14-136>.
- [134] B.A. Afolabi, O.C. Olagoke, D.O. Souza, M. Aschner, J.B.T. Rocha, A.L.A. Segatto, Modified expression of antioxidant genes in lobster cockroach, *Nauphoeta cinerea* exposed to methylmercury and monosodium glutamate, *Chem. Biol. Interact.* 318 (2020). <https://doi.org/10.1016/j.cbi.2020.108969>.
- [135] B.C. Piccoli, J.C. Alvim, F.D. da Silva, P.A. Nogara, O.C. Olagoke, M. Aschner, C.S. Oliveira, J.B.T. Rocha, High level of methylmercury exposure causes persisted toxicity in *Nauphoeta cinerea*, *Environ. Sci. Pollut. Res.* (2019). <https://doi.org/10.1007/s11356-019-06989-9>.
- [136] B.A. Afolabi, O.C. Olagoke, High concentration of MSG alters antioxidant defence system in lobster cockroach *Nauphoeta cinerea* (Blattodea: Blaberidae), *BMC Res. Notes*. 13 (2020) 217. <https://doi.org/10.1186/s13104-020-05056-8>.
- [137] N.R. Rodrigues, M.E.M. Nunes, D.G.C. Silva, A.P.P. Zemolin, D.F. Meinerz, L.C. Cruz, A.B. Pereira, J.B.T. Rocha, T. Posser, J.L. Franco, Is the lobster cockroach *Nauphoeta cinerea* a valuable model for evaluating mercury induced oxidative stress?, *Chemosphere*. 92 (2013) 1177–1182. <https://doi.org/10.1016/J.CHEMOSPHERE.2013.01.084>.
- [138] R. Jacob, X. Fan, M. Evans, ... J.D., Brain glucose levels are elevated in chronically hyperglycemic diabetic rats: no evidence for protective adaptation by the blood brain barrier, *Metab.* ... (2002). [https://www.metabolismjournal.com/article/S0026-0495\(02\)00153-1/abstract](https://www.metabolismjournal.com/article/S0026-0495(02)00153-1/abstract) (accessed March 29, 2019).
- [139] J.J. Hwang, L. Jiang, M. Hamza, E.S. Rangel, F. Dai, R. Belfort-Deaguiar, L. Parikh, B.B. Koo, D.L. Rothman, G. Mason, R.S. Sherwin, Blunted rise in brain glucose levels during hyperglycemia in adults with obesity and T2DM, (2017). <https://doi.org/10.1172/jci.insight.95913>.

- [140] G. Parker, R. Taylor, D. Jones, D. McClain, Hyperglycemia and inhibition of glycogen synthase in streptozotocin-treated mice: Role of O-linked N-acetylglucosamine, *J. Biol. Chem.* 279 (2004) 20636–20642. <https://doi.org/10.1074/jbc.M312139200>.
- [141] F.M. Ashcroft, M. Rohm, A. Clark, M.F. Brereton, Is Type 2 Diabetes a Glycogen Storage Disease of Pancreatic β Cells?, *Cell Metab.* 26 (2017) 17–23. <https://doi.org/10.1016/j.cmet.2017.05.014>.
- [142] A. Moore, A. Shindikar, I. Fomison-Nurse, F. Riu, P.E. Munasinghe, T. Parshu Ram, P. Saxena, S. Coffey, R.W. Bunton, I.F. Galvin, M.J. Williams, C. Emanuelli, P. Madeddu, R. Katare, Rapid onset of cardiomyopathy in STZ-induced female diabetic mice involves the downregulation of pro-survival Pim-1, *Cardiovasc. Diabetol.* 13 (2014) 68. <https://doi.org/10.1186/1475-2840-13-68>.
- [143] A.W. Stitt, Y.M. Li, T.A. Gardiner, R. Bucala, D.B. Archer, H. Vlassara, Advanced glycation end products (AGEs) co-localize with AGE receptors in the retinal vasculature of diabetic and of AGE-infused rats., *Am. J. Pathol.* 150 (1997) 523–31. <http://www.ncbi.nlm.nih.gov/pubmed/9033268> (accessed May 11, 2019).
- [144] A. Loboda, M. Damulewicz, E. Pyza, A. Jozkowicz, J. Dulak, Role of Nrf2/HO-1 system in development, oxidative stress response and diseases: an evolutionarily conserved mechanism, *Cell. Mol. Life Sci.* (2016). <https://doi.org/10.1007/s00018-016-2223-0>.
- [145] A. Pitoniak, D. Bohmann, Mechanisms and functions of Nrf2 signaling in *Drosophila*, *Free Radic. Biol. Med.* (2015). <https://doi.org/10.1016/j.freeradbiomed.2015.06.020>.
- [146] D.H.F. Mak, S.P. Ip, P.C. Li, M.K.T. Poon, K.M. Ko, Alterations in tissue glutathione antioxidant system in streptozotocin-induced diabetic rats, *Mol. Cell. Biochem.* (1996). <https://doi.org/10.1007/BF00227543>.
- [147] K. Shah, S. DeSilva, T. Abbruscato, The role of glucose transporters in brain disease: Diabetes and Alzheimer's disease, *Int. J. Mol. Sci.* 13 (2012) 12629–12655. <https://doi.org/10.3390/ijms131012629>.
- [148] J.A. Sanchez, D. Mesquita, M.C. Ingaramo, F. Ariel, M. Milan, A. Dekanty, Eiger/TNF α -mediated Dilp8 and ROS production coordinate intra-organ growth in *drosophila*, *PLoS Genet.* 15 (2019) e1008133.

<https://doi.org/10.1371/journal.pgen.1008133>.

- [149] I. Louradour, A. Sharma, I. Morin-Poulard, M. Letourneau, A. Vincent, M. Crozatier, N. Vanzo, Reactive oxygen species-dependent Toll/NF- κ B activation in the drosophila hematopoietic niche confers resistance to wasp parasitism, *Elife*. 6 (2017). <https://doi.org/10.7554/eLife.25496>.
- [150] R.P. Sorrentino, J.P. Melk, S. Govind, Genetic Analysis of Contributions of Dorsal Group and JAK-Stat92E Pathway Genes to Larval Hemocyte Concentration and the Egg Encapsulation Response in *Drosophila*, *Genetics*. 166 (2004) 1343–1356. <https://doi.org/10.1534/genetics.166.3.1343>.
- [151] V.M. Wright, K.L. Vogt, E. Smythe, M.P. Zeidler, Differential activities of the *Drosophila* JAK/STAT pathway ligands Upd, Upd2 and Upd3, *Cell. Signal*. 23 (2011) 920–927. <https://doi.org/10.1016/j.cellsig.2011.01.020>.
- [152] C.J. Champion, J. Xu, The impact of metagenomic interplay on the mosquito redox homeostasis, *Free Radic. Biol. Med.* 105 (2017) 79–85. <https://doi.org/10.1016/j.freeradbiomed.2016.11.031>.
- [153] K.J. Dietz, Redox signal integration: From stimulus to networks and genes, *Physiol. Plant*. 133 (2008) 459–468. <https://doi.org/10.1111/j.1399-3054.2008.01120.x>.
- [154] H. Lu, Y. Yang, E.M. Allister, N. Wijesekara, M.B. Wheeler, The identification of potential factors associated with the development of type 2 diabetes: A quantitative proteomics approach, *Mol. Cell. Proteomics*. 7 (2008) 1434–1451. <https://doi.org/10.1074/mcp.M700478-MCP200>.
- [155] N. Lester-Coll, E.J. Rivera, S.J. Soscia, K. Doiron, J.R. Wands, S.M. De La Monte, Intracerebral streptozotocin model of type 3 diabetes: Relevance to sporadic Alzheimer's disease, *J. Alzheimer's Dis*. 9 (2006) 13–33. <https://doi.org/10.3233/JAD-2006-9102>.
- [156] M. Tatar, A. Kopelman, D. Epstein, M.P. Tu, C.M. Yin, R.S. Garofalo, A mutant *Drosophila* insulin receptor homolog that extends life-span and impairs neuroendocrine function, *Science* (80-.). 292 (2001) 107–110. <https://doi.org/10.1126/science.1057987>.
- [157] O. Puig, M.T. Marr, M.L. Ruhf, R. Tjian, Control of cell number by *Drosophila* FOXO:

Downstream and feedback regulation of the insulin receptor pathway, *Genes Dev.* 17 (2003) 2006–2020. <https://doi.org/10.1101/gad.1098703>.

[158] L. Adhikary, F. Chow, D.J. Nikolic-Paterson, C. Stambe, J. Dowling, R.C. Atkins, G.H. Tesch, Abnormal p38 mitogen-activated protein kinase signalling in human and experimental diabetic nephropathy, *Diabetologia.* 47 (2004) 1210–1222. <https://doi.org/10.1007/s00125-004-1437-0>.

[159] J.L. Rains, S.K. Jain, Oxidative stress, insulin signaling, and diabetes, *Free Radic. Biol. Med.* 50 (2011) 567–575. <https://doi.org/10.1016/j.freeradbiomed.2010.12.006>.